

NOTE TO USERS

This reproduction is the best copy available.

UMI[®]

**BIODYNAMIC RESPONSE AND BODY INTERACTIONS WITH THE SEAT
PAN AND THE BACKREST UNDER VERTICAL VIBRATION**

Huainan Zhang

A thesis
in
the Department
of
Mechanical Engineering

Presented in Partial Fulfillment of the Requirements
for the Degree of Master of Applied Science
at Concordia University
Montréal, Québec, Canada

March 2005

© Huainan Zhang, 2005



Library and
Archives Canada

Bibliothèque et
Archives Canada

Published Heritage
Branch

Direction du
Patrimoine de l'édition

395 Wellington Street
Ottawa ON K1A 0N4
Canada

395, rue Wellington
Ottawa ON K1A 0N4
Canada

Your file Votre référence

ISBN: 0-494-04436-5

Our file Notre référence

ISBN: 0-494-04436-5

NOTICE:

The author has granted a non-exclusive license allowing Library and Archives Canada to reproduce, publish, archive, preserve, conserve, communicate to the public by telecommunication or on the Internet, loan, distribute and sell theses worldwide, for commercial or non-commercial purposes, in microform, paper, electronic and/or any other formats.

The author retains copyright ownership and moral rights in this thesis. Neither the thesis nor substantial extracts from it may be printed or otherwise reproduced without the author's permission.

AVIS:

L'auteur a accordé une licence non exclusive permettant à la Bibliothèque et Archives Canada de reproduire, publier, archiver, sauvegarder, conserver, transmettre au public par télécommunication ou par l'Internet, prêter, distribuer et vendre des thèses partout dans le monde, à des fins commerciales ou autres, sur support microforme, papier, électronique et/ou autres formats.

L'auteur conserve la propriété du droit d'auteur et des droits moraux qui protègent cette thèse. Ni la thèse ni des extraits substantiels de celle-ci ne doivent être imprimés ou autrement reproduits sans son autorisation.

In compliance with the Canadian Privacy Act some supporting forms may have been removed from this thesis.

Conformément à la loi canadienne sur la protection de la vie privée, quelques formulaires secondaires ont été enlevés de cette thèse.

While these forms may be included in the document page count, their removal does not represent any loss of content from the thesis.

Bien que ces formulaires aient inclus dans la pagination, il n'y aura aucun contenu manquant.


Canada

ABSTRACT

BIODYNAMIC RESPONSES AND BODY INTERACTIONS WITH THE SEAT PAN AND THE BACKREST UNDER VERTICAL VIBRATION

Huainan Zhang

Enhancement of driver comfort related to vibration environment of road vehicles involves characterization of vibration environment, biodynamic response of the driver and seating dynamics. The human driver's responses, when exposed to automotive vibration along the vertical axis, have been widely characterized, assuming body interactions with the seat pan alone. The standardized ranges reported in ISO-5982 (2001) are considered applicable for human occupants seated on a flat pan with no back support. Moreover, the data used in the synthesis are believed to correspond to relatively high magnitudes of vertical vibration. The sitting postures in automotive seats are known to be considerably different from those considered in the standard and the reported data. Most importantly, the human drivers exposed to vertical vibration exhibit significant simultaneous interactions with the backrest. In this dissertation research, the body interactions with both the seat pan and the backrest are investigated under vertical automotive vibration and representative posture. An experiment design is realized on the basis of typical automotive seat to characterize the biodynamic interactions at the seat pan and the backrest. The measured data are analyzed to illustrate the significance of the seated body weight, magnitude of vertical vibration and a few posture-related factors, namely, the hands position and feet position. The results suggest strong influence of the

body mass and built, and the hands position, and most of all significant interactions with the backrest.

The apparent mass response characteristics of 24 individuals are measured under postural and vibration conditions representative of those applicable to automobile drivers and passengers, with appropriate considerations of the interactions with the backrest and the pan. The measured total body forces at the seat pan and the upper body forces transmitted to the seat backrest are analyzed to identify important contributing factors and target response curves for model development. The results clearly demonstrated strong interactions between the upper body and the backrest apart from those between the seated body and the pan. A four-degree-of-freedom linear biodynamic model of the seated occupant is developed, with the objective of satisfying the apparent mass response at both the seat pan and the seat backrest. The model parameters are identified through solution of a constrained optimization function comprising magnitude and phase components of both the apparent mass response functions measured at the pan and the backrest. Owing to the strong dependence of the biodynamic response on the body weight, the measured data are grouped under four different body mass ranges. The body mass dependent models are then explored on the basis of the parameters identified for the baseline model. The variations in the model parameters with the body mass are expressed by linear regression functions, to facilitate the prediction of biodynamic responses of individual subjects. The validity of the proposed generalized model is demonstrated by comparing the model responses with the data acquired for a few subjects.

ACKNOWLEDGEMENTS

I am sincerely grateful to my supervisors, Dr. Subhash Rakheja and Dr. Ion-Stiharu, for their initiation of the project and their constant guidance and dedication throughout the thesis work. Their valuable advice and contributions have helped to make the completion of this thesis. I also wish to acknowledge the contribution of various researchers whose data have been employed in this study.

The encouragement and understanding of my wife, Ran, make the completion of this thesis possible. Her essential assistance in the final stage is further acknowledged. I dedicate this thesis to her and my son who will come into this world in two months.

TABLE OF CONTENTS

LIST OF FIGURES	vii
LIST OF TABLES	xiii
LIST OF ABBREVIATIONS AND SYMBOLS	xiv

CHAPTER 1

HUMAN RESPONSE TO WHOLE BODY VIBRATION

1.1	Introduction	1
1.2	The Biodynamic response of seated occupants exposed to WBV	4
1.3	Review of the published data on the whole-body biodynamic response	8
1.3.1	Factors affecting biodynamic response functions	15
1.3.2	Influence of the seated posture on APMS and DPMI magnitude	16
1.3.3	Influence of subject mass and build	25
1.3.4	Influence of excitation magnitude and frequency	28
1.3.5	Influence of gender	32
1.4	Biodynamic models of seated occupants	34
1.5	Scope and objectives of the dissertation research	40
1.6	Thesis organization	42

CHAPTER 2

MEASUREMENT OF THE BIODYNAMIC RESPONSE TO WHOLE-BODY VIBRATION

2.1	Introduction	44
2.2	Test apparatus	45

2.3	Test methodology	51
2.4	Test matrix	53
2.5	Summary	56

CHAPTER 3

APPARENT MASS RESPONSE CHARACTERISTICS

3.1	Introduction	57
3.2	Static analysis of body mass supported by the pan and the backrest	58
3.3	APMS response of the seated subjects	64
3.3.1	Influence of body weight	65
3.3.2	Influence of BMI and BF	89
3.3.3	Correlation between the measured APMS magnitude at seat pan and backrest	91
3.3.4	The APMS data normalization	94
3.3.5	The influence of the magnitude and the type of vibration excitation	100
3.3.6	Influence of the hands position	103
3.3.7	Influence of gender	106
3.4	Summary	107

CHAPTER 4

DEVELOPMENT OF HUMAN BODY MODEL ON SEAT

4.1	Introduction	111
4.2	Model development	113

4.2.1	Formulation of a non –dimensional model	116
4.3.2	Backrest APMS of the model	117
4.3	Model parameters estimation	119
4.4	Development of body weight-dependent seated occupant models	125
4.5	Summary	132

CHAPTER 5

CONCLUSIONS AND RECOMMANDATIONS FOR FURTHER WORK

5.1	Major highlights or contributions	138
5.2	Conclusions	141
5.2	Recommendations for future studies	142
REFERENCE		143

LIST OF FIGURES

Figure 1.1	Effect of sitting posture and body mass on the mean DPMI magnitude17
Figure 1.2	Effects of sitting posture and body mass on the equivalent APMS magnitude derived from the reported DPMI data17
Figure 1.3	Effect of sitting posture on the DPMI magnitude and phase response under sine sweep excitations ($1.0\text{-}2.0\text{ ms}^{-2}$)19
Figure 1.4	Effect of contact with a rigid flat backrest on the mean STHT response of 12 subjects 20
Figure 1.5	Diagrammatic representation of the nine postures21
Figure 1.6	Inter-quartile ranges for normalized apparent masses for 12 subjects using nine postures at 1.0 m/s^2 r.m.s 22
Figure 1.7	Inter-quartile ranges for seat vertical to pelvis rotation transmissibility for 12 subjects using nine postures at 1.0 m/s^2 r.m.s 22
Figure 1.8	Schematic representations of different sitting postures 23
Figure 1.9	Effect of seat height on the mean APMS magnitude response of 27 subjects for different postures (excitation: $1.0\text{ m/s}^2\text{ rms}$) 24
Figure 1.10	Influence of hands position and back support condition on the mean APMS magnitude response of 27 subjects 25
Figure 1.11	The effect of body mass on the DPMI magnitude27
Figure 1.12	The effect of body mass on the APMS magnitude, derived from the reported DPMI data27
Figure 1.13	Effect of excitation magnitude on the mean DPMI response of 15 male subjects29
Figure 1.14	Effect of excitation level on the DPMI magnitude29
Figure 1.15	Effect of excitation level on the APMS magnitude derived from the reported DPMI data 30
Figure 1.16	Effect of excitation level on the mean DPMI magnitude30
Figure 1.17	Effect of excitation level on the absorbed power normalized by average sitting weight32

Figure 1.18 Inter-subject variability in the backrest apparent mass measured at the back	34
Figure 1.19 Single-degree-of-freedom mechanical models of the seated occupant exposed to vertical vibration	36
Figure 1.20 Two-DOF mechanical equivalent models of the seated occupant exposed to vertical vibration	36
Figure 1.21 Three-DOF mechanical equivalent models of the seated occupant exposed to vertical vibration	37
Figure 1.22 Four-DOF biodynamic models of the seated occupant exposed to vertical vibration	37
Figure 1.23 Lumped parameter models of seated human body proposed by Yasunao and Griffin	41
Figure 2.1 Top and side views of the rigid test seat	47
Figure 2.2 A pictorial view of the test seat mounted on the platform	48
Figure 2.3 Location of the load cells within the force platform	49
Figure 2.4 The rms spectra of the platform acceleration measured under white- noise excitations	50
Figure 2.5 PSD of the platform acceleration measured under seat track- measured vibration	51
Figure 3.1 Comparison of APMS responses of 24 subjects measured at seat pan	67
Figure 3.2 Comparison of APMS responses of 24 subjects measured at seat pan	68
Figure 3.3 Comparison of APMS responses of 24 subjects measured at seat pan	69
Figure 3.4 Comparison of APMS responses of 24 subjects measured at seat pan	70
Figure 3.5 Comparison of APMS responses of 24 subjects measured at seat pan	71
Figure 3.6 Comparison of APMS responses of 24 subjects measured at seat pan	72
Figure 3.7 Comparison of APMS responses of 24 subjects measured at seat pan	73
Figure 3.8 Comparison of APMS responses of 24 subjects measured at seat pan	74

Figure 3.9	Comparison of APMS responses of 24 subjects measured at the backrest	75
Figure 3.10	Comparison of APMS responses of 24 subjects measured at the backrest	76
Figure 3.11	Comparison of APMS responses of 24 subjects measured at the backrest	77
Figure 3.12	Comparison of APMS responses of 24 subjects measured at the backrest	78
Figure 3.13	Comparison of APMS responses of 24 subjects measured at the backrest	79
Figure 3.14	Comparison of APMS responses of 24 subjects measured at the backrest	80
Figure 3.15	Comparison of APMS responses of 24 subjects measured at the backrest	81
Figure 3.16	Comparison of APMS responses of 24 subjects measured at the backrest	82
Figure 3.17	Dependence of the peak seat pan APMS magnitude and the corresponding frequency on the body mass (hands-in-lap)	84
Figure 3.18	Dependence of the peak seat pan APMS magnitude and the corresponding frequency on the body mass (hands-on-steering wheel)	84
Figure 3.19	Dependence of the peak backrest APMS magnitude and the corresponding frequency on the body mass (hands-in-lap)	85
Figure 3.20	Dependence of the peak backrest APMS magnitude and the corresponding frequency on the body mass (hands-on-steering wheel)	85
Figure 3.21	Mean APMS magnitude responses measured at: (a) seat pan; and (b) backrest, as a function of body mass (hands-in-lap)	86
Figure 3.22	Mean APMS magnitude responses measured at: (a) seat pan; and (b) backrest, as a function of body mass (hands-on-steering wheel)	86

Figure 3.23	Comparisons of mean, maximum and minimum values of the measured seat pan APMS response (hands in lap) with the ranges reported in ISO-5982	88
Figure 3.24	Comparisons of mean, maximum and minimum values of the measured seat pan APMS response (hands on steering wheel) with the ranges reported in ISO-5982	88
Figure 3.25	Dependence of the peak seat-pan and backrest APMS magnitude on the BMI	89
Figure 3.26	Dependence of the peak seat-pan and backrest APMS magnitude on BF	90
Figure 3.27	Comparisons of the APMS magnitude responses measured on the seat-pan and the backrest	92
Figure 3.28	Correlations between the APMS magnitudes measured at the seat pan and the backrest	93
Figure 3.29	The normalized APMS magnitude response of 24 subjects measured at the seat pan under different levels of vertical vibration	95
Figure 3.30	The normalized APMS magnitude response of 24 subjects measured at the seat pan under different levels of vibration	96
Figure 3.31	The normalized APMS magnitude response of 24 subjects measured at the seat backrest under different levels of vibration	97
Figure 3.32	The normalized APMS magnitude response of 24 subjects measured at the seat backrest under different levels of vibration	98
Figure 3.33	The mean, standard deviation, and lower and upper bounds of the normalized APMS magnitude and phase responses measured at the seat pan	99

Figure 3.34	The mean, standard deviation, and lower and upper bounds of the normalized APMS magnitude and phase responses measured at the seat backrest	100
Figure 3.35	The mean APMS response on the seat pan attained for different magnitude and types of vibration excitations	101
Figure 3.36	The mean APMS response on the seat backrest attained for different magnitude and types of vibration excitations	103
Figure 3.37	The comparison of the mean APMS magnitude responses measured on the seat pan and backrest for different hands positions	105
Figure 3.38	Variation in the ratio of the pan APMS magnitude to the backrest APMS magnitude	93
Figure 3.39	The comparisons of mean APMS responses measured on the seat backrest with 12 male and 12 female subjects	108
Figure 4.1	The proposed structure of the seated human biodynamic model	114
Figure 4.2	Comparisons of apparent mass responses of the seated occupant model with the mean measured response (hands-in-lap posture)	124
Figure 4.3	Comparisons of apparent mass responses of the seated occupant model with the mean measured response (hands-on-steering wheel posture)	125
Figure 4.4	Correlations of the model stiffness parameters with the body mass	128
Figure 4.5	Correlations of the model damping parameters with the body mass	128
Figure 4.6	Comparisons of the mass-dependent model results with the mean measured response of seated occupants within different mass ranges (hands-in-lap)	129

Figure 4.7	Comparisons of the mass-dependent model results with the mean measured response of seated occupants within different mass ranges (hands on steering wheel)	130
Figure 4.8	The comparison of the estimated seat pan APMS responses with the body weight dependent model response for both hands positions	132
Figure 4.9	Comparisons of the estimated APMS magnitude and phase responses with the measured responses of the subject with total body mass of 56.9 kg	133
Figure 4.10	Comparisons of the estimated APMS magnitude and phase responses with the measured responses of the subject with total body mass of 77.3 kg	134
Figure 4.11	Comparisons of the estimated APMS magnitude and phase responses with the measured responses of the subject with total body mass of 95.3 kg	135

LIST OF TABLES

Table 1.1	Summary of experimental conditions employed in different studies9
Table 1.2	Factors influencing the biodynamic response characteristics15
Table 1.3	The parameters of the reported model38
Table 2.1	Physical characteristics of the test subjects55
Table 2.2	The test matrix56
Table 3.1	Average Body Weight Supported by the Seat Pan and the Backrest59
Table 3.2	Comparisons of measured and estimated values of the seat pan static force for all subjects seated with hands in lap and hands on steering wheel postures62
Table 3.3	Comparisons of measured and estimated values of the seat back static force for all subjects seated with hands in lap and hands on steering wheel postures63
Table 4.1	Model Parameters based upon the mean mass of 71.2 kg 122
Table 4.2	Parameters of the automotive body weight-dependent occupant models	...127
Table 4.3	Regression functions of the model parameters128
Table 4.4	The estimated model parameters of three selected subjects131

LIST OF ABBREVIATIONS AND SYMBOLS

ABBREVIATIONS

APMS	Apparent mass
DPMI	Driving-point mechanical impedance
STHT	Seat-to-head transmissibility
ISO	International Standard Organization
PSD	Power spectral density
rms	Root-mean-square
WBV	Whole-body vibration
EBS	Erect back support
ENS	Erect back not supported
SLO	Sitting in a slouched posture
WBVS	Whole-body vehicle vibration simulator
SDOF	Single-degree-of-freedom
PUF	Polyurethane foams
LAP	Hands-in-lap posture
SW	Hands-on-steering wheel posture

SYMBOLS

α	inclination angle of the backrest with respect to vertical
β	inclination angle of the seat pan with respect to horizontal axis
k_1, k_2, k_{b1}, k_{b2}	stiffness coefficients (N/m)
c_1, c_2, c_{b1}, c_{b2}	viscous damping coefficients (Ns/m)
ω	angular frequency (rad/s)
$Z(j\omega)$	complex DPMI
$M(j\omega)$	complex APMS
$H(j\omega)$	complex seat-to-head transmissibility
$F(j\omega)$	driving force
$a(j\omega)$	driving point acceleration
$a_H(j\omega)$	head response acceleration
f_n	undamped natural frequency (Hz)
a_v	magnitude of vertical acceleration measured at the seat base
a_{bn}	magnitudes of acceleration components normal to the inclined backrest
a_{pn}	magnitudes of acceleration components normal to the inclined seat pan
\bar{a}_v	overall r.m.s acceleration
T	exposure duration
$M_{s0}(j\omega)$	complex APMS of the total seat of seat along

$M_{b0}(j\omega)$	complex APMS of the total seat backrest along
$M_s(j\omega)$	complex APMS of the subject alone as measured on the seat pan
$M_b(j\omega)$	complex APMS of the subject alone as measured on the seat backrest
F_p	driving point fore at the seat pan along an axis normal to the seat pan
m_0, m_1, m_2	model masses
x_1, x_2	motion of masses m_1 and m_2
x_0	displacement coordinate of base mass m_0
X_0, X_1, X_2	Laplace transformation of x_0, x_1, x_2
M_T	total body mass
$\omega_1, \omega_2, \omega_{b1}, \omega_{b2}$	natural frequency of the uncoupled masses
$\xi_1, \xi_2, \xi_{b1}, \xi_{b2}$	damping ratios of the uncoupled masses
μ_0, μ_1, μ_2	the ratio of model masses to the total body mass
$U(\chi)$	weighted minimization function
$U_p(\chi)$	squared errors resulting from APMS response at the seat pan
$U_b(\chi)$	squared errors resulting from APMS response at the seat backrest
χ	vector of model parameters to be identified
$M_p(\omega_i)$	magnitude of the pan APMS response of the model
$\phi_p(\omega_i)$	phase of the pan APMS response of the model
$M_b(\omega_i)$	magnitude of the backrest APMS response of the model
$\phi_b(\omega_i)$	phase of the backrest APMS response of the model
ψ, ρ	weighting factors

Chapter 1 Human Response to Whole Body Vibration

1.1 Introduction

Whole-body vibration (WBV) occurs when the body is supported on a surface which is vibrating. Humans are exposed to vibrations of the whole body nature when: sitting on a vibrating seat, standing on a vibrating floor, or lying on a vibrating bed. Heavy road and off road vehicles, due to their interactions with uneven terrains, are known to yield considerable levels of vibration to the driver and the passengers. Continued exposures to high magnitude of vibration could result in acute damage to body structures. Prolonged exposure to vehicular vibration and shocks has been related to discomfort, reduced working efficiency, and various health and safety risks.

Many studies have suggested that the exposure to whole-body vibration (WBV) can affect the lumbar spine and the connected nervous system [1,2]. Biodynamic experiments have shown that WBV exposure, combined with constrained sitting postures, can put the lumbar intervertebral disc at the risk of failure [3]. Epidemiologic studies have indicated that long-term exposure to the occupational WBV is associated with the degeneration of the spine and with low back pain disorders [4]. A critical evaluation of the epidemiologic literature on the effects of long-term WBV exposure on the spinal system indicated that low back pain, early degeneration of the lumbar spinal system and herniated lumbar disc were the most frequently reported adverse effects in worker exposed to WBV [5]. There are also many chronic health problems and unwanted physiological and psychophysical effects caused by long-term occupational exposure to such vibration in the 0.5-80 Hz frequency range, including abdominal pain digestive and vision problems, etc. [6].

In the U.S.A., Canada, and some European countries, it has been estimated that 4 to 7% of all employees are exposed to potentially harmful WBV [7], mainly the drivers of vehicles, such as dumpers, excavators, scrapers, buses and trucks. In view of severe health and safety risks posed by exposure to vibration and shock environment of off road vehicles, knowledge of how vibration is transmitted to and through the human body is a prerequisite to a full understanding of the cause-effect relationship between WBV and health, comfort and performance.

The dynamic response of the seat plays a critical role in enhancing the ride vibration environment of off road vehicles. Most seats are compliant and modify the vibration by amplifying low frequency vibration and attenuating high frequency vibration. One objective of the seat designer is to achieve an overall reduction in vibration discomfort of the seat occupant compared with the discomfort that would be experienced with a rigid seat [1]. It has been established that the human-seat system performance is affected not only by the seat design but also by the biodynamics of the human occupant [8]. The seated occupant response to vibration contributes considerably in shaping the vibration transmission performance of a seat, which may be attributed to dissipation / absorption of vibration energy by the biological system. The characterization of the contribution due to the seated occupant and the human responses to vibration are quite complex, as the human body is a complex active dynamic system.

The human responses to vibration have been mostly characterized by the biodynamic responses expressed either in terms of transmission of motion through the body or by the force-motion relationships at the driving-point [1]. The driving-point mechanical impedance (DPMI) or apparent mass (APMS) response characteristics of

seated human occupants exposed to vertical vibration have been widely investigated to enhance an understanding of the human responses to vibration and to develop mechanical equivalent models for applications in seating dynamics [8,10]. The reported investigations, however, are based upon the force-motion relationship at a single driving-point formed by the seat-pan and body interface, while the interactions with the back support are ignored.

The human response to vibration is strongly dependent upon the support conditions provided by the seat and the workstation. These may include the back supported against an inclined backrest and hands resting on a steering wheel. The dynamic interactions between the body and the supports other than the seat pan have been characterized only in a few recent studies [66,67]. The international standard, ISO-5982 [10], defines the ranges of DPMI of seated occupants exposed to vertical vibration, which are applicable only for sitting postures without a back support. The seated human interactions with the backrest have been studied in a single recent study, where the backrest is considered to be perfectly vertical [67]. Considering that the automotive seats are designed with inclined seat pan and backrest to provide comfortable and controlled sitting posture, the reported data for a vertical backrest may not be considered applicable.

This dissertation research explores the force-motion behavior of the seated occupant at two driving points, namely the seat pan and the seat backrest, while exposed to vertical vibration. The biodynamic responses of the seated occupant associated with the two driving points are constructed as a function of the vibration magnitude and hands position. A mechanical equivalent model of the occupant is proposed to characterize the APMS characteristics at the seat pan as well as the backrest.

1.2 The biodynamic response of seated occupants exposed to WBV

It has been suggested that the human responses to vibration and role of the human occupant in the coupled seat-occupant dynamics may be characterized by its biodynamic response measured at the driving-point between the seat and the occupant. Two functions have often been used interchangeably to describe ‘to the body’ force-motion relationship at the human-seat interface, namely the driving-point mechanical impedance (DPMI) and the apparent mass (APMS) [1,8].

The term ‘mechanical impedance’ is often used as a generic term for all relations between the driving force of a system at a particular frequency and the resultant movement (acceleration, velocity or displacement) at that frequency. Force and acceleration are always in phase for a rigid mass and, at any frequency, the ratio of their root-mean-square (r.m.s) magnitudes indicates the mass of the object. In practice, at high frequencies the object will no longer be rigid and the force and acceleration will become out of phase in a manner depending on the stiffness and the damping at each frequency. The ratio of force to acceleration can still be calculated but it no longer equals the static mass of the object and, therefore, it is termed as ‘apparent mass’. The DPMI relates the driving force and resulting velocity response at the driving point, and is given by:

$$Z(j\omega) = \frac{F(j\omega)}{V(j\omega)} \quad (1.1)$$

Where $Z(j\omega)$ is the complex DPMI, and $F(j\omega)$ and $V(j\omega)$ are the driving force and response velocity at the driving point, respectively. ω is the angular frequency in rad/s and $j = \sqrt{-1}$ is the complex phasor.

The APMS relates the driving force and the resulting acceleration response, and is related to the DPMI by:

$$M(j\omega) = \frac{F(j\omega)}{a(j\omega)} = \frac{Z(j\omega)}{j\omega} \quad (1.2)$$

Where $M(j\omega)$ is the complex apparent mass and $a(j\omega)$ is the driving point acceleration.

The magnitude of DPMI can be obtained by multiplying the APMS by the angular frequency, thus tending to make the resonant peaks appear more apparent at high frequencies, than if they were represented in terms of APMS. From the definitions of DPMI and APMS, it is apparent that DPMI leads the APMS by 90 degrees.

The DPMI and APMS response functions are applied to study the force-motion relations for the vibration exposed seated occupant [1,8]. The quantity APMS has the advantage that it can be obtained directly from the signals provided by accelerometers and force transducers. Furthermore, Newton's second law of motion gives APMS a simple intuitive meaning: 'a force applied to a body accelerates the body by an amount proportional to the force, the constant of proportionality being the mass of the body.' When the human body is effectively rigid (e.g. at very low frequencies in the vertical axis) the apparent mass of the body is equal to its static mass and the force and acceleration are in phase. As the frequency of motion increases, the presence of one or more resonances and/or the visco-elastic properties of the biological system tend to alter the APMS response and introduce a phase difference between the force and the acceleration. At higher frequencies the upper body is only loosely coupled, the dynamic force is thus dominated by the masses near the driving point resulting in lower magnitude of the APMS.

The other biodynamic response function may be referred to as 'through the body' biodynamic function, termed as seat-to-head transmissibility (STHT). This function

describes the vibration transmission through the body, usually from the seat to the head, and expressed as:

$$H(j\omega) = \frac{a_H(j\omega)}{a(j\omega)} \quad (1.3)$$

Where $H(j\omega)$ is the complex seat-to-head transmissibility function and $a_H(j\omega)$ is the head response acceleration.

At low frequencies, the motion at the human-seat interface is transmitted directly to the head due to the effectively rigid mass behavior of the human body, leading to unity value of transmissibility magnitude and zero phase difference. A number of studies have investigated the STHT responses of the seated occupants under vertical vibration [13,14,18]. The reported data are intended to assess the comfort perception of the exposed human body, and to assess the spinal stresses caused by vibration. A few have attempted to measure the transmission of vibration to specific locations on the spine [9].

The characterization of vibration transmitted to the body segments poses considerable measurement challenges. The reported data thus exhibit extreme differences in the responses, even though they have been performed under comparable and controlled experimental conditions. Alternatively, the functions based upon ‘to-the-body’ measurement, namely DPMI and APMS, are conveniently used to characterize the human responses to vibration. The measurements of these functions require instrumentation at the driving-point surfaces and thus yield more repeatable data with relatively lower inter-subject variabilities.

ISO-5982 (2000) [10] characterizes the ranges of idealized values of biodynamic responses of seated human occupants on the basis of a synthesis of data acquired in different studies under comparable experimental conditions. The proposed ranges are

considered applicable for no back support posture and believed to correspond to relatively high magnitudes of vertical vibration. These ranges do not represent the conditions encountered in automotive seating, mostly due to lack of consideration of the back support.

During the exposure to WBV there are many physiological, psychophysical and physical factors which are relevant for the development of unwanted effects. These could be individual susceptibility, the body constitution and the posture, together with the frequency, direction, magnitude and duration of the vibration exposure. The amount of vibration energy absorbed and/or exchanged between the source and the body, has therefore been suggested as a better measure of the physical stress on the body since it takes into consideration of the interactions between the vibration structure and the body [11]. The instantaneous power P_{Tr} transmitted to the body, represents of the product of the driving-point force $F(t)$ and the velocity $V(t)$, such that:

$$P_{Tr} = F(t)V(t) \equiv P_{Abs}(t) + P_{El}(t) \quad (1.4)$$

Where P_{Abs} is the absorbed part of the power accounting for the energy necessary for keeping pace with the energy dissipated through the structural damping. The elastic power $P_{El}(t)$ is continuously delivered to and removed from the body during each period of excitation and averages to zero for each sinusoidal cycle of motion. Thus, the time-averaged absorbed power \bar{P}_{Abs} equals the transmitted power \bar{P}_{Tr} :

$$\bar{P}_{Abs} = \bar{P}_{Tr} = F(t)V(t) \quad (1.5)$$

The above equation may be modified to express the movement in terms of displacement or acceleration or to replace the force by a measure of the impedance. It is

therefore possible to determine the absorbed power by measuring the force and either the displacement, velocity or acceleration, Alternatively, if the impedance or the apparent mass is known, the absorbed power can be estimated by measuring only the movement. Although not yet thoroughly evaluated, absorbed energy may be a better quantity for risk assessment than the acceleration as specified in ISO-2631, since it takes into account the dynamic force applied to the human body [12].

The above four functions have been employed to characterize the human biodynamic response by performing measurements under a variety of test conditions. Based on the measured data, a number of mechanical-equivalent biodynamic models have also been proposed in the literature for the purpose of estimating the magnitudes of the forces transmitted to particular subsystems within the body, (e.g. the spine) and/or establishing potential damage mechanisms, and assessing the tolerance to vibration under the exposure to intensive vibration levels.

1.3 Review of the published data on the whole-body biodynamic response

In this chapter, the published data on whole-body biodynamic response characteristics are reviewed together with the test conditions. Table 1.1 summarizes the goals and experimental conditions of various reported studies on DPML/APMS, STHT and Absorbed Power. In many of the earlier studies, such as those conducted by Coermann [15] and Miwa [21], the number of subjects included was usually small and there were few considerations of the many factors, such as the seating postures, the subject characteristics, and vibration excitations. In some studies the feet of the subjects were either not supported or supported but not vibrated [21,28]. The majority of the studies have employed limited number of male subjects, while input vibration has been limited to 20 Hz.

Table 1.1: Summary of experimental conditions employed in different studies.

Authors	Subject			Excitation			Reported Functions
	Number and sex	Body mass (kg)	Posture	Type	Level	Frequency Range(Hz)	
Guignard (1959)[13]	10 males	Not stated	Ejection seat with no backrest contact. Two postures: 'slack and attentive'	Sine	1g peak	8-60 Discrete frequencies	STHT
Guignard and Irving (1960)[14]	10 males	5 'large' and 5 'small'	Normal sitting posture with no backrest	Sine	2.5g	2-13.5	STHT
Coermann (1960)[15]	8 males	70-99	Standing, sitting with feet not supported, no backrest	Sine	0.1, 0.2 and 0.3g	1-20	DPMI and STHT
Schmitz and Simons (1960)[16]	18 males	Not stated	Relaxed sitting posture with contoured wooden backrest	Sine	0.15, 0.18, 0.3 and 0.35g	2.5 and 3.5	STHT
Edwards and Lange (1964)[17]	2 males	77 and 84	Supine; Lateral; Standing	Sine	0.2-0.5g	1-20	DPMI
Dennis (1965)[18]	6 males	Not stated	Comfortable sitting posture on a foam padded tank seat with foam padded backrest	Sine	0.5 and 1.0g	5-37	STHT
Vogt et al. (1968)[19]	10 males	79(mean)	Erect sitting, loosely restrained, feet supported, but not vibrated	Sine	0.5g with increased gravity of 1, 2 and 3 g	2-15	Mean DPMI and phase, mean STHT magnitude
Suggs et al. (1969)[20]	11 males	58-90	Sitting upright with hands in lap, feet supported, no backrest	Sine	0.10g peak to peak	1.75-10	Mean DPMI and phase
Miwa (1974)[21]	5 males	50-76	Standing; kneeling; sitting erect and relaxed, feet not vibrated	Sine	0.1g r.m.s	3-200	Mean DPMI and phase
Griffin (1975)[22]	12 males	60-88	For maximum and minimum head vibration, no backrest	Sine	0.2-0.4m s ⁻² r.m.s	7-75	Mean STHT

Table 1.1: Summary of experimental conditions employed in different studies. (continued)

Rowlands (1977)[23]	6 males	Not stated	Various: slumped, normal, erect "back-off" with hard-flat backrest	Sine sweep	2,2.8 and 4 ms^{-2}	2-25	Mean STHT
Cohen et al. (1977)[24]	6 males	55-82	Comfortable neutral sitting posture Tractor non-cushioned seat no backrest	Sine	0.69 ms^{-2} r.m.s	2.5-5	Mean STHT
Bennet et al. (1978)[25]	12 males	Not stated	Upright and semi-reclined posture with soft cushion backrest	Random	0.21,0.28 and 0.35g r.m.s	0-5	Mean STHT
Griffin et al. (1978)[26]	56 males 28 females 28 children	Not stated	Sitting, increasing height of footrest, no backrest	Sine	1 ms^{-2} r.m.s	4 and 16	Mean STHT
Griffin et al. (1979)[27]	18 males 18 females	Not stated	Various:comfortable,upright, relaxed, stiff,Increasing height of footrest, no backrest	Sine	1 ms^{-2} r.m.s	1-100	Mean STHT
Mertens (1978)[28]	6 males 3 females	57-90	Upright sitting with feet not supported	Sine	0.4g r.m.s with increased gravity of 1,2, 3 and 4g	2-20	Mean DPMT STHT
Moseley et al. (1981)[29]	12 males	Not stated	Comfortable normal sitting,one hard and one soft backrest	Sine sweep	1.5 ms^{-2} r.m.s	0-65	Mean STHT
Furness (1981)[30]	6 males	62-78	"Back-on" and harnesssed with hard flat inclined backwards at 13°	Sine sweep	1.0 ms^{-2} r.m.s	0-40	Mean STHT
Rao (1982)[31]	8 males	Not stated	Car seat belt used in one condition use backrest in some conditions	Sine	0.64, 1.32and 2 ms^{-2} r.m.s	2.5-30	Mean STHT
Sandover (1982)[32]	6 (sex not stated)	52.7-87.2	Erect with various conditions of feet and arms	Random	1.2 and 2.3 ms^{-2} r.m.s	1-25	Individual APMS

Table 1.1: Summary of experimental conditions employed in different studies. (continued)

Donati and Bonthoux (1983)[33]	15 males	49-74	Erect, feet supported, hands on steering wheels	Sine and Broadband random	1.6 ms^{-2}	1-10	Mean DPMI
Fairley and Griffin (1983)[34]	1 male	63	Sitting, no backrest, feet supported /not supported, soft/hard seat	Vertical gaussian random	1 ms^{-2} r.m.s	0.25-20	APMS magnitude
Fairley and Griffin (1986)[35]	8 males	57-85	Normal posture, feet supported and vibrated	Random	1 ms^{-2} r.m.s	0.25-20	Individual APMS
Hagena et al. (1986)[36]	9 males 2 females	Not stated	Erect sitting posture no backrest	Sine	0.2g	3-40	Mean STHT
Hinz and Seidel (1987)[37]	4 males	56-83	Moderately erect sitting no backrest	Sine	1.5 and 3.0 ms^{-2} r.m.s	2-12	Mean DPMI and STHT
Paddan and Griffin (1988)[38]	12 males	58-81	Two postures: sitting with backrest and without backrest	Random	1.75 ms^{-2} r.m.s	25	Mean STHT
Fairley and Griffin (1989)[39]	24 males 24 females 12 children	Not stated	Upright, no backrest, footrest Vibrating, hands in lap	Random	1 ms^{-2} r.m.s	20	Individual APMS
Fairley and Griffin (1989)[39]	8 males	57-85	4 seated postures: Normal, upright erect, upright tense upright back supported; Feet supported o footrest moving with platform	Random	0.25, 0.5, 1.0, 2.0 ms^{-2} r.m.s	20	Mean APMS magnitude
Paddan (1991)[40]	31	Not stated	“back-on” comfortable upright	Random	1.0 ms^{-2} r.m.s	0-16	Mean STHT
ISO-5982 (1993)[65]	39	51-94	Vaguely defined 10 persons had feet supported by footrest moving with seat, various restraint system	Sine	$1-2\text{ ms}^{-2}$ r.m.s	0.5-31.5	Mean DPMI and STHT

Table 1.1: Summary of experimental conditions employed in different studies. (continued)

Smith (1993)[41]	3 males 2 females	64-86	Sitting upright with back support and constraint	Sine and random	1 and 2 ms^{-2} r.m.s	3-21	Mean DPMI
Holmlund et al (1993)[42]	15 males 15 females	57-92 54-93	Relaxed and erect upper body	Sine	0.5,0.7,1.0,1.4 ms^{-2} r.m.s	2-100	Mean DPMI
Seidel (1996)[43]	37 males	49-103	Hard seat without backrest feet supported and vibrated	Random	0.7,1.0 and 4 ms^{-2} r.m.s	0-20	Mean DPMI
Boileau and Rakheja (1998)[44]	7 males	54-80.9	Erect sitting with back support erect sitting without back support	Sine and random	1,1.5 and 2.0 ms^{-2} r.m.s	0-10Hz	Mean DPMI and phase
R.Lundstron And Holmlund (1998)[45]	15 males 15 females	54-93	Relaxed and erect upperbody posture	Sine	0.25-1.4 ms^{-2}	1.13-80	Absorption power
Kubo et al. (1999)[46]	5 males	Not stated	Comfortable sitting posture with a inclined backrest	Sine	Not stated	2.5,8,11, 14,17,20	Physical and physiological reactions
Mansfield and Griffin (1999) [57]	12 males	Not stated	Comfortable upright posture, without backrest	Random	Six level: 0.25- 2.5 ms^{-2} r.m.s	0.2-20	Individual absorbed power
Cho and Yoon (2001)[47]	5 males 5 females	48-77	Comfortable posture without Backrest or with backrest inclined Backward 21°	Random	1.0 ms^{-2} r.m.s	1-25	Mean STHT
Mansfield and Griffin (2001)[48]	12	74.5 (Mean)	9 sitting postures	Random	0.2,1.0,2.0 ms^{-2} r.m.s	1-20	Individual APMS and STHT
Nawayseh and Griffin (2004) [67]	12 males	63-103	4 sitting postures	Sine	0.125,0.25,0.625, 1.25 ms^{-2} r.m.s	0.25-10	APMS
Nawayseh and Griffin (2004) [68]	12 males	62-106	4 sitting postures	Sine	0.125,0.25,0.625, 1.25 ms^{-2} r.m.s	0.25-20	APMS

The sitting postures in automotive seats are known to be considerably different from those employed in the reported studies. These differences mostly arise from inclined pan or cushion, inclined backrest, relatively low seat height and occupants making full use of the back support. Most of the reported studies have been performed with subjects seated with either no back support or limited back support with a vertical backrest, while hands resting in the lap. Moreover, all of the studies only focus on a single driving point of vibration entering the body, with the exception of a single recent study that attempts the measurement of dynamic force imparted on a vertical backrest [67].

The seated occupants exposed to WBV are simultaneously exposed to local vibration of the head (e.g. from a head-rest), the hands (e.g. on a steering wheel) and the feet (e.g. on the floor). Apart from this, considerable vibration may excite the body when seated with back support on an inclined backrest. There exist multiple points of entry, depending on the sitting posture, the feet position, the hands on steering wheel, and the back support. The characterization of the human response to vibration thus requires the consideration of multiple driving points, which is a formidable task when added complexities of the biological system are considered.

Among the different points of vibration entry, the seat pan and the backrest represent the most significant due to more comprehensive contacts with both surfaces. The reported studies including the ISO-5982 ignore the body interactions with the backrest. The presence of a backrest vibrating vertically along with the seat tends to increase the magnitude of vibration transmitted to the head [1]. Also, the changes in body posture when leaning against a backrest may alter the vibration modes of the body and thus the vibration transmissibility and human perception of vibration. The effects of

vertical vibration can be further complicated by the resonance of the backrest structure. If the seat is significantly inclined backwards there may, again, be increased transmission in the region of body resonance. The backrest in the car seat contributes to decrease the muscle tensions and helps maintain a controlled sitting posture in driving.

Although many studies have been conducted to study human perception of vibration and biodynamic response under vertical vibration, only a few have explored the contributions due to the hands posture. The majority of the experiments have been performed with subjects' hands in the lap, which does not characterize the sitting posture of a driver. It is obvious that most of the reported data could only be valid for no-back support posture and hands in lap. A recent study on the biodynamic response of seated occupants in an automotive posture has clearly emphasized the significance of hands position [70].

Moreover, most of the reported studies have presented the mean values of a biodynamic response measures derived from data acquired with subjects of considerably different body masses. While the influence of the body mass on the biodynamic response has not been clearly identified [43,69,70], the ensuing mechanical models and the test dummies are derived to characterize the mean biodynamic response, which is perhaps most representative of subjects with body mass in the vicinity of mean mass of the test subject population considered in a study [1]. For automotive seating applications, the knowledge of the body mass dependence of the biodynamic response is perhaps important due to the strong dependency of the energy restoring and the dissipative properties of polyurethane foam cushions upon the seated body mass [49].

From the review of the reported studies, it is evident that although all these studies have significantly contributed to the understanding of the human biodynamic response, while very limited results could be considered applicable to the automotive seating. Most of the reported studies have been performed with subjects seated with either no back support or limited back support with a vertical backrest, and no study has attempted to measure the biodynamic response characteristics of seated subjects at an inclined backrest.

1.3.1 Factors affecting biodynamic response functions

The reported studies have shown that many subject, seat, and vibration related factors affect the biodynamic responses. These include the individual anthropometric parameters, seat geometry, sitting posture and nature of vibration (magnitude and frequency) [22,39,45]. Table 1.2 summarizes some of the factors that have been considered in a number of studies. The effects of these factors are discussed in the following subsections.

Table 1.2: Factors influencing the biodynamic response characteristics.

Subject-related	Seat-related	Vibration-related
Body mass, height, build and gender	Seat height, seat geometry, hands and feet position	Vibration type (sine, random), magnitude (r.m.s, peak magnitude), frequency range

1.3.2 Influence of the seated posture on APMS and DPMI magnitude

Occupants of different vehicles may assume a variety of postures. For example, the car drivers usually sit with an inclined backrest while the drivers of industrial trucks usually sit with an upright back posture. The posture has been shown to have a insignificant influence on the biodynamic response characteristics [1,38,48,68]. The reported data sets obtained through measurements at the seat pan alone are discussed in terms of both functions in this section in order to demonstrate the different trends arising from the two functions, which may affect the analysis.

Miwa [21] measured the DPMI response of the seated subjects corresponding to kneeling, sitting and standing postures. In the experiments, the subjects sat on a vertical vibrator with feet hanging freely. Based on the mean values the responses attained with five subjects, it was observed that the DPMI magnitude without a footrest was larger than that with a footrest over the entire frequency range, from 3-200Hz.

The influence of sitting erect and relaxed postures has been demonstrated by Seidel [43], who analyzed data acquired with a group of 37 subjects. The subjects sat on a hard seat without backrest, with feet supported and vibrated on a footrest. The two postures were defined as relaxed posture, and erect posture with a straight back and the arms crossed in front of the chest. The mean DPMI magnitudes corresponding to two mass groups (60-70kg and 70-80kg) and two different postures are shown in Figure 1.1. For both postures, DPMI response exhibits peaks near 5Hz, 7Hz and 13Hz. The relaxed posture, however yields significantly lower magnitude of DPMI than the erect posture at frequencies above 4Hz. The first resonant frequency established from DPMI data occurred at a higher frequency with the erect posture than that with the relaxed posture.

When the data sets are converted to APMS, the shift of the first resonance frequency is observed more clearly, as shown in Figure 1.2. With a relaxed posture, the resonant frequency, as seen from the APMS data, is around 3.7Hz and with an erect posture the resonant frequency is near 5Hz. It can be postulated that the erect posture with high muscle tension increases the stiffness of the human body, and thus the resonant frequency.

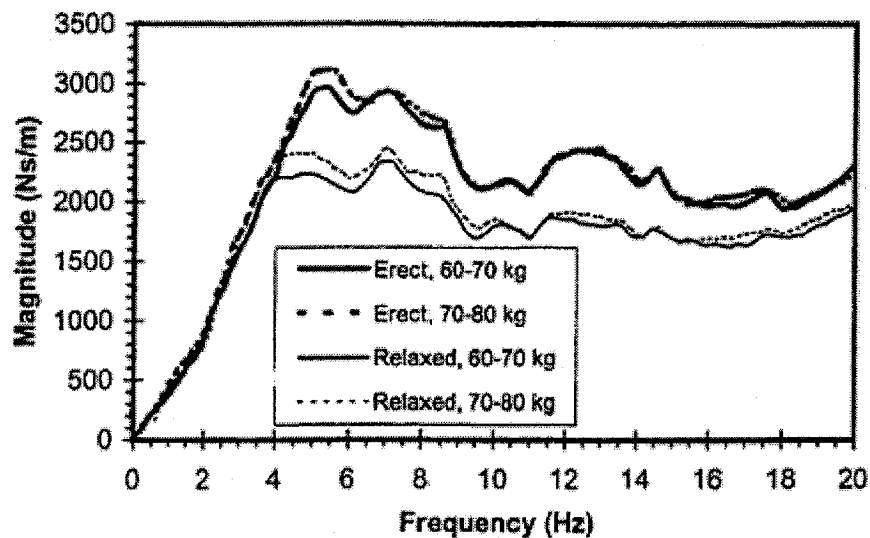


Figure1.1: Effect of sitting posture and body mass on the mean DPMI magnitude [43].

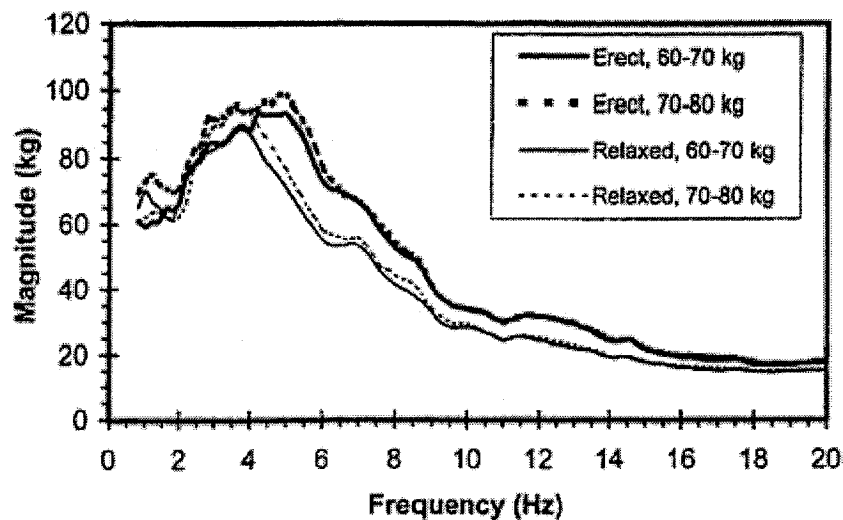


Figure 1.2: Effects of sitting posture and body mass on the equivalent APMS magnitude derived from the reported DPMI data [43].

The influence of a backrest and variations in its inclination angle has been investigated by Boileau and Rakheja [44], involving a total 7 male subjects. In this study, the subjects were asked to maintain their hands in the lap with their feet resting flat on a vibration simulator platform. The evaluation was performed for three sitting postures: 1) sitting erect with back unsupported, referred to as the 'erect back not supported' (ENS) posture; 2) sitting erect with most of the back in contact with the backrest, also referred to as 'erect back supported' (EBS) posture; 3) sitting in a slouched (SLO) posture, the upper body having a more pronounced inclination towards the front than with the ENS posture, while the lower back is in contact with the backrest. Although the majority of the measurements were performed with a seat backrest angle of 0° , a few experiments were also conducted with a back inclined at 14° with respect to the vertical axis. The mean DPMI magnitude and phase responses, illustrated in Figure 1.3, reveal significant influence of the sitting posture. An ENS posture yields higher DPMI magnitude at frequencies above 4 Hz and a higher resonant frequency than those observed for the EBS posture. The SLO posture yields a slightly higher resonant frequency and higher DPMI magnitude than those observed for the EBS posture. It can be therefore generally concluded that the DPMI and APMS magnitudes appear to be higher for back not supported posture than for the back supported posture.

Although the influences of various factors on the DPMI and APMS response have been extensively studied, only a few studies have reported their influence on the seat to head vibration transmissibility of the seated subjects [27,37,38,48]. Griffin et al. [27] investigated the STHT of a single subject assuming eight different postures ranging from 'slouched' to 'erect', and five head positions ranging from looking 50° down to looking

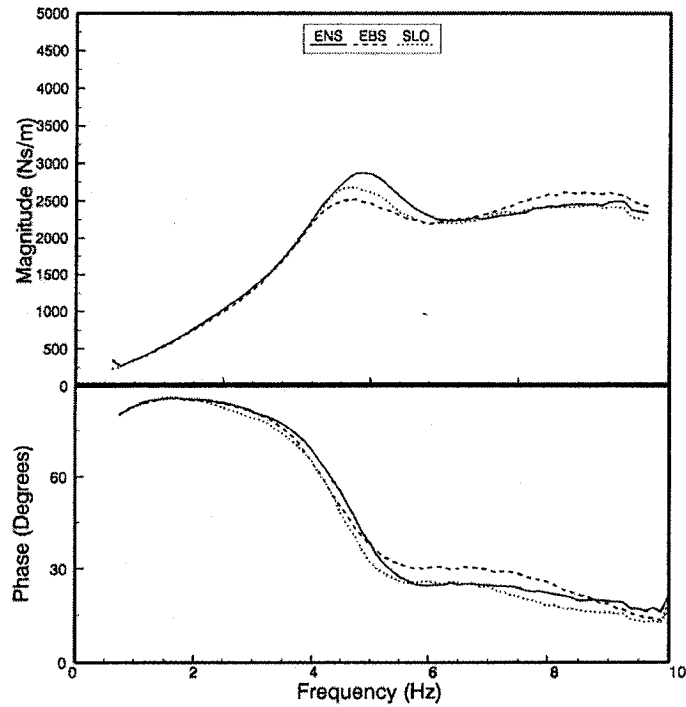


Figure1.3: Effect of sitting posture on the DPMI magnitude and phase response under sine sweep excitations ($1.0\text{-}2.0\text{ ms}^{-2}$)[44].

50° up under sinusoidal excitations of 1.0 ms^{-2} r.m.s in the 0-50Hz frequency range. The erect posture resulted in an increase in the STHT magnitude at all frequencies above 3Hz, and approximately 4 to 1 increase in the range of 15-25Hz for individuals. The slouched posture, however, resulted in STHT magnitude well below unity at frequencies above 3Hz. In the same study, the mean transmissibility determined for 18 male subjects, revealed that a stiff posture resulted in increased STHT magnitude at frequencies above 6Hz, and lower STHT magnitude at frequencies below 6Hz, when compared to those obtained for a relaxed posture. It has been reported that increased muscle tension results in higher STHT from 5 to 10Hz. Paddan and Griffin [38] investigated the influence of leaning against a rigid backrest when evaluating the STHT through experiments involving 12 subjects. The mean STHT response characteristics of 12 subjects with and

without backrest support are illustrated in Figure 1.4. The results clearly show that the contact with a backrest yields significant increase in the transmission of vertical vibration at frequencies above 4.5Hz and below 6.2Hz. It is probable that some of the increase is associated with the different orientation of the head and the neck, and with the vibration transmission from the backrest.

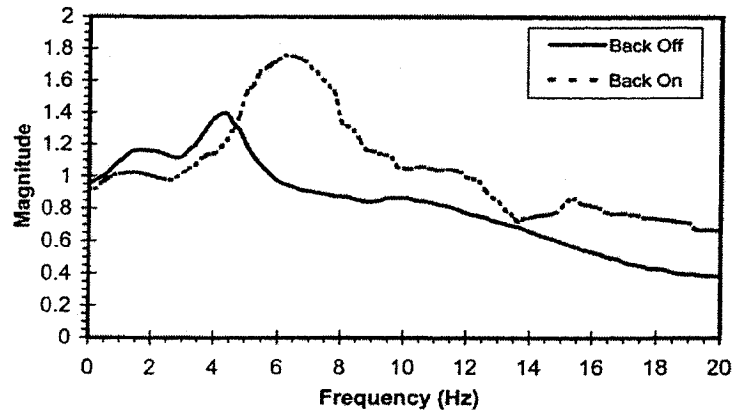


Figure1.4: Effect of contact with a rigid flat backrest on the mean STHT response of 12 subjects [38].

A footrest may further affect the STHT, since it influences the sitting posture, the muscle tension, and the area of contact between the vibrating surface and the body. The STHT measurements performed by Griffin et al. [27] revealed that presence of a footrest (normal height) or its absence (legs hanging free) do not considerably influence the STHT.

Mansfield and Griffin [48] reported a study on the effects of variations in the sitting posture on the apparent mass and seat to pelvis pitch transmissibility. Each of the 12 subjects was exposed to vertical random vibration in the 1 to 20 Hz frequency ranges, while assuming nine different sitting postures. Figure 1.5 shows a schematic representation of the nine postures considered. Figures 1.6 and 1.7 show the median and

inter-quartile ranges of the normalized apparent masses and the transmissibilities for 12 subjects using nine different sitting postures at 1.0 m/s^2 r.m.s. It was observed that peaks in the apparent masses occurred near 5 and 10Hz and in the seat to pelvis pitch transmissibilities were near 12Hz. There was most variability in apparent mass over the 4-15 Hz frequency range and all conditions show more pelvis rotation in the frequency range from 10 to 18 Hz than at lower frequencies. There were only small changes in the apparent mass or transmissibility with posture, although peaks were lower for the apparent mass in the 'kyphotic' posture and were lower for the transmissibility in the 'belt' posture.

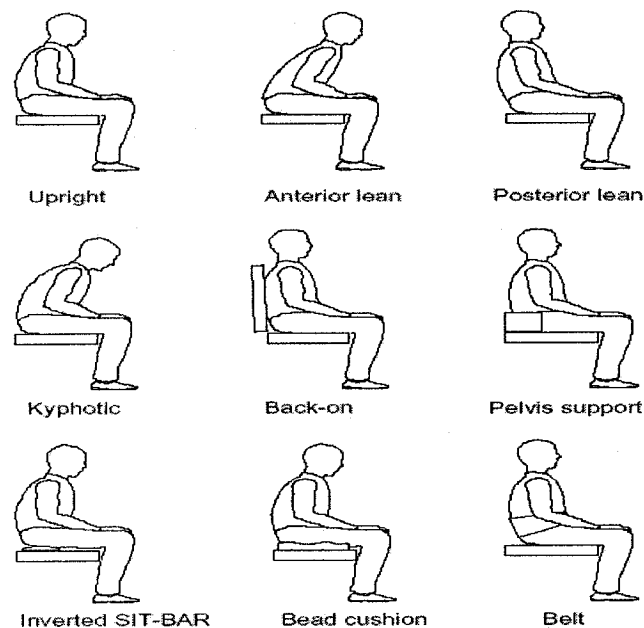


Figure 1.5: Diagrammatic representation of the nine postures [48].

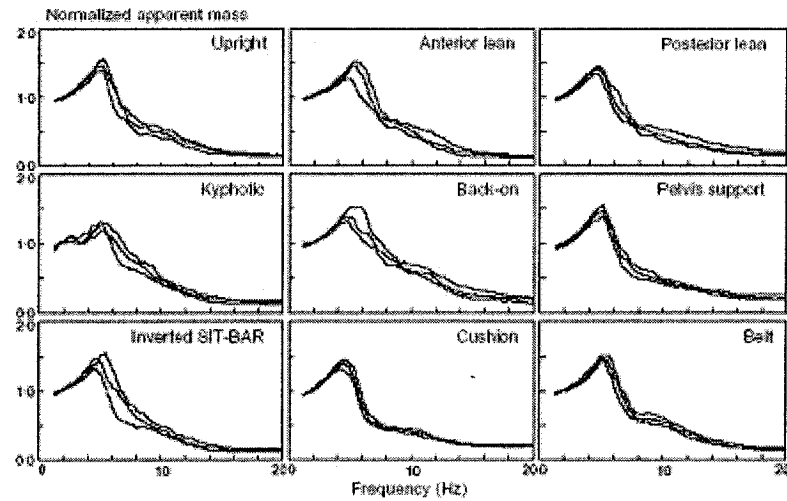


Figure 1.6: Inter-quartile ranges for normalized apparent masses for 12 subjects using nine postures at 1.0 m/s^2 r.m.s [48].

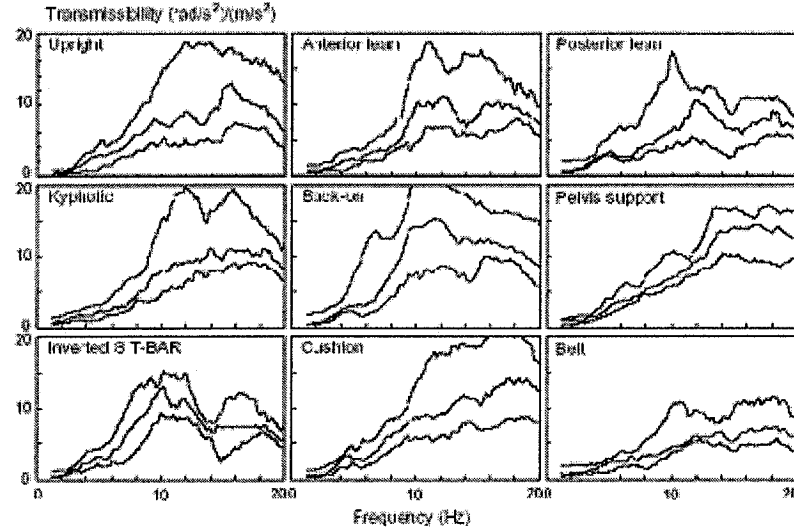


Figure 1.7: Inter-quartile ranges for seat vertical to pelvis rotation transmissibility for 12 subjects using nine postures at 1.0 m/s^2 r.m.s [48].

All of the above studies have considered sitting on a flat and rigid back with back not supported or supported against a vertical backrest, and hands in the lap or crossed against the chest. The effects of inclined pan, inclined backrest and hands position on APMS responses have been presented in a recent study by Wang et al. [68]. The measurements were performed for a total of 36 different sitting postural configurations realized through variations in hands position, three seat heights (510, 460 and 410mm),

and seat design factors involving two different pan orientations (0° and 7.5°). The six different seat dependent postures are shown in Figure 1.8: (1) seated on an inclined seat pan and back supported by the inclined backrest (BIP); (2) inclined pan with back supported by a vertical backrest (BVP); (3) a flat pan with back supported by a vertical backrest (BVF); (4) a flat pan with back supported by an inclined backrest (BIF); (5) inclined pan with back not supported (NVP); and (6) a flat pan with back not supported (NVF). Figure 1.9 illustrates a comparison of the mean APMS magnitude response of 27 subjects measured on seats with three different heights considered in the study. For a given posture, the effect of seat height on the primary resonant frequency is observed to be minimal. The peak APMS magnitude is strongly affected by the hands position and seat height, a lower seat height generally yields lower magnitude response in majority of the frequency range.

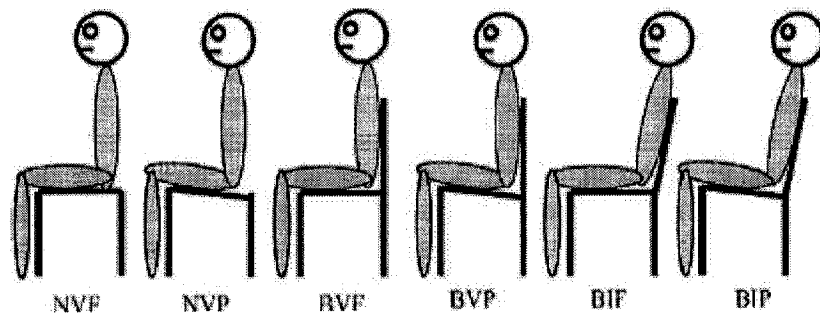


Figure 1.8: Schematic representations of different sitting postures [68].

The measured data acquired for 0° and 7.5° inclinations were analyzed to study the influence of seat pan angle on the biodynamic response. The results show negligible effect of the seat pan variations considered in this reported study. Figure 1.10 shows a comparison of mean magnitude responses of 27 subjects obtained for six different postures involving a flat pan. The mean magnitude responses attained for no back support

(NVF), and supported against a vertical (BVF) and an inclined backrest (BIF) are compared for two different hands positions in Fig. 1.10(a). The effect of hands position on the mean magnitude response for each back support condition is further shown in Fig. 1.10(b). The results show that the hands position becomes relevant only for postures involving back support conditions. The APMS responses of the subjects seated without back support exhibit relatively sharp resonant response for both hands position, and the bandwidth of the peak response increases when the back is supported. This bandwidth increases further when the back is supported by an inclination backrest. Back supported on an inclined backrest coupled with hands on steering wheel yields a more pronounced secondary mode near 10 Hz. The effect of hands position on the magnitude response, however, is not evident at frequencies above 12 Hz.

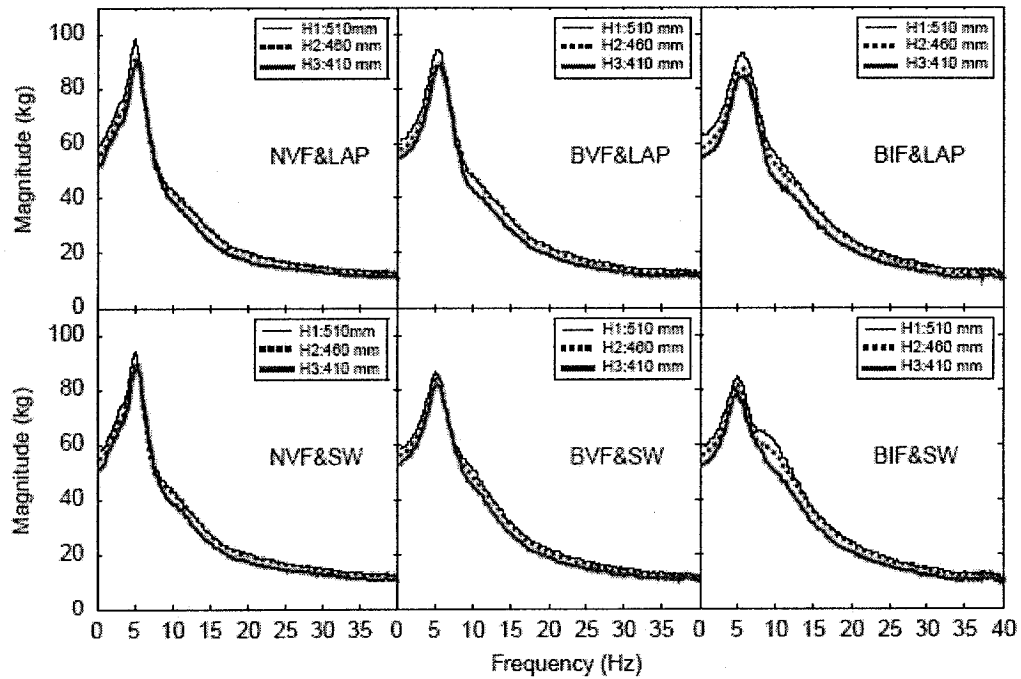


Figure 1.9: Effect of seat height on the mean APMS magnitude response of 27 subjects for different postures (excitation: $1.0m/s^2rms$) [68].

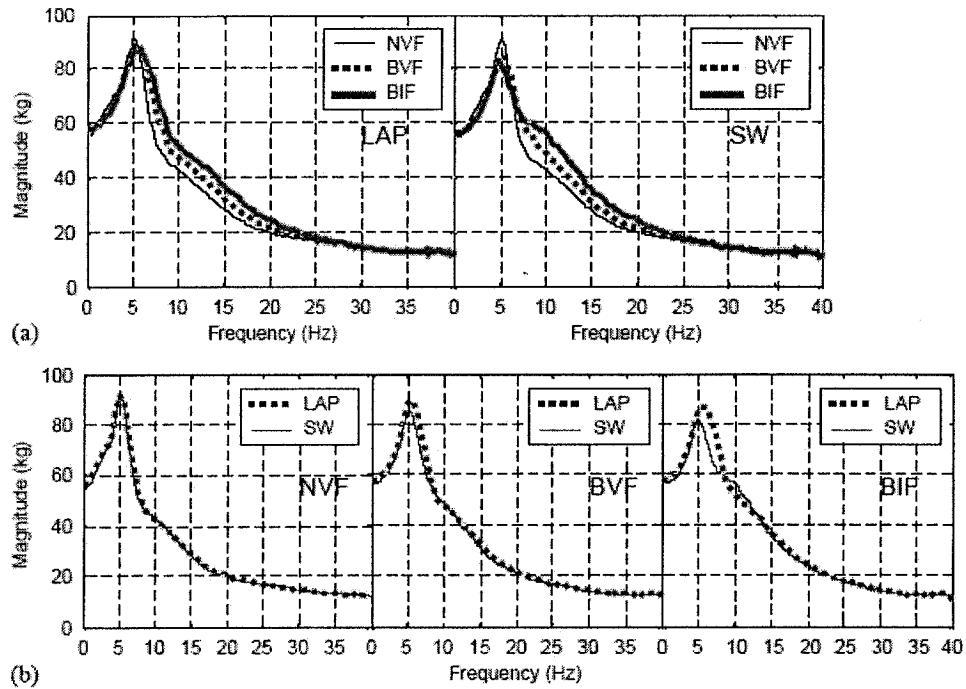


Figure 1.10: Influence of hands position and back support condition on the mean APMS magnitude response of 27 subjects: (a) hands position; and (b) back support condition [68].

1.3.3 Influence of subject mass and build

The DPMI, APMS and absorbed energy of seated body are strongly affected by the body weight. Fairley and Griffin [39] reported the APMS responses of 60 seated subjects including 24 males, 24 females and 12 children, which revealed large scatter in the data due to the large variations in the subject masses. The scatter in magnitude response at lower frequencies could be reduced considerably by normalizing the magnitude data with respect to the static seated mass of each subject. The DPMI characteristics, reported by Seidel [43] for a total of 37 male subjects assuming an erect sitting posture, was grouped into four sets based upon different ranges of subject mass, namely less than 60kg,

between 60-70kg, between 70-80kg, and higher than 80kg. This grouping method can also be found in the study by Rakheja et al. [69]. Figure 1.11 illustrates the DPMI magnitude response of subjects in different mass ranges. Figure 1.12 illustrates the same data sets converted into APMS, which clearly illustrates considerably larger differences in the peak APMS magnitudes for different mass groups. Wang et al. [68], investigated the correlation between the APMS magnitude and the body mass as a function of the excitation frequency. The results obtained from the regression analysis between the measured APMS magnitude at selected frequencies (3, 6 and 12 Hz) and the body mass, corresponding to specific sitting postures, suggest linear dependence of APMS magnitude on the body mass at selected frequencies, irrespective of the postural configuration considered.

Only a few studies have explored the influence of variation in the body mass and size on the STHT magnitude. A definite influence of such variations, however, could not be established due to the considerable variations in the measured STHT responses of individuals. For both male and female seated subjects, it has been reported that larger subjects tend to be relatively less sensitive to low frequency vibration (less than 6.3Hz) and more sensitive to high frequency vertical vibration [1]. In these investigations, the correlations with body size were determined for weight, height, hip size, thigh size, and upper and lower leg length.

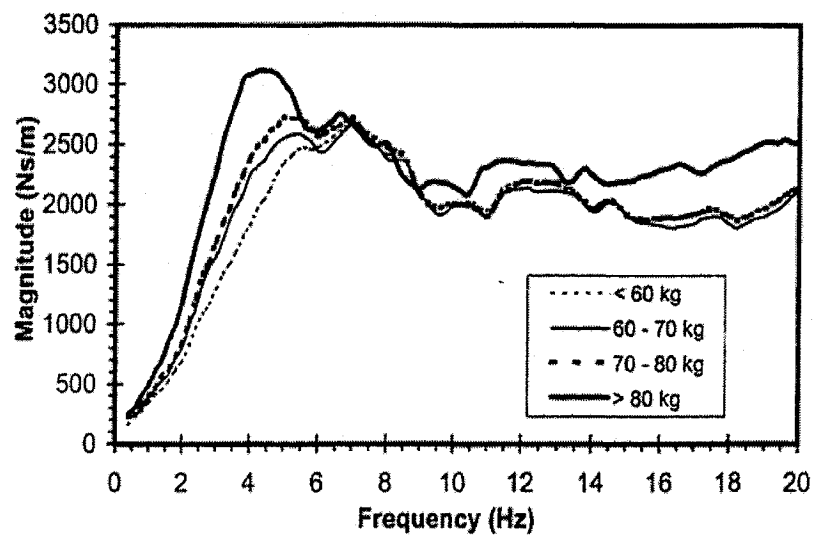


Figure 1.11: The effect of body mass on the DPMI magnitude [43].

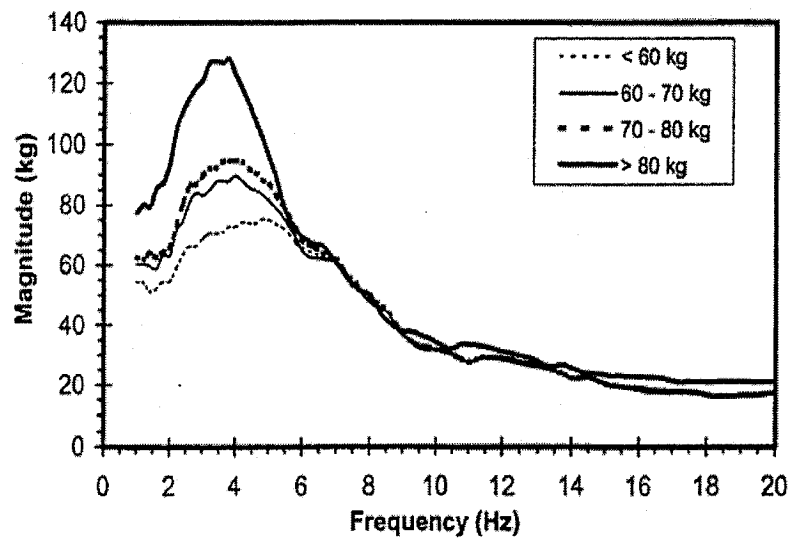


Figure 1.12: The effect of body mass on the APMS magnitude, derived from the reported DPMI data [43].

1.3.4 Influence of excitation magnitude and frequency

The biodynamic response characteristics of the seated human body under different types of whole body vibration have been investigated in several studies. Holmlund et al. [42] reported the DPMI magnitude responses for a group of 15 male subjects exposed to different vibration levels, with relaxed and erect sitting posture, as shown in Figure 1.13. It can be observed that both the peak impedance magnitude and the two resonant frequencies decrease with increasing vibration level. This may be attributed to the ‘softening’ of the human body under higher levels of vibration excitation. These observations are further supported by the studies performed by Seidel [43], Wu [8], Rakheja et al. [44] and Wang et al. [68]. Different studies, however, have reported considerably different quantitative variations in the DPMI or the APMS magnitudes with the varying magnitude of vibration excitation. The mean DPMI data acquired for four male subjects exposed to sinusoidal vibration (2-12Hz) of two different magnitudes (1.5 and 3.0 ms^{-2} r.m.s), as shown in Figure 1.14, has been reported by Hinz and Seidel [37]. Figure 1.15 illustrates the corresponding APMS magnitude data derived from the reported DPMI data. The dependency of the DPMI or the APMS magnitude on the magnitude of vibration excitation suggests nonlinear response behavior of the human body. The above studies may further suggest that the biodynamic response behavior becomes increasing nonlinear under higher levels of excitation.

The mean DPMI data reported by Boileau and Rakheja [44] for a total of 7 subjects maintaining an ENS posture exposed to three different levels of sinusoidal excitations is further examined to verify the above observation. Although the mean DPMI, shown in Figure 1.16, reveals a slight decrease in the primary resonant frequency, the peak

magnitude reduces by only 3.2%, from 2786 to 2699 Nsm^{-1} , when the excitation level increases from 1.0 to 2.0 ms^{-2} r.m.s. This observation also holds true for the data obtained under EBS postures. The study further showed that the sinusoidal and random vehicular vibration of comparable magnitudes yield similar DPMI responses.

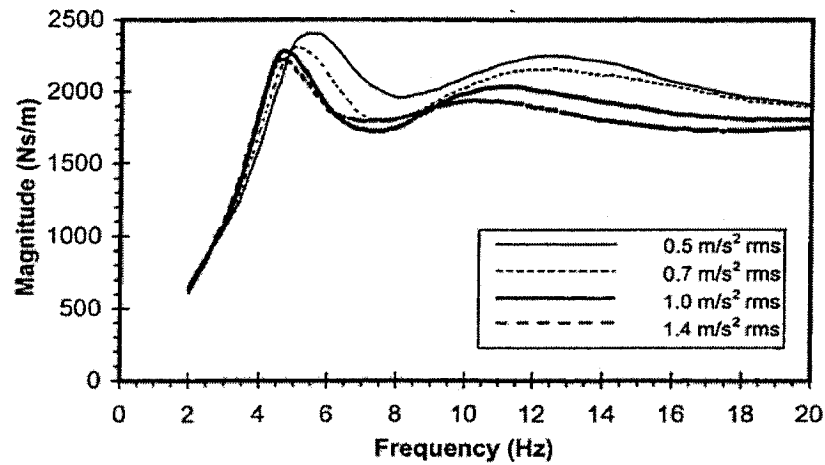


Figure 1.13: Effect of excitation magnitude on the mean DPMI response of 15 male subjects [42].

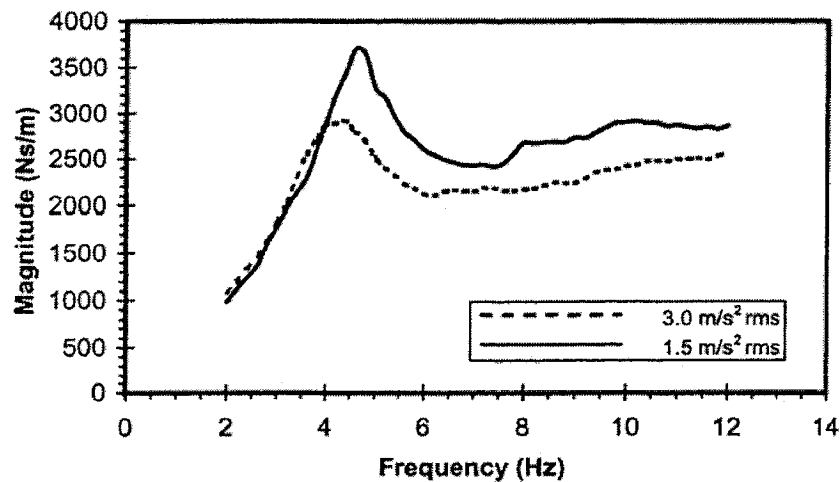


Figure 1.14: Effect of excitation level on the DPMI magnitude [37].

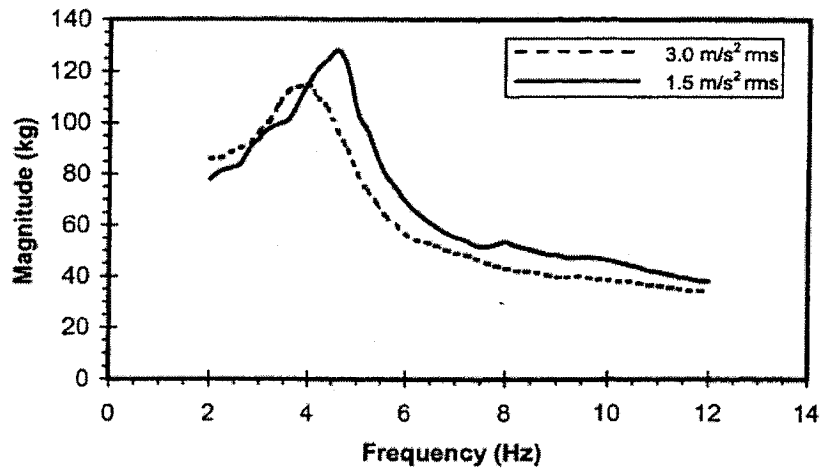


Figure 1.15: Effect of excitation level on the APMS magnitude derived from the reported DPMI data [37].

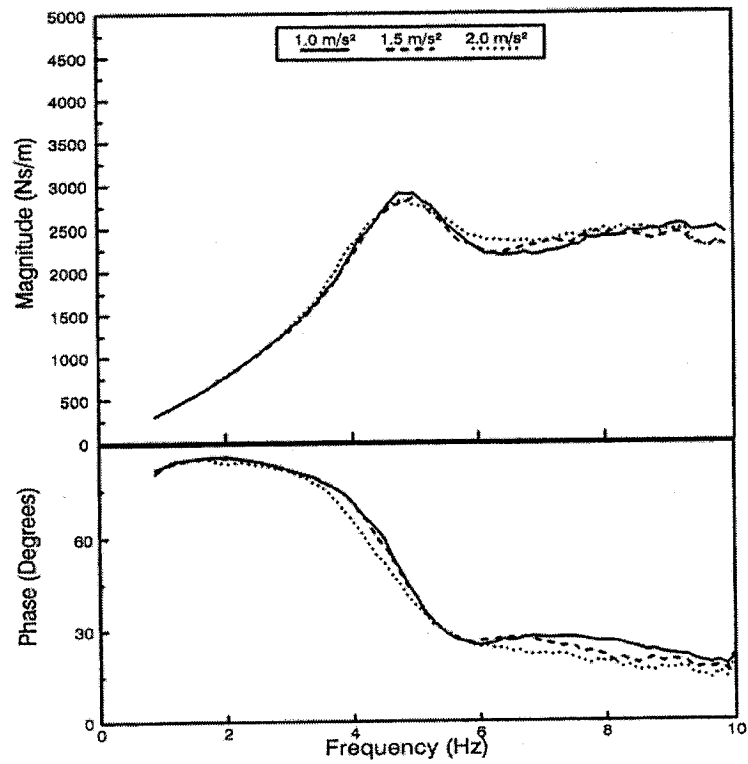


Figure 1.16: Effect of excitation level on the mean DPMI magnitude [44].

The influence of the excitation magnitude on the STHT, however, is small, when compared with the contributions due to inter-and intra-subject variations. Variations in the back support and head inclination are known to cause greater effects on STHT than that caused by variations in magnitude of the vibration [1].

Lundstrom and Holmlund [45] reported the absorbed power characteristics of 30 seated subjects exposed to vertical vibration. Opposed to the DPMI or the APMS response, the absorbed power was found to be strongly dependent upon the magnitude of acceleration due to vibration. The study further showed that the power absorbed by the body depends upon the body weight. Figure 1.17 illustrates the influence of different acceleration levels on the magnitude of absorbed power. The power absorbed by under exposure to vertical whole body vibration at six different magnitudes of random vibration (0.25, 0.5, 1.0, 1.5, 2.0, 2.5 ms^{-2} r.m.s) has been measured using 12 male subjects by Mansfield and Griffin [57]. The results showed the largest absorbed power at about 5Hz, and the frequency of the peak value reduced with increasing vibration magnitude. The total absorbed power increased approximately in proportion to the square of the acceleration magnitude.

The possible influence of type of vibration excitation on the DPMI magnitude has been investigated by Boileau [51]. The study used 3 types of excitation signals, including swept sinusoidal, broad-band random excitation in the 1.0 to 2.0 ms^{-2} r.m.s range, and different random excitations defined for off-road vehicles. The DPMI data were averaged over various vibration excitation levels for different postures. It was concluded that the DPMI magnitude vary only slightly for all the excitation signals and the seated postures considered in the study. It was thus suggested that the DPMI characteristics determined

under sinusoidal or broad-band random vibration of similar magnitudes can be conveniently applied for off-road vehicle vibration applications.

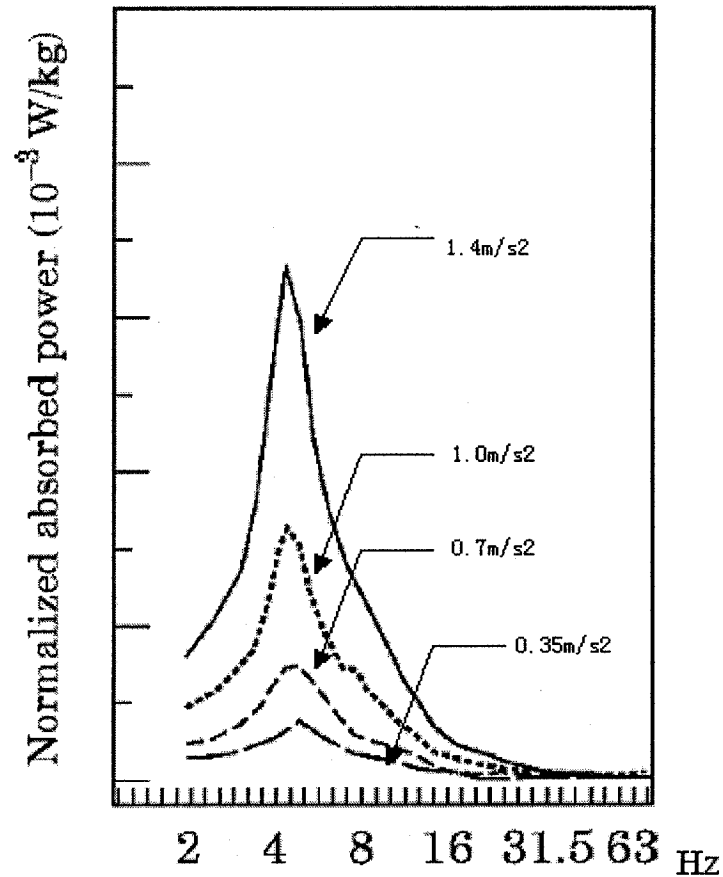


Figure 1.17: Effect of excitation level on the absorbed power normalized by average sitting weight [45].

1.3.5 Influence of gender

A few studies have specifically investigated the influence of gender on the biodynamic response of the seated human body exposed to vertical vibration. Fairley and Griffin [39] reported insignificant gender effect on the biodynamic response based upon measurements performed with 24 males, 24 females and 12 children. Another study performed with 12 males and 12 females also reported insignificant gender effect on the basis of energy absorption of the seated occupants [42]. A study of inter-subject

variability reported by Griffin and Whitham [1] found a non-significant trend for seated females to be relatively more sensitive to 16Hz than the widely known 4Hz vertical vibration as compared with seated males. Since the above studies are performed under postures and excitation levels that are not representative of the automotive environment, it is necessary to acquire the data under a representative automotive environment to study the influence of gender on the biodynamic response characteristics of the seated human occupants. Wang et al. [68] investigated the influence of gender on the APMS magnitude response through the analysis of selected data attained for a total of 10 subjects, including 5 male and 5 female. The results showed the presence of a more clear second resonance in the frequency range above 15 Hz, and higher APMS magnitude response at higher frequencies for the female subjects. An further analysis of covariance on the gender dependency in this study also revealed that gender effect could be observed only in the frequency range above 15 Hz.

The findings of all of the above-mentioned studies on DPMI and APMS are based upon measurements performed on the single driving – point, while the interactions between the upper body and the backrest are neglected. A recent study has attempted to measure the dynamic force response at the backrest, while seated against a vertical backrest and exposed to vertical vibration [67]. The study measured the forces in the fore-and-aft direction at the backrest for 12 male subjects in four sitting postures and exposed to different four vibration magnitudes. Figure 1.18 illustrates the reported backrest APMS magnitude response of all the subjects for four different postures. The results revealed minimal magnitudes of dynamic response at the backrest due to contact against the vertical backrest.

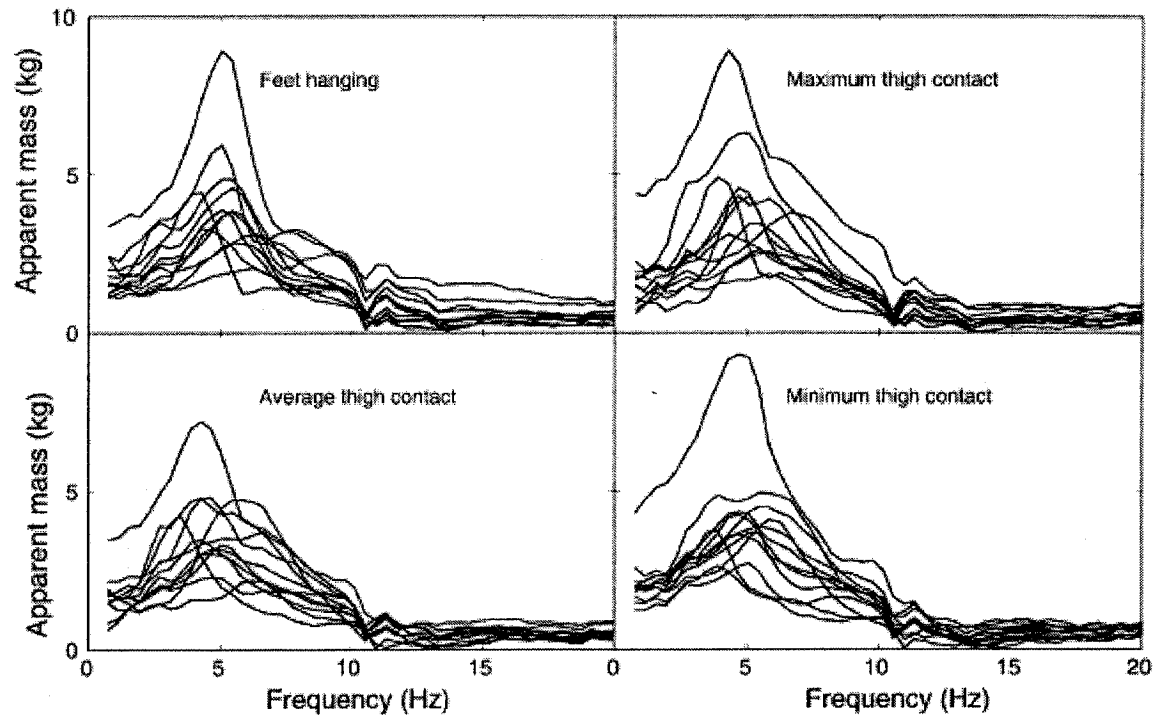


Figure 1.18: Inter-subject variability in the backrest apparent mass measured at the back [67].

1.4 Biodynamic models of seated occupants

‘Biodynamics’ concerns with the physical, biological and mechanical properties or responses of the body, its tissues and organs, either with reference to the induced forces or motion, or in relation to the body’s own mechanical activity. Biodynamic models of the seated occupant exposed to vibration are formulated to describe biodynamic measurements, represent the body modes, to predict the effects of motion on human health, comfort or performance, and to study the vibration behavior of the coupled seat-occupant system. The last aspect is vital for the design of seats and requires formulation of mechanical-equivalent models of the human body. Biodynamic models of seated occupants exposed to vertical vibration have been attempted on the basis of measured responses at the seat pan. Models of varying complexities have been proposed to achieve

certain similarity with the human behavior under vertical vibration [55]. However the complexity of a model structure and its similarity with the human body, does not necessary imply that the model is correct for simulation of the mechanical behavior of the human body subjected to vibration. The only way of justifying the model correctness is to demonstrated reasonably good similarity between the dynamic response of the model and the behavior of the human body.

Majority of the models proposed in the literature are lumped-parameter models, where the mechanical properties of the biodynamic system are represented by one or more lumped masses, and energy restoring and dissipative elements. The model parameters are usually identified from the measured biodynamic response data using either curve-fitting or optimization based system identification techniques. While most of the studies have applied the DPMI or APMS magnitude and phase data for parameter identification [47,56,60], a few studies have used additional STHT magnitude and phase data to enhance the uniqueness of solutions of the minimization problem [8,70].

A number of lumped parameter models ranging from simple single-degree-of-freedom (SDOF) to several DOF have been proposed to characterize the biodynamic behavior of the seated body under vertical vibration. These include SDOF models proposed by Coermann [15] and Fairley and Griffin [39]; 2-DOF models proposed by Suggs et al. [20] and Allen [52]; 3-DOF linear and non-linear models proposed by Rakheja et al. [70] and Demic [53]; 4-DOF models proposed by Payne and Band [54], and Boileau [51]. A few of these models have also been included in the International Standard, ISO 5982 [10]. Figures 1.19 to 1.22 illustrate the schematics of the reported single, two-, three- and four- DOF models, respectively. The parameters of the reported biodynamic human body models above are summarized in Table 1.3. The model

parameters are mostly identified from either the measured driving-point mechanical impedance or the vibration transmissibility characteristics (e.g. magnitude and phase transmissibility of the seat to head motion) of selected human subjects. Some models' parameters have been derived from both the DPMI/APMS and the SHTT magnitude and phase data [8,51,70].

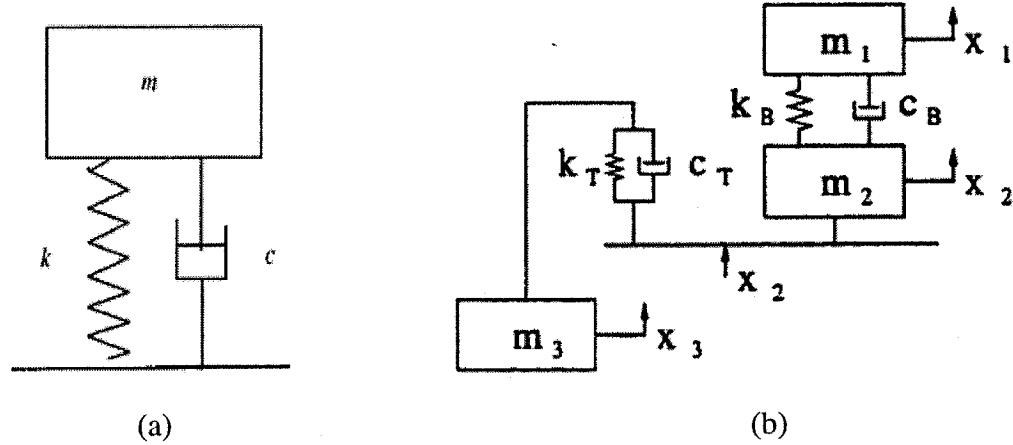


Figure 1.19: Single-degree-of-freedom mechanical models of the seated occupant exposed to vertical vibration: (a) model proposed by Coermann [15]; (b) model proposed by Fairly and Griffin [39] (SDOF when dynamics due to leg mass m_3 is ignored).

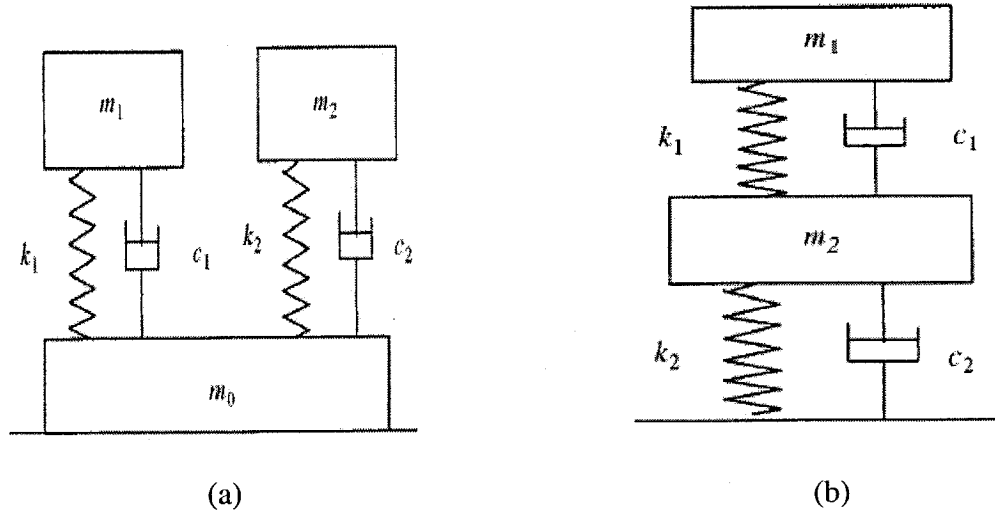
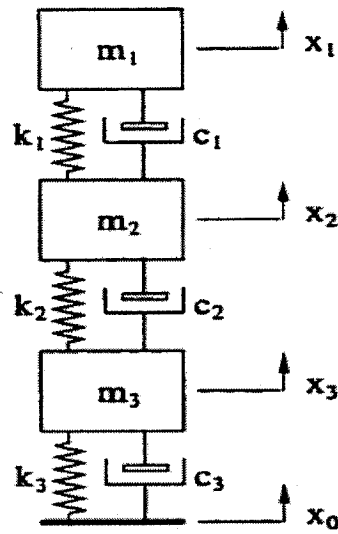
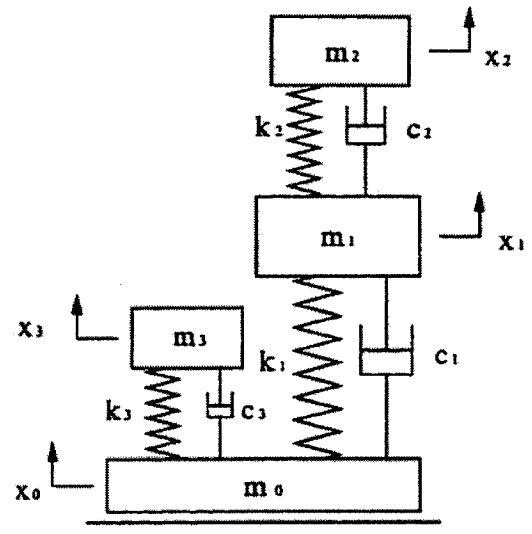


Figure 1.20: Two-DOF mechanical equivalent models of the seated occupant exposed to vertical vibration: (a) model proposed by Suggs [20]; and (b) model proposed by Allen [52].

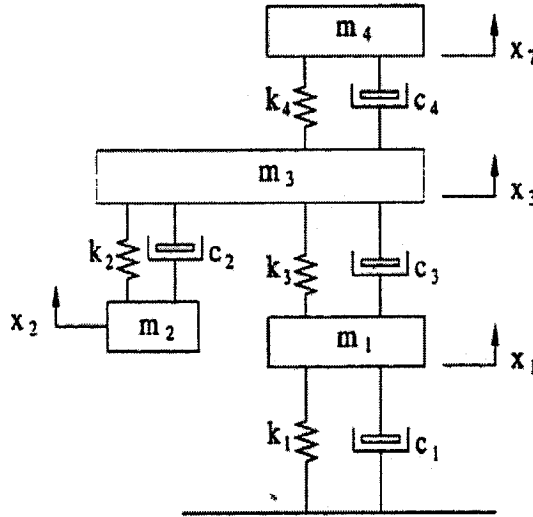


(a)

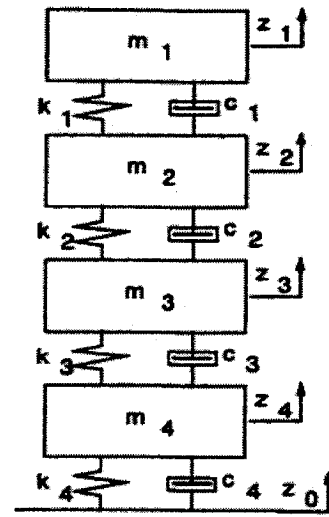


(b)

Figure 1.21: Three-DOF mechanical equivalent models of the seated occupant exposed to vertical vibration:(a) model proposed by Demic [53]; and (b) model proposed by Rakheja et al. [70].



(a)



(b)

Figure 1.22: Four-DOF biodynamic models of the seated occupant exposed to vertical vibration:(a) model proposed by Payne and band [54]; and (b) model proposed by Boileau [51].

Table 1.3: The parameters of the reported model.

Model	Model Parameters
Coermann (1962) [15]	$m=83.7 \text{ kg}$, $k=131181 \text{ N/m}$, $\xi=0.57$, $f_n=6.3\text{Hz}$
Fairley and Griffin(1989) [39]	$m_1=45.6 \text{ kg}$, $m_2=36.4\text{kg}$, $\xi_B=0.475$, $c_B=1360\text{Ns/m}$, $f_{nB}=5\text{Hz}$, $k_T=0$, $\xi_T=0$
Suggs (1969) [20]	$m_0=5.7\text{kg}$, $m_1=36.4\text{kg}$, $m_2=18.6\text{kg}$, $k_1=25968\text{N/m}$, $k_2=41549\text{N/m}$, $c_1=485\text{Ns/m}$, $c_2=884\text{Ns/m}$
Allen (1978) [52]	$m_1=50\text{kg}$, $m_2=5\text{kg}$, $\xi_1=0.3$, $\xi_2=0.05$, $f_{n1}=5\text{Hz}$, $f_{n2}=17\text{Hz}$
Demic (1987) [53]	$m_1=42\text{kg}$, $m_2=23\text{kg}$, $m_3=5\text{kg}$, $k_1=10000\text{N/m}^3$, $k_2=5000\text{N/m}^3$, $k_3=10000\text{N/m}^3$, $c_1=c_2=2\text{Ns}^3/\text{m}^3$, $c_3=10\text{Ns}^3/\text{m}^3$
Payne and Band (1971) [54]	$m_1=29\text{kg}$, $m_2=6.8\text{kg}$, $m_3=21.8\text{kg}$, $m_4=5.45\text{kg}$, $k_2=2838\text{N/m}$, $k_4=204820\text{N/m}$, $\xi_1=0.25$, $\xi_2=0.5$, $\xi_3=0.1$, $\xi_4=0.15$
Boileau (1995) [51]	$m_1=5.31\text{kg}$, $m_2=28.49\text{kg}$, $m_3=8.62\text{kg}$, $m_4=12.78\text{kg}$, $k_1=310\text{kN/m}$, $k_2=183\text{kN/m}$, $k_3=162.8\text{kN/m}$, $k_4=90\text{kN/m}$, $c_1=400\text{Ns/m}$, $c_2=4750\text{Ns/m}$, $c_3=4585\text{Ns/m}$, $c_4=2064\text{Ns/m}$
Rakheja et al. (2002) [70]	Hands-in-lap model: $m_0=2\text{kg}$, $m_1=10.3\text{kg}$, $m_2=16.5\text{kg}$, $m_3=25\text{kg}$, $k_1=126.6\text{kN/m}$, $k_2=600.3\text{kN/m}$, $k_3=61.3\text{kN/m}$, $c_1=2122\text{Ns/m}$, $c_2=899\text{Ns/m}$, $c_3=594\text{Ns/m}$, Hands-on-steering wheel model: $m_0=2\text{kg}$, $m_1=12.9\text{kg}$, $m_2=14.1\text{kg}$, $m_3=23.9\text{kg}$, $k_1=136.4\text{kN/m}$, $k_2=750.4\text{kN/m}$, $k_3=46\text{kN/m}$, $c_1=1933\text{Ns/m}$, $c_2=674\text{Ns/m}$, $c_3=742\text{Ns/m}$

* f_n :undamped natural frequency, ξ : damping ratio.

Boileau [51] proposed a 4-DOF linear biodynamic model, shown in Figure 1.22, based upon measured and synthesized values of DPMI and STHT magnitude and phase data. The baseline model is established for erect back not supported posture, while the model components correspond to the various body segments. The fundamental resonant frequency of the model was obtained as 5.5Hz, compared to 4.875Hz derived from the target values. The peak model response was observed to be quite close to the corresponding target value, while an error of approximately 1.2%. The DPMI phase response of the model correlated well with the target value at frequencies up to 6 Hz, while the phase error increased at higher frequencies. The STHT response derived from the model revealed a resonant peak of 1.77 at 4.8Hz, while the corresponding target value

was 1.45 at 5Hz. A relatively good agreement was also observed for the STHT phase response at frequencies below 6 Hz.

A 3-DOF model, shown in Figure 1.21 was proposed by Rakheja et al. [70]. The baseline model was derived to satisfy both the mean APMS and the STHT responses proposed in ISO-5982 [10] applicable for mean body mass of 71.2 kg. The model structure was further used to characterize the APMS responses of occupants with body mass within four different mass groups and exposed to vertical vibration. The model results showed reasonably good agreement with the measured data, particularly at frequency below 10Hz, for the hands in lap and hands on steering wheel postures.

Majority of the above models can provide useful approximate input-output relationships, under the experiment conditions considered, which cannot be considered applicable for automotive seating. Vehicle driving usually involves different postures (leaning against a backrest, sitting erect or sitting with a slouched posture), hands in contact with a steering wheel, and feet supported either on the floor or on pedals, while the vibration excitation is random in nature. All of the above-mentioned models have been derived on the basis of the biodynamic response data acquired for subjects seated without a back support. The 3-DOF model proposed by Rakheja et al. [70] forms an exception, which is derived on the basis of data acquired with a back supported posture. The model parameters, however, are identified on the basis of APMS magnitude and phase data alone.

The development of an effective biodynamic or biomechanical model poses considerable complexities in identifying the model structures and properties of the biological system. The tuning and validation of the model further require the

measurements of motions/forces developed by different model/body components, which is a formidable measurement task. Although a mechanistic model has been proposed to characterize the force motion behavior more accurately, the essential experimental data needed to derive or validate the model is not widely available. Figure 1.23 shows a mechanistic model proposed by Yasunao and Griffin [56]. Modeling of the dynamic responses of the seated body has been sufficiently justified by the desire to identify potential injury mechanism, and to reduce the adverse effects of vibration or mechanical shock on human health through development of appropriate interventions. A vibration model to predict the relations between the psychological and physiological reactions of humans exposed to vibration has been proposed by Kubo et al. [46]. In this study, 5 male subjects were exposed to external vertical vibration at various frequencies, the relationship between the physical reaction and the resulting psychological and physiological reactions was expressed in terms of multiple regression functions. However, the prediction of the forces and movements in the body provides only a small step towards the prediction of effects of vibration on health, considering that the injury-mechanism is highly complex and time-dependent.

1.5 Scope and objectives of the dissertation research

From the review of the reported studies discussed in the above sections, it is apparent that the passenger and driver comfort in an automobile, among many other factors, is strongly dependent upon the intensity of low frequency whole-body vibration. Although the vibration related comfort performance of automobiles strongly relies upon many design factors, such as the suspension, chassis, interior and panel design, the

automotive seats further contribute to enhancement of the vibration comfort [61]. It is thus highly desirable to design seats, which can further attenuate the whole-body vehicular vibrations, specifically in the vicinity of the primary human body resonant frequency. The designing of automotive seats and assessments of their vibration comfort performance are mostly based upon repetitive field or laboratory tests, often based upon subjective feedbacks. The development of an effective biodynamic model could permit the preliminary design and analyses of seats through computer simulations.

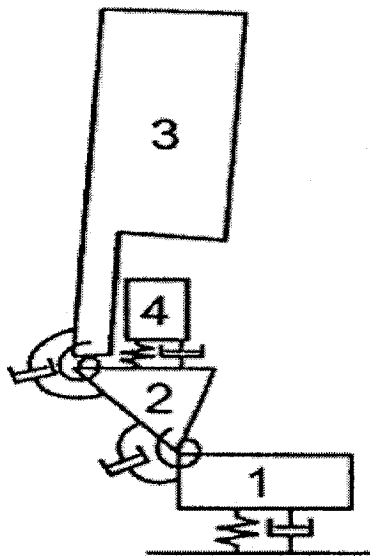


Figure 1.23: Lamped parameter models of seated human body proposed by Yasunao and Griffin [56].

The reported biodynamic models, however, are not applicable for automotive applications. Furthermore, the reported biodynamic models are based upon the force-motion relationship at the seat-pan alone, while the sitting posture is limited to unsupported back only. No attempts have been made to characterize the force-motion

relationship at the upper body and backrest interface, when the backrest is inclined as in the case of automobile seats.

The primary objective of this dissertation research is thus formulated to develop a human biodynamic model, which could be effectively characterize the biodynamic response behavior at both the seat pan and the backrest of the seated occupants in the automotive vibration environment. The specific objectives of the research are formulated as follows: (i) Derive the apparent mass response characteristics of the seated occupants at the seat pan and the backrest; (ii) Analyze the measured APMS data to establish the influences of various test variables and contributing factors, and identify most significant factors that affect the APMS response; (iii) Propose the target curves, which are considered to represent the biodynamic behavior of occupants under automotive types of postures and vertical vibration excitations; and (iv) Develop body mass dependent biodynamic models of seated occupants on the basis of the identified target curves.

1.6 Thesis organization

This dissertation is organized into five chapters describing the systematic developments in realizing the above objectives. The literature is reviewed in the first chapter highlighting the research contributions. The first chapter also presents the results of a complete review of published data on whole-body biodynamic response and some human body models. Chapter 2 presents the illustration of the test methodology. The influence of various factors on the measured APMS response is investigated in Chapter 3, to propose the target data for the model development. Chapter 4 presents the work of model development. A seated human body model is proposed based on the measured

biodynamic response data at both seat pan and backrest, obtained simultaneously under a predefined set of test conditions. Finally, the highlights of the dissertation research, conclusions and the recommendations for future studies are presented in Chapter 5.

Chapter 2

Measurement of the Biodynamic Response to Whole-body Vertical Vibration

2.1 Introduction

The vibration-related comfort characteristics of the automotive seats are frequently assessed through subjective and objective ride performance tests [55]. While subjective evaluations yield considerable data on the relative ride ranking, they do not provide quantitative information to the designer. Furthermore, the subjective evaluations are, in general, considered to be complex and expensive, specifically when repetitive tests need to be performed with a large number of seats. The subjective evaluations, however, can be effectively used to obtain ride perception, when a relatively small numbers of prototype seats are involved. Alternatively, objective assessments of seats provide important quantitative information on the design. The objective assessments may be performed either in the field or in the laboratory under representative postures and excitations [1,32]. The field evaluations tend to be more demanding on the financial and human resources, and may pose certain challenges in the interpretation of the results due to lack of repeatability and possible variations in the test conditions. While a relative assessment of vibration performance of the automotive seats can be effectively carried out in the laboratory by loading the seat with a rigid load or a dummy [49]. Such an approach, however, does not provide an assessment of the seat-human interactions. The assessment methods involving extensive use of human subjects, also pose many ethical concerns. It is thus desirable to derive effective occupant-seat models, which can be applied to assess the vibration performance of the coupled system and to serve as a design tool.

The identification of effective model of the seated occupant would also facilitate the development of a anthropodynamic manikin that could be conveniently employed in repetitive laboratory assessment tasks. The model formulation, however, must be based upon the human response data acquired under conditions representative of the automotive seating posture. These should include the representative posture involving full contact with an inclined back support, hands place either in the lap or on the steering wheel, and relatively low seated height. The human perception of vertical vibration or the biodynamic responses in an automotive posture should involve characterizations of the multiple driving-point behaviours, namely the seat pan buttocks and inclined backrest-upper body interfaces.

The experiment design and methods formulated to acquire the biodynamic response characteristics of occupants seated with automotive postures and exposed to vertical vibration, are described in this chapters. A rigid automotive seat structure is designed to represent the typical dimensions and geometry, and to provide representative automotive postures in consultations. The seat is instrumented to measure the biodynamic response characteristics of a large sample of male and female subjects under white-noise and track measured whole-body vibration, considered to represent the automobile vibration environment.

2.2 Test apparatus

For the purpose of biodynamic characterization of seated occupants exposed to vertical vibration, a test seat must be designed to provide sitting postures representative of the automobile driver/passenger postures. Moreover, the vibration exciter must be capable of reproducing the representative vibration environment in a safe manner for the

test occupants. The test fixture used in this study involves a whole-body vehicle vibration simulator (WBVS) capable of producing vertical vibration of deterministic as well as random nature. A steering column is installed on the WBVS to allow for experiments under a driver sitting posture. The WBVS is also equipped with a force platform to measure the total dynamic force developed by the occupant and the seat. The WBVS comprises two vertical electro-hydraulic actuators with a number of safety control loops that limit the peak displacement, peak force and peak acceleration to preset levels.

A rigid seat is designed using hollow square-section steel bars to reduce its total weight. The steel tubes are welded to achieve the geometric configuration illustrated in Figure 2.1. The seat-pan is rigidly fixed on the truss structure, while the backrest is mounted through two load cells, which are installed to measure the total dynamic force exerted by the driver to the backrest. The seat was configured to realize geometry representative of automotive seats. The entire seat is installed on a flat rigid plate, which is installed on a whole-body vibration simulator platform through four identical load cells. The seat and the force platform are positioned to achieve the overall center of gravity of the seat-occupant system near the geometric center of the four load cells. Figure 2.2 illustrates a pictorial view of the seat installed on the simulator. The 450 mm x 450mm seat pan is installed at an angle of 13° with respect to horizontal, while the angle between the pan and the backrest is fixed at 101° . The backrest provides a support surface of 450 mm x 500 mm. The seat is installed to provide a seated height of 220 mm, measured from the base of the backrest to the platform. This height was selected to achieve both the driver and passenger sitting postures, characterized by the hands placed on a steering wheel and in the lap, respectively. The weight of the entire assembly

including the base plate, the seat structure and the two backrest load cells was measured as 36 kg.

The seat is instrumented to measure the total body force acting on the seat pan and the backrest using a total of six force sensors. Four 1.112 kN load cells are mounted under the base plate of the seat to measure the total body force under vertical vibration. The force exerted on the backrest is measured using two 0.44 kN load cells, installed between the backrest and the seat structure.

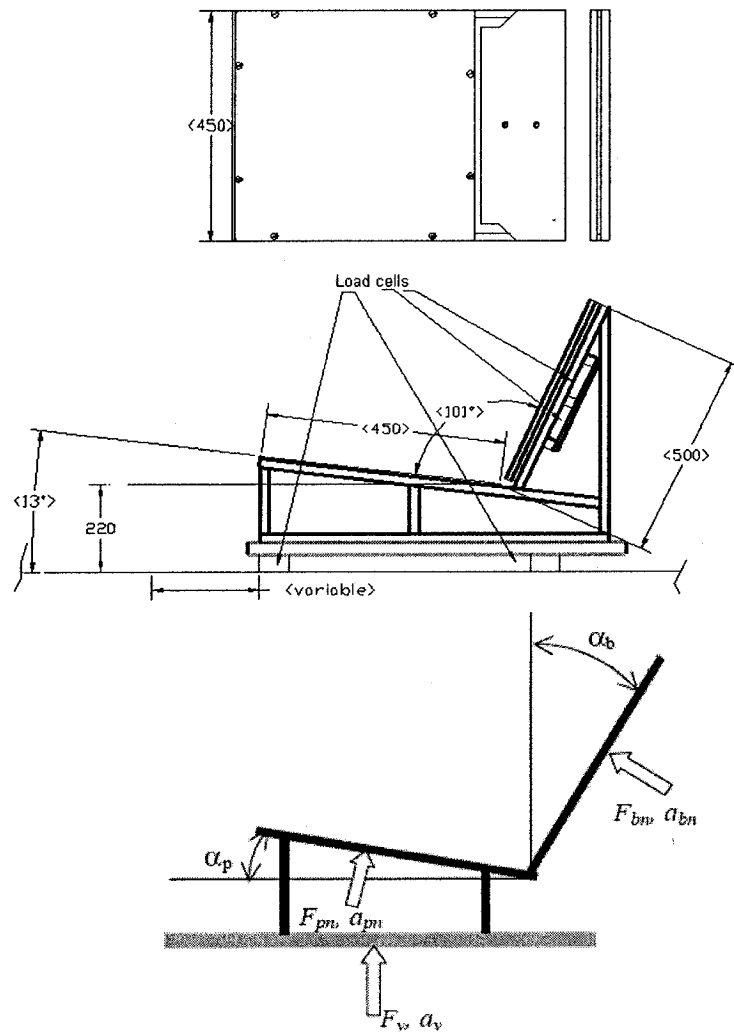


Figure 2.1: Top and side views of the rigid test seat.

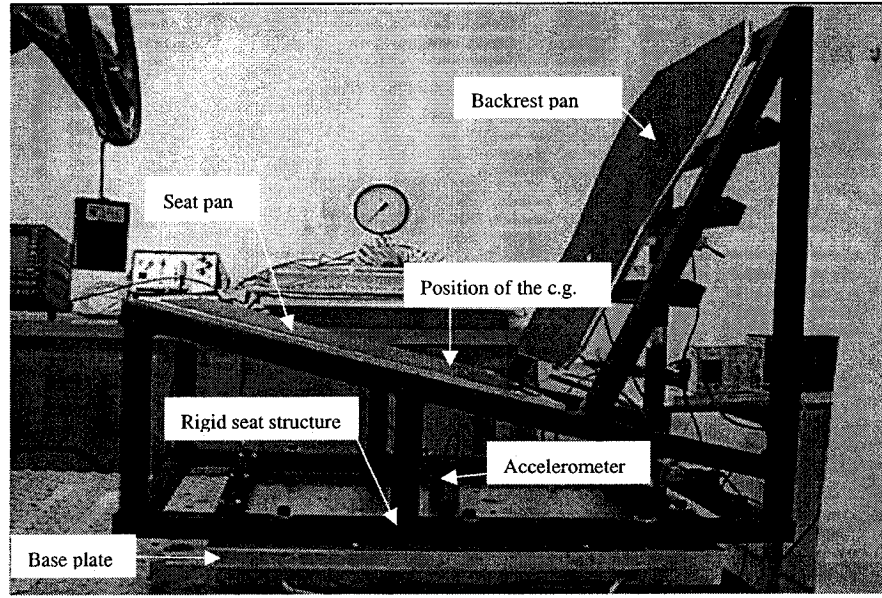


Figure 2.2: A pictorial view of the test seat mounted on the platform.

Figure 2.3 illustrates the location of the load cells supporting the seat. One accelerometer was installed on the seat base to measure the acceleration due to input vertical vibration. A second accelerometer was installed on the backrest along a direction normal to the backrest to measure the normal component of the acceleration due to backrest vibration. It should be noted that under vertical vibration of the rigid seat, the backrest acceleration is related to the vertical acceleration by the seat geometry:

$$a_{bn} = a_v \sin(\alpha) \quad \text{and} \quad a_{pn} = a_v \cos(\beta)$$

Where a_v is the magnitude of vertical acceleration measured at the seat base, a_{bn} and a_{pn} are the magnitudes of acceleration components normal to the inclined backrest and pan, respectively, as shown in Figure 2.1. Angles α and β are inclinations of the backrest and seat pan with respect to vertical and horizontal axes, respectively. The backrest inclination is 24° with respect to a vertical axis, while the seat pan is inclined at 13° with respect to the horizontal axis.

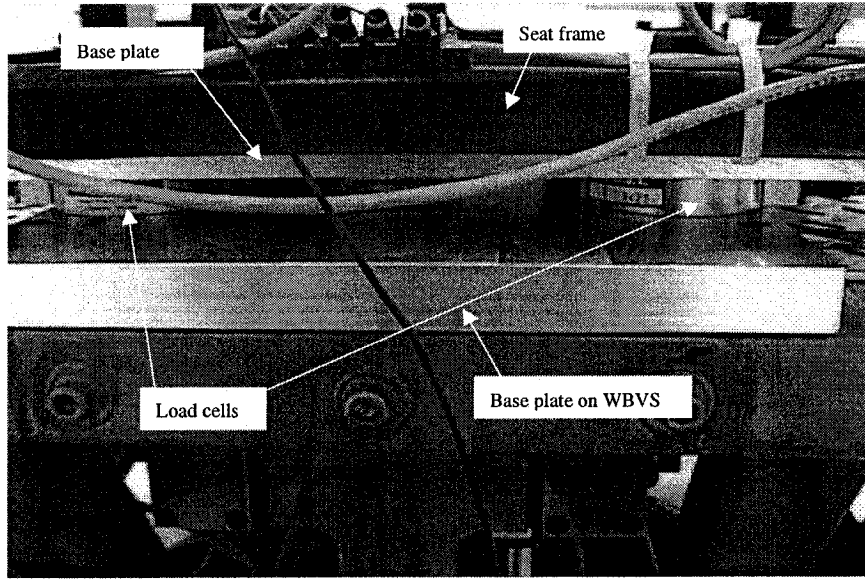


Figure 2.3: Location of the load cells within the force platform.

The vibration simulator is operated using the synthesized white-noise and track-measured vibration spectra in the 0.5 to 40 Hz frequency range. Three different levels of broad-band excitations, were synthesized to yield overall r.m.s acceleration values of 0.25, 0.5 and 1 m/s^2 , computed from:

$$\bar{a}_v = \sqrt{\frac{1}{T} \int_0^T a_v^2 dt} \quad (2.1)$$

Where \bar{a}_v is the overall r.m.s acceleration and T is the exposure duration.

In Addition to the broad band excitation, a track-measured vibration signal was synthesized to perform the experiments under typical automobile vibration. The WBVS was operated under a selected synthesized excitation, and the resulting acceleration response of the platform was acquired using a two-channel signal analyzer. The measured signals were analyzed to derive the rms and power spectral density (PSD) of the WBVS acceleration. Figures 2.4 and 2.5 illustrate the rms acceleration spectra due to white noise

excitation and PSD of the track-measured acceleration, respectively. An examination of the acceleration PSD due to the track-measured seat vibration reveals predominance of vibration in the vicinity of 1.2 Hz, 5 Hz, 9 Hz and 12 Hz, most likely attributed to bounce mode of the sprung mass, chassis and the unsprung masses, respectively. The results also show the absence of mechanical resonance of the platform in the 0-40 Hz frequency range, while the broad-band acceleration spectra show nearly flat magnitude in the frequency range of interest.

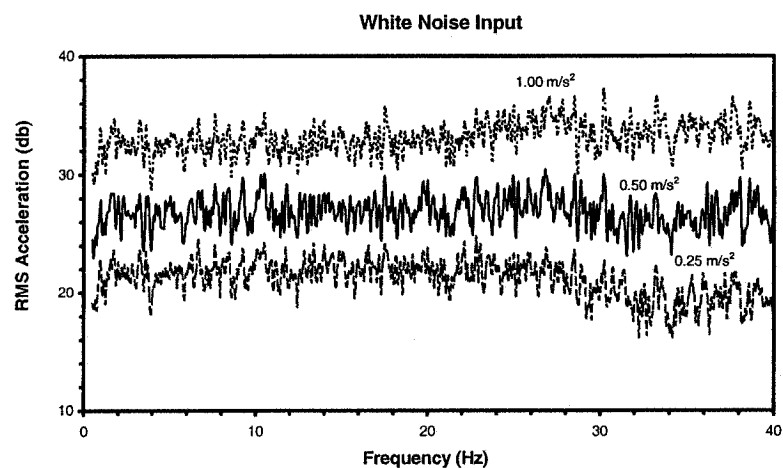


Figure 2.4: The rms spectra of the platform acceleration measured under white- noise excitations.

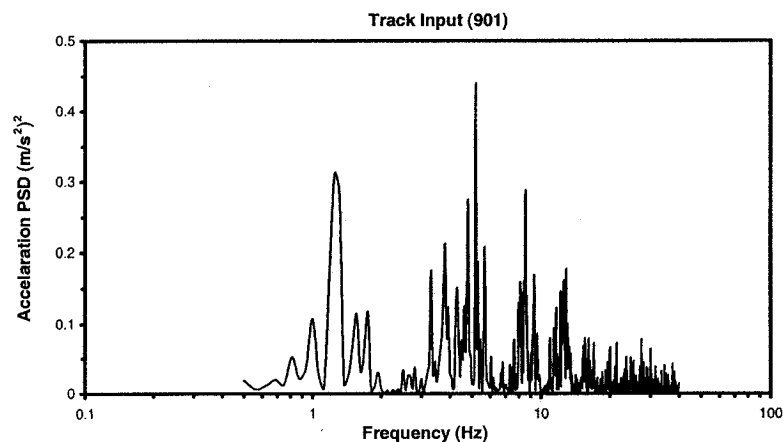


Figure 2.5: PSD of the platform acceleration measured under seat track-measured vibration.

2.3 Test methodology

Measurements are initially performed to measure the APMS response of the test seat alone, which will be used to perform the inertia cancellation of the measured biodynamic response. The seat without an occupant is thus subject to vertical vibration (white-noise and track measured), and the resulting acceleration and force signals are acquired using two two-channel B&K 2635 signal analyzers. Two different analyzers, both calibrated prior to the tests, are used to analyze the forces and accelerations acquired from the seat pan and the backrest. The apparent masses of both the seat and the backrest are derived and examined to identify the resonance of the seat, if any. The apparent mass of the total seat is computed from the measured force and acceleration in the following manner:

$$M_{s0}(j\omega) = \frac{F_s(j\omega)}{a_v(j\omega)} \quad (2.2)$$

$$M_{b0}(j\omega) = \frac{F_b(j\omega)}{a_{bn}(j\omega)} \quad (2.3)$$

Where $M_{s0}(j\omega)$ and $M_{b0}(j\omega)$ are the complex APMS of the total seat and backrest of the seat alone corresponding to the excitation frequency of ω . F_s and F_b are the forces measured at the seat base and the backrest, respectively. It should be noted that the force and acceleration at the backrest were measured along a direction normal to the backrest surface. The apparent mass measured at seat pan, however, is based on the vertical components of the seat force and the WBVS acceleration. The consideration of the normal components at the seat would also yield identical APMS response, such that:

$$M_{son}(j\omega) = \frac{F_{sn}(j\omega)}{a_{sn}(j\omega)} = \frac{F_s \cos \beta}{a_v \cos \beta} = M_{so}(j\omega) \quad (2.4)$$

The measured APMS response of seat and the backrest revealed constant magnitudes equal to the respective masses, and negligible phase between the forces and accelerations, in the 0.5 – 40 Hz range. These measurements further confirmed the absence of a structural resonance in the frequency range of interest.

A total of 24 adult subjects were employed for the study. After providing a brief description of the experimental procedures and obtaining the informed consent, each subject was asked to assume a posture with specified hands and feet position. The body weight supported by the seat pan and the backrest were recorded in the corresponding position from the static force signals displayed to the experimenter. The simulator was operated to produce the motion signals corresponding to a selected excitation and the resulting force and acceleration signals were acquired using the signal analyzer. An on-line signal analysis was performed to derive the two different APMS magnitude and phase responses of the coupled seat-subject system, as derived from the measured force and acceleration at the seat base and at the backrest, computed from the backrest force and the acceleration. The apparent mass responses of the seated subject alone were extracted by performing the necessary corrections for the inertial forces due to the seat assembly and the backrest. The complex APMS response of the seated occupant were thus derived from:

$$\begin{aligned} M_s(j\omega) &= M_{ss}(j\omega) - M_{s0}(j\omega) \\ M_b(j\omega) &= M_{bs}(j\omega) - M_{b0}(j\omega) \end{aligned} \quad (2.5)$$

Where M_s and M_b are the complex APMS responses of the subject alone as measured on the seat pan and the backrest, respectively. M_{ss} and M_{bs} represent the respective APMS responses of the coupled seat-occupant system. M_{s0} and M_{b0} are the

APMS responses of the seat assembly and the backrest, as defined in Equations (2.2) and (2.3). The vehicular vibration simulator was operated to produce the motion signals corresponding to a selected excitation and the resulting force and acceleration signals were acquired using the signal analyzers. The data analyses were performed using a bandwidth of 100 Hz with resolution of 0.125 Hz. The data analyses involved 27 averages, hanning window and a sample overlap of 75%.

2.4 Test matrix

A total of 24 (12 male and 12 female) subjects were considered to perform the characterization of biodynamic responses of seated occupants under vertical vibration. Table 2.1 summarizes the physical description of the subjects selected for the study. The weight of the selected subjects ranged from 58 kg to 100.0 kg for the males, and from 48 kg to 111.4 kg for the female subjects. The height of the male and female subjects varied from 169 to 181 cm and 153 to 175 cm, respectively. The body fat percentages of the selected subjects were further computed using the body fat calculator and summarized in the Table 2.1. The body fat of the test subjects varied from 6% to 39% for the male subjects and from 19% to 41% for the female subjects. The mean weights of the male and female subjects were computed as 78.5 kg and 64 kg, respectively, while the mean heights were obtained as 175.5 cm and 166.6 cm. While the age of participants varied from 21 to 53 years for male subjects and 26 to 52 years for female subjects, the mean ages of the male and female participants were 38.1 and 41 years, respectively.

Each subject was seated on the test seat with specified hands position and assuming a comfortable but stable posture with respect to the back support and the feet position.

The selected feet position was considered as the nominal position, and referred to as '*M*'. The knee hinge position corresponding to this posture was measured, while the selected foot position was marked on the platform for the particular subject. Two additional feet positions, 7.5 cm ahead of the '*M*' position (referred to as '*L*') and 7.5 cm behind the '*M*' position (referred to as '*S*') are also considered for the study. The tests were also performed with subject hands in the lap and on the steering wheel, representing the passenger and driver like sitting posture.

Biodynamic response characteristics of the participants were measured under two different excitations: white-noise random excitations in the 0.5 to 40 Hz frequency range, and random vibration measured at the seat base of a vehicle on a relatively rough track [57]. Three different levels of white-noise random excitations (0.25 m/s^2 , 0.5 m/s^2 and 1.0 m/s^2 rms acceleration) were synthesized in the laboratory to represent a wide range of vibration levels, which are most likely to occur in an automobile. The track measured random excitation was synthesized in the laboratory to study the biodynamic response under typical automotive vibration. The overall rms acceleration due to track-measured acceleration was computed as 1.07 m/s^2 [57]. A total of 24 tests were thus performed on each subject involving three levels of feet position, two levels of hands position, 3 levels of broad band excitation and single level of track-measured excitation. Table 2.2 summarizes the test matrix used for the study. Each experiment was conducted three times and the data were used to examine the repeatability of the measurement. The white-noise excitations of overall rms acceleration of 0.25 m/s^2 , 0.5 m/s^2 and 1.0 m/s^2 are referred to as '*W1*', '*W2*' and '*W3*' in Table 2.2. The hand positions '*SW*' and '*L*' refer to 'hands on the steering wheel' and 'hands in the lap', respectively. The static body

weights supported by the seat base and backrest were recording before and after each trial.

A particular trial was repeated if the static values acquired after the test different from those acquired prior to the test by more than 10%.

Table 2.1: Physical characteristics of the test subjects.

Subject Identification	Weight (kg)	Height (cm)	Age (years)	Body Fat (%)
Male Subjects				
01	75.0	175	45	15
02	58.5	170	47	11
03	100.0	174	53	39
04	94.0	180	40	24
05	86.4	180	43	21
06	76.7	177	38	29
07	77.0	175	36	33
09	69.4	169	32	15
10	58.0	177	29	06
11	74.0	180	21	13
16	95.3	181	32	22
19	77.3	178	42	22
Mean	78.5	176.3	38.2	
STDV	13.4	4.1	6.8	---
Female Subjects				
08	70.8	163	38	37
12	48.0	160	48	24
13	55.0	170	30	22
14	70.0	170	52	32
15	57.0	164	49	28
17	68.0	170	48	27
18	70.0	175	51	29
22	56.0	164	28	19
23	61.0	162	35	26
25	111.4	170	38	41
26	49.4	153	26	23
27	51.0	164	42	19
Mean	64.0	165.4	40.4	
STDV	17.1	4.7	7.9	---
Mean all	71.2	171	39.3	
STDV	16.8	6	7.4	---

Table 2.2: The test matrix.

Test Condition	Excitation			
	White Noise			Track-Measured
	W1 – 0.25m/s ²	W2 – 0.5 m/s ²	W3 – 1.07 m/s ²	1.07 m/s ²
Hands Position	SW, L	SW, L	SW, L	SW, L
Feet Position	S, M, L	S, M, L	S, M, L	S, M, L

2.5 Summary

A rigid seat was designed to realize automotive sitting postures and applied to perform the biodynamic measurements on 24 male and female subjects exposed to vertical vibration levels considered to be representative of the automotive vibration environment. The data was analyzed to derive the seated occupant and biodynamic response to whole-body vertical vibration. The tests were performed with two different hand positions (driver posture-hands on the steering wheel, and passenger posture-hands in the lap), three different feet positions, medium-M, long-L, and short-S and different levels of broad band excitations. The measured data was analyzed to establish biodynamic response characteristics of male and female seated subjects, upon performing the necessary corrections for the inertial forces of the seat assembly and the backrest structure. The analyses of the measured data provided the biodynamic response characteristics of male and female seated subjects, as reflected on the seat pan and the backrest as function of the feet position, hands position, and excitation type and magnitude. The response characteristics are discussed in the following chapter and applied to derive mechanical equivalent models.

Chapter 3 Apparent Mass Response Characteristics

3.1 Introduction

The biodynamic response characteristics of seated human subjects have been extensively reported. [44,51,57,62], These studies have contributed greatly to the understanding of seated occupant response to whole-body vertical vibration. The biodynamic response characteristics have been applied for development of mechanical equivalent models of seated occupants and anthropodynamic dummies for vibration assessment of seat-occupant system [60,64]. Considerable differences among the reported datasets, however, have been observed due to the wide range of test conditions used in different studies, such as sitting posture, frequency and amplitude of vibration excitation, number and physical characteristics of subjects [62]. The ranges of the idealized values of apparent mass, the driving-point mechanical impedance, and the seat-to-head transmissibility of seated body biodynamic response under vertical vibration have also been proposed in ISO-5982 [59] on the basis of a synthesis of various datasets reported under comparable test conditions.

The ranges of idealized values presented in ISO-5982 [59] are not intended to characterize the biodynamic response of seated human occupants under automotive postures and vibration conditions, since they are based upon data acquired with no back support and under relatively high magnitudes of vertical vibration. The application of the vast majority of reported data to automotive seating postures also raises many concerns due to considerably different posture and vibration conditions of automobiles. The reported studies, with only few exceptions, have considered the subjects seated with either no back support or support with a vertical backrest, hands-in-lap and high levels of

input vibration, which do not represent the postures and vibration environment of the automobiles. Moreover, no study has attempted to quantify the dynamic interactions with an inclined seat backrest, as encountered in the automobile seats, which may yield further knowledge on the seated occupant response to whole-body vertical vibration.

In this study, the apparent mass response characteristics are derived through measurements of force and motions on both the seat pan and the back rest using 24 individuals under postural and vibration conditions representative of those applicable to automobile drivers and passengers. The measurements are performed to establish the influence of hands position, body weight, vibration excitation level and type of vibration on the seated body apparent mass response. On the basis of these results, the mean apparent mass characteristics of seated automobile occupants are derived for development of mechanical equivalent models.

3.2 Static analysis of body mass supported by the pan and the backrest

The total body weight supported by the seat pan and the backrest was recorded before and after each experiment corresponding to different postures to ensure consistent sitting posture during a trial. The static forces data were further used to derive the mean body weight supported by the seat pan and the backrest. The average body weight supported by the seat pan and the backrest by the 12 male and 12 female seated subjects are summarized in Table 3.1. The table also presents the body mass index (BMI), a measure of the frame of the subjects, computed from a standard BMI calculator [71]. The results show that the body weight supported by the seat pan ranges from 72.5% to 79.9%

for male subjects and from 74.9% to 80.8% for female subjects, when the subjects are seated with their hands in the lap and selected feet position (M). The weight supported

Table 3.1: Average Body Weight Supported by the Seat Pan and the Backrest.

Subject ID	Body Mass (kg)	Height (cm)	BMI	Percent Body Weight Supported by				
				SEAT PAN		BACKREST		
				Hands Position				
				LAP	SW	LAP	SW	
Male	10	58	177	19	73.6	70.3	30.0	29.1
	2	58.5	170	20	78.4	76.2	26.3	22.9
	9	69.4	169	24	77.6	72.9	27.1	23.8
	11	74	180	23	74.3	70.9	30.9	23.5
	1	75	175	24	77.7	72.9	25.2	17.5
	6	76.7	177	24	79.9	75.4	27.0	35.1
	7	77	175	25	76.7	74.0	26.8	31.7
	19	77.3	178	24	75.7	71.5	27.9	30.8
	5	86.4	180	27	72.5	69.4	31.9	26.5
	4	94	180	29	73.0	69.3	38.4	33.8
	16	95.3	181	29	74.0	72.1	29.3	29.3
	3	100	174	33	74.1	74.0	31.6	31.4
Mean		78.47	176.33	25.08	75.6	72.4	29.4	27.9
Female	12	48	160	19	79.0	76.2	25.6	30.0
	26	49.4	153	21	74.9	72.5	24.9	20.0
	27	50.8	164	19	76.4	74.0	31.7	29.9
	13	55	170	19	78.5	74.2	28.2	24.2
	22	55.8	164	21	75.3	71.5	25.8	28.0
	15	56.9	164	21	77.9	76.1	28.3	20.7
	23	60.8	162	23	79.1	76.8	27.0	19.7
	17	67.8	170	23	79.6	76.0	35.1	32.1
	14	70	170	24	76.0	72.6	40.0	37.6
	18	70.1	175	23	76.7	72.5	39.4	36.4
	8	70.8	163	27	80.8	78.1	35.5	29.9
	25	111.4	170	39	76.6	73.5	35.8	30.3
Mean		63.9	165.4	23.3	77.6	74.5	31.4	28.2
Mean (all)		71.2	170.9	24.2	76.6	73.5	30.4	28.1
STDEV(all)		16.8	6.0	--	2.3	2.4	4.7	5.5

by the backrest under same conditions varies from 25.2% to 38.4% for males, and from 24.9% to 40% for females. The mean values of the body weights supported by the seat pan and the backrest for male and female subjects, however, are quite comparable. The overall mean values of the body weight supported by the pan and the backrest, computed for all 24 subjects, are obtained as 76.6% and 30.4%, with standard deviation of 2.3 and 4.7 respectively for hands-in-lap position.

The body weight supported by the seat pan and the backrest decreases slightly in most cases, when the hands are placed on the steering wheel (SW), as illustrated in Table 3.1. The body weight supported by the seat pan ranges from 69.3% to 76.2% for male subjects and from 71.5% to 78.1% for female subjects, when the subjects are seated with their hands on the steering wheel and selected feet position (M). The weight supported by the backrest under same conditions varies from 17.5% to 33.8% for males, and from 19.7% to 37.6% for females. The mean values of the body weights supported by the seat pan and the backrest for male and female subjects under this posture are also quite comparable. The overall mean values of the body weight supported by the pan and the backrest, computed for all 24 subjects, are obtained as 73.5% and 28.1%, with standard deviation of 2.4% and 5.5% respectively.

The body weight supported by the seat pan and the backrest are also estimated from the reported anthropometric data for male and female population [58]. The anthropometry suggests that the human upper body mass, including the masses due to head, neck, trunk and arms, accounts for nearly 67.8% of the total body mass for the hands-in-lap position, and 65.6% of the total body mass for the hands-on-steering wheel position. The static force on the seat pan is thus estimated from the sum of the total upper

body mass and the mass due to thighs resting on the pan, considered to be 10% of the total body mass. This sum is multiplied by $\cos \beta$ to determine the effective vertical load on the seat. Table 3.2 presents comparisons of the measured seated body weight supported by the seat pan for all the subjects with the estimated values. Columns B and D in the table represent the calculated forces for the hands in lap and the hands on steering wheel positions, respectively, while the values in columns A and C represent the corresponding measured forces. The table also lists the ratio of the measured static force to the estimated force, A/B and C/D , for the hands in lap and hands on steering wheel postures. The results show reasonably good agreement between the estimated and measured values. The mean values of the ratios of the measured to estimated forces are obtained as 1.01 and 1.00, respectively, for the hands in lap and hands on the steering wheel (SW) postures. The peak deviation between the measured and estimated values is observed to be 7%.

The seated body weight supported by the backrest is further estimated from the upper body mass and the backrest inclination. The normal component of the upper body mass acting on the backrest is obtained by multiplying the upper body mass with $\sin \alpha$. This estimation assumes that the entire upper body is supported against the backrest, which may not be valid when the subjects assume a slouched posture. Table 3.3 illustrates comparisons of the estimated static force supported by the backrest with the measured data for all 24 subjects seated with 'LAP' and 'SW' postures. The columns B and D present the calculated static force at the seat back, comparing to 'LAP' and 'SW' postures, while columns A and C represent the corresponding measured values. The table

also presents the ratios of the measured to estimated static forces for both postures (A/B and C/D).

Table 3.2: Comparisons of measured and estimated values of the seat pan static force for all subjects seated with hands in lap and hands on steering wheel postures.

Subject ID	Body Mass (kg)	Static seat pan force (kg)						
		LAP			SW			
		A	B	A/B	C	D	C/D	
Male 10	58	42.69	43.77	0.98	40.77	42.53	0.96	
2	58.5	45.86	44.15	1.04	44.58	42.9	1.04	
9	69.4	53.85	52.37	1.03	50.59	50.89	0.99	
11	74	54.98	55.84	0.98	52.47	54.27	0.97	
1	75	58.28	56.6	1.03	54.68	55	0.99	
6	76.7	61.28	57.88	1.06	57.83	56.25	1.03	
7	77	59.06	58.11	1.02	56.98	56.47	1.01	
19	77.3	58.52	58.34	1	55.27	56.69	0.98	
5	86.4	62.64	65.2	0.96	59.96	63.36	0.95	
4	94	68.62	70.94	0.97	65.14	68.93	0.95	
16	95.3	70.52	71.92	0.98	68.71	69.89	0.98	
3	100	74.1	75.47	0.98	74	73.33	1.01	
Female 12	48	37.92	36.22	1.05	36.58	35.2	1.04	
26	49.4	37	37.28	0.99	35.82	36.23	0.99	
27	50.8	38.81	38.34	1.01	37.59	37.25	1.01	
13	55	43.18	41.51	1.04	40.81	40.33	1.01	
22	55.8	42.02	42.11	1	39.9	40.92	0.98	
15	56.9	44.33	42.94	1.03	43.3	41.73	1.04	
23	60.8	48.09	45.88	1.05	46.69	44.59	1.05	
17	67.8	53.97	51.17	1.05	51.53	49.72	1.04	
14	70	53.2	52.83	1.01	50.82	51.33	0.99	
18	70.1	53.77	52.9	1.02	50.82	51.41	0.99	
8	70.8	57.21	53.43	1.07	55.29	51.92	1.07	
25	111.4	85.3	84.07	1.01	81.9	81.69	1	
Mean	71.2	54.38	53.72	1.01	52.2	52.2	1	
STDEV	16.1	12.22	12.68	0.03	11.9	12.3	0.03	

Table 3.3: Comparisons of measured and estimated values of the seat back static force for all subjects seated with hands in lap and hands on steering wheel postures.

Subject ID	Body Mass (kg)	Static seat back force (kg)						
		LAP				SW		
		A	B	A/B		C	D	C/D
Male 10	58	17.4	16.12	1.079		16.9	15.6	1.083
2	58.5	15.4	16.26	0.947		13.4	15.73	0.852
9	69.4	18.8	19.29	0.975		16.5	18.67	0.884
11	74	22.9	20.57	1.113		17.4	19.9	0.874
1	75	18.9	20.85	0.907		13.1	20.17	0.649
6	76.7	20.7	21.32	0.971		26.9	20.63	1.304
7	77	20.6	21.4	0.962		24.4	20.71	1.178
19	77.3	21.6	21.49	1.005		23.8	20.79	1.145
5	86.4	27.6	24.02	1.149		22.9	23.24	0.985
4	94	36.1	26.13	1.382		31.7	25.28	1.254
16	95.3	27.9	26.49	1.053		27.9	25.63	1.088
3	100	31.6	27.8	1.137		31.4	26.9	1.167
Female 12	48	12.3	13.34	0.922		14.4	12.91	1.115
26	49.4	12.3	13.73	0.896		9.9	13.29	0.745
27	50.8	16.1	14.12	1.14		15.2	13.66	1.112
13	55	15.5	15.29	1.014		13.3	14.79	0.899
22	55.8	14.4	15.51	0.928		15.6	15.01	1.039
15	56.9	16.1	15.82	1.018		11.8	15.3	0.771
23	60.8	16.4	16.9	0.97		12	16.35	0.734
17	67.8	23.8	18.85	1.263		21.8	18.24	1.195
14	70	28	19.46	1.439		26.3	18.83	1.397
18	70.1	27.6	19.49	1.416		25.5	18.85	1.352
8	70.8	25.1	19.68	1.275		21.2	19.04	1.113
25	111.4	39.8	30.97	1.285		33.7	29.96	1.125
Mean	71.2	21.95	19.79	1.094		20.29	19.15	1.044
STDEV	16.1	7.32	4.634	0.169		7.074	4.484	0.205

The measured static force data presented in Tables 3.2 and 3.3 show good agreements with those estimated from the anthropometric data. The results show that the ratio of the measured seat pan force to the computed force ranges from 0.96 to 1.05 for

the male subjects and from 0.99 to 1.07 for the female subjects, when the subjects are seated with their hands in the lap. The standard deviations of the ratio are 0.03 for the male subjects and 0.025 for the female subjects. Similar results are obtained for the subjects seated with their hands on steering wheel. The results show larger variations in the ratio of the seat back measured force to that estimated from the anthropometric data, as evident from relatively high standard deviations. The ratio ranges from 0.95 to 1.38 for male subjects and from 0.92 to 1.43 for female subjects, when the subjects are seated with their hands in lap. For the subjects seated with their hands on steering wheel, the ratios range from 0.65 to 1.3 for male subjects and from 0.73 to 1.39 for female subjects. The extreme variations were clearly evident for shorter subjects with hands-on-steering wheel posture; since these subjects tended to shift their torso to maintain adequate contact with the steering wheel. The female subjects with relatively large body mass also revealed larger variations.

3.3 APMS response of the seated subjects

The force and acceleration signals acquired at the seat pan and the backrest are analyzed to compute the APMS response characteristics of the coupled seat-occupant system. The APMS responses of the seated occupants are derived upon performing the inertial correction, as stated in Equation (2.5). The response characteristics attained during the three trials corresponding to a selected test condition are examined for repeatability and averaged to obtain the mean responses for each subject as reflected at the seat pan and the backrest. The mean responses attained with 24 subjects corresponding to each test condition are compared to identify important trends. The comparisons revealed considerable scatters in the data. The high degree of inter-subject variability could be attributed to subject weight, height and build. It has been widely

reported that the body mass affects the APMS response most significantly [26,39]. The individual data sets are evaluated in an attempt to quantify the effects of hands and feet position, and the magnitude of excitation. The representative data sets are then identified to develop mechanical-equivalent models. The data sets obtained for the seat pan and the backrest are presented in the following sections to discuss the important trends.

3.3.1 Influence of body weight

The APMS responses of the seated body measured at the seat pan and the backrest under vertical vibration are most strongly affected by the body weight, as shown in Figures 3.1 through 3.16 for different experimental conditions. Figures 3.1 to 3.8 illustrate the APMS magnitude and phase responses measured on the seat pan for all 24 subjects seated with two different hands positions, subject-selected feet position (M) and exposed to different levels of white noise and track-measured vibration. Figures 3.9 to 3.16 illustrate the corresponding APMS magnitude and phase responses measured on the seat back. The results show considerable scatter in both the pan and the back APMS magnitude data, specifically at frequencies below 14 Hz, while the scatter is wider for hands-on-steering wheel posture.

The results show that the peak magnitude of the backrest APMS is comparable to that of the seat pan APMS, irrespective of the test condition. The backrest APMS, therefore, can not be neglected and may provide considerable insight into the human responses to vibration, when seated against an inclined backrest. While the seat pan APMS magnitudes mostly predominate around a single frequency in the 6-8 Hz range, the backrest APMS magnitude responses generally reveal three notable peaks in the

vicinity of 2.5 Hz (which might be associated with the pitch motion of the head), 6-8 Hz, and 12-16 Hz. The backrest APMS responses exhibit considerably larger scatter in the data when compared with that observed in the seat pan responses. This is in-part attributed to the sitting habits of individuals causing considerable variations in the upper body-backrest contact force, as it is evident from the variations in the measured static forces summarized in the Table 3.3. The measured phase responses converge asymptotically towards -90° at frequencies below 10 Hz. Considerable deviations in the phase response are also observed at frequencies below 10 Hz.

The body mass is believed to be the primary factor leading to the scatter among the individual data sets, which has been identified in a large number of earlier studies [26,39,44,62]. It has thus been suggested that the APMS magnitude response be normalized with the respect to the static sitting weight [8]. The normalized APMS responses could be effectively used to study the effects of other factors. The normalization process generally diminishes the scatter among the individual data sets considerably. The reported studies have thus applied the static sitting weight on the seat pan to obtain normalized seat APMS response. It has been reported that the seat pan supports approximately 67%-75% of the total body weight, depending upon the seat height and the sitting posture [65]. The static weight supported by the backrest, however, has been attempted in a single study [68], which would vary with the inclination angle.

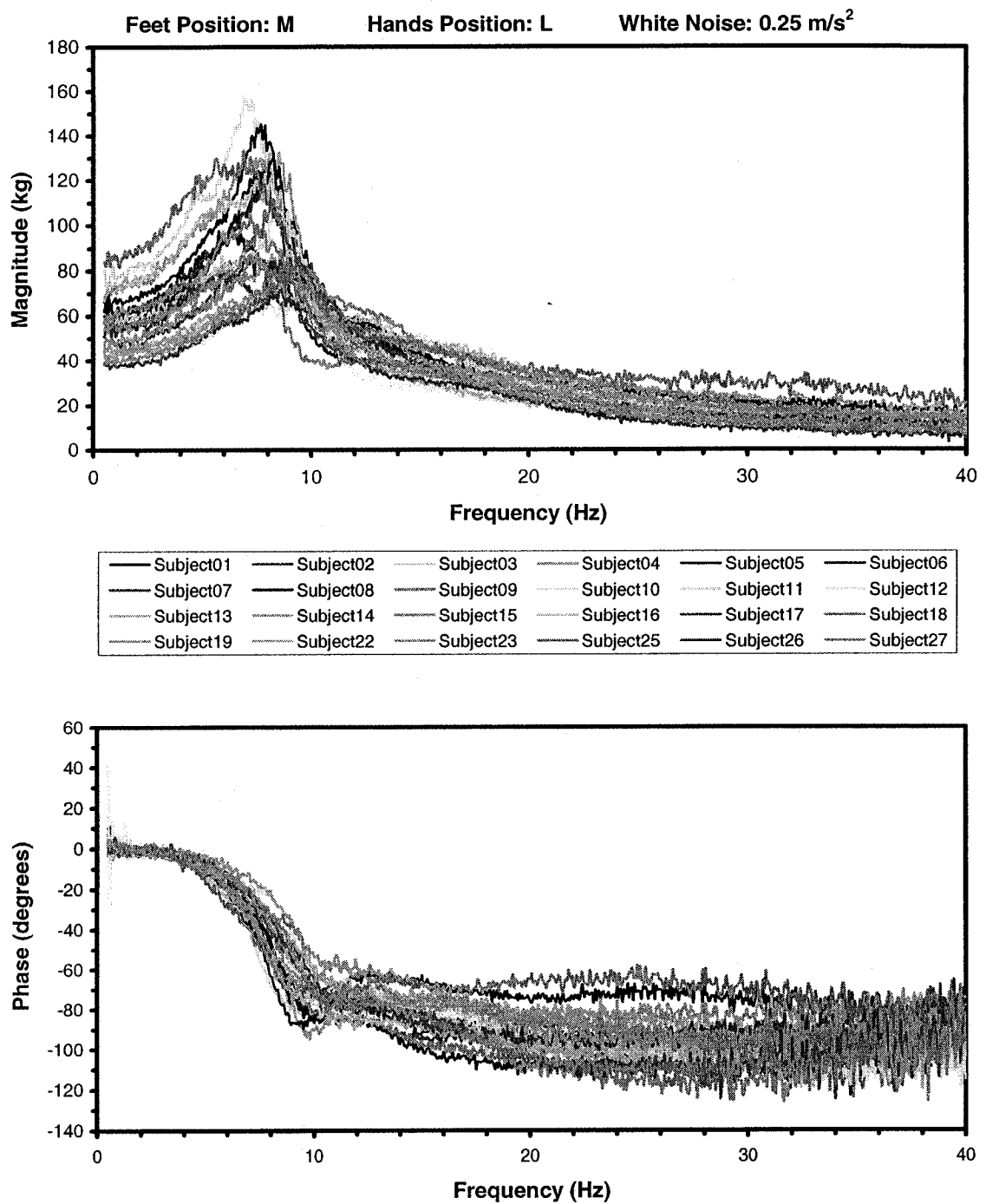


Figure 3.1: Comparison of APMS responses of 24 subjects measured at seat pan.

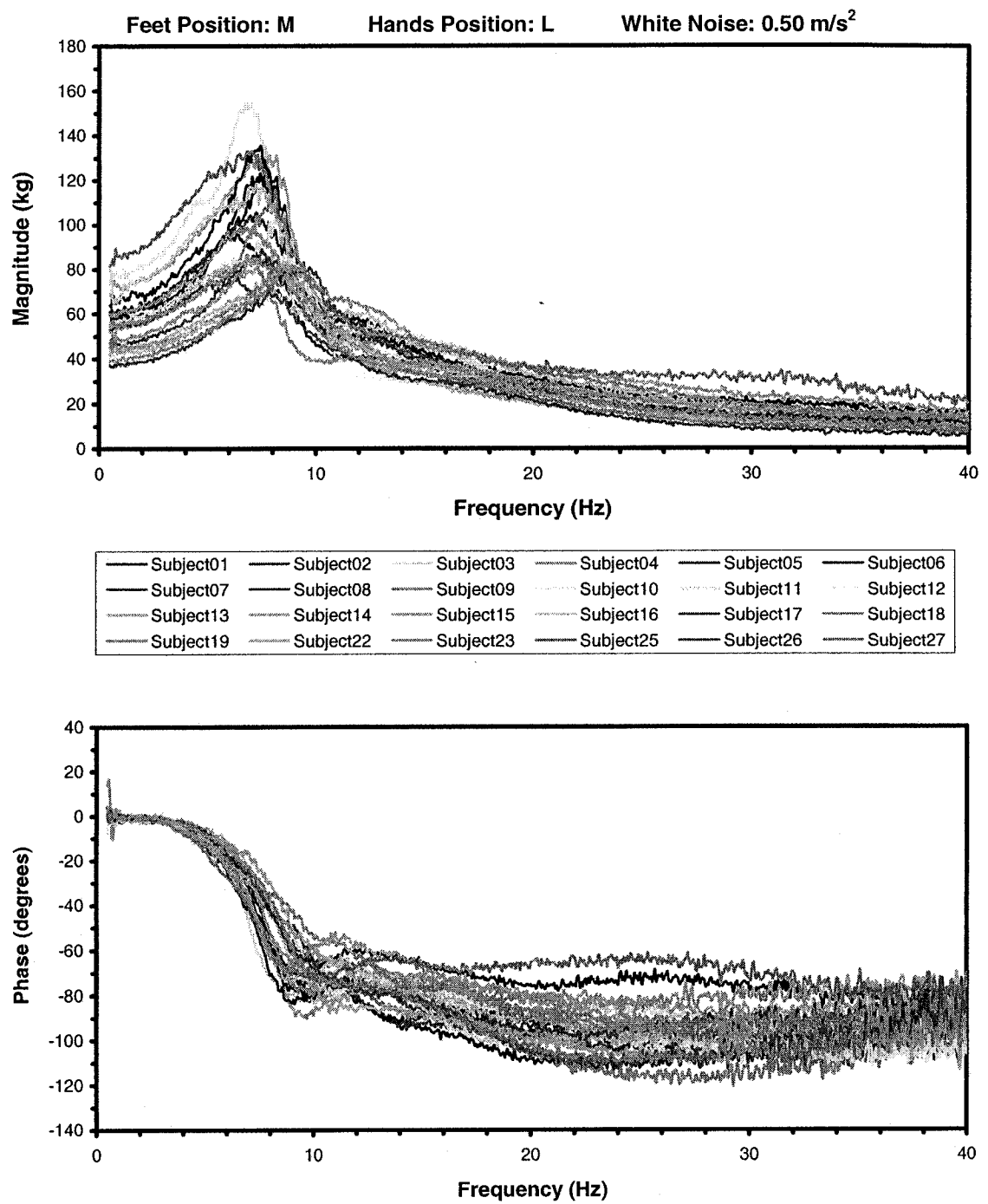


Figure 3.2: Comparison of APMS responses of 24 subjects measured at seat pan.

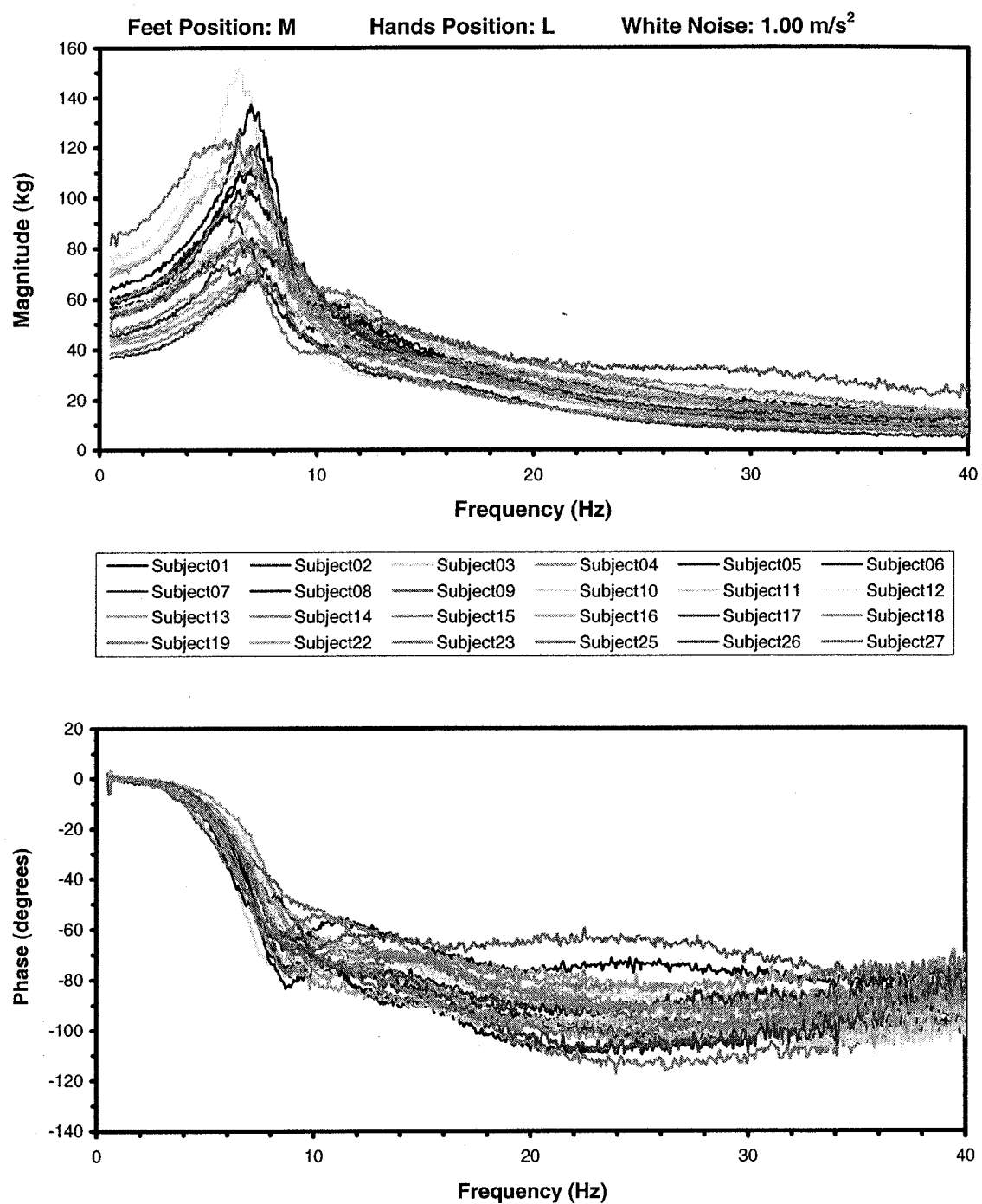


Figure 3.3: Comparison of APMS responses of 24 subjects measured at seat pan.

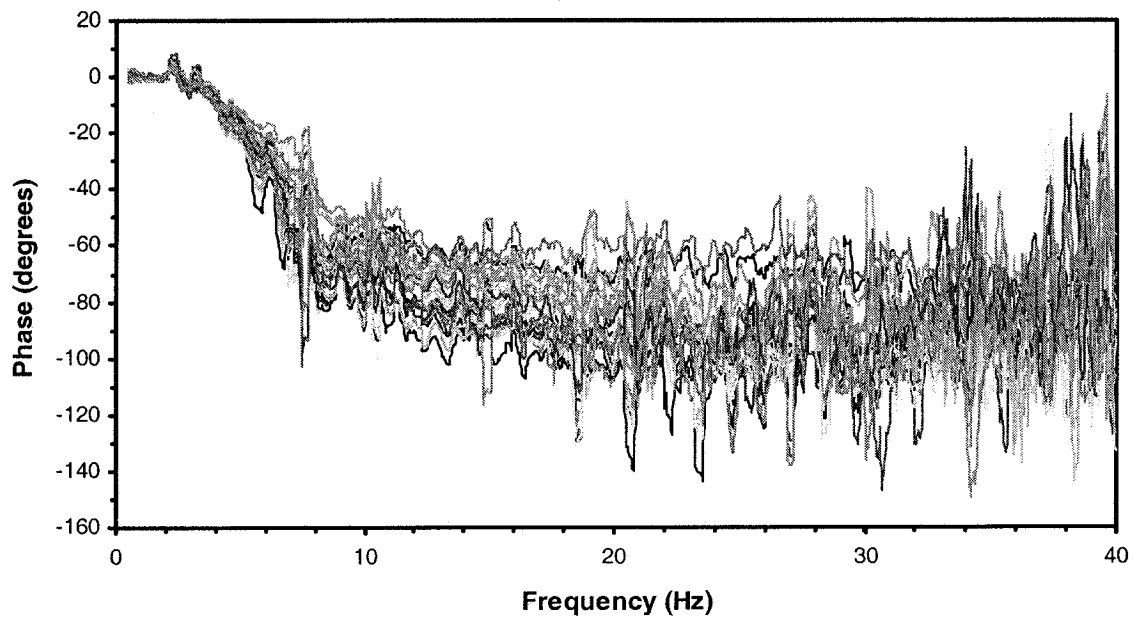
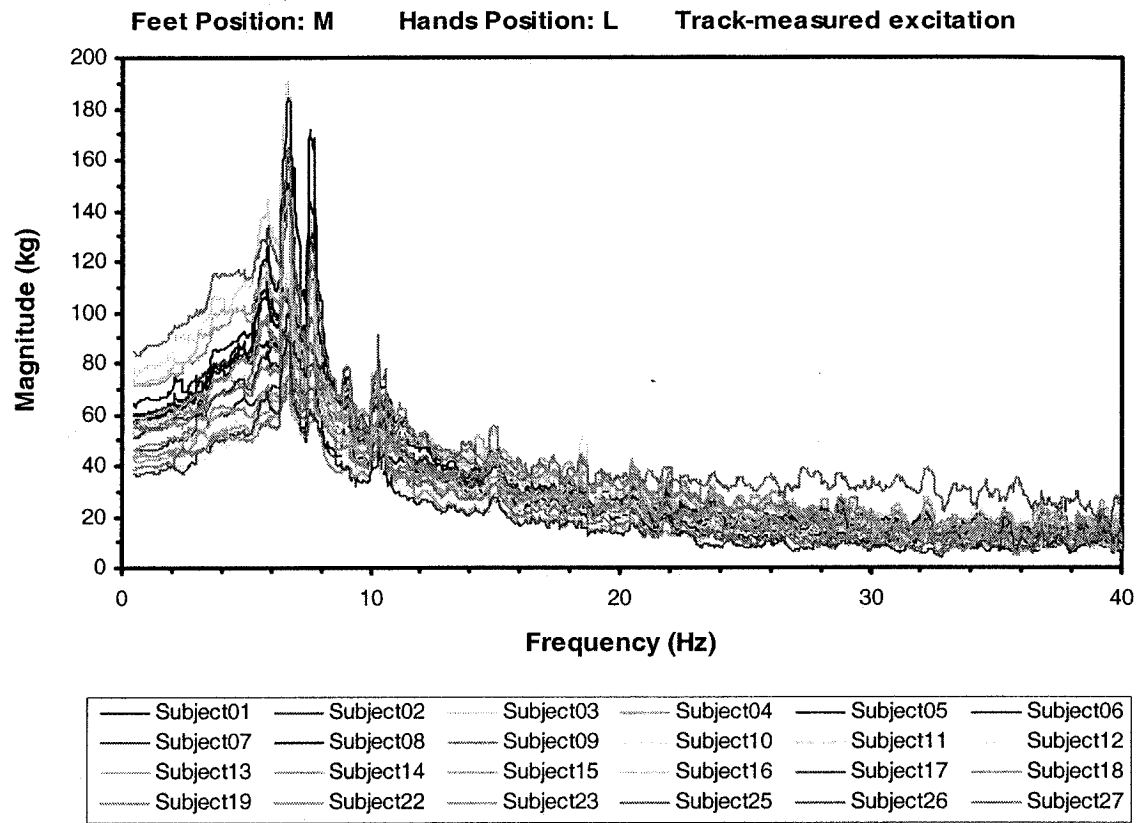


Figure 3.4: Comparison of APMS responses of 24 subjects measured at seat pan.

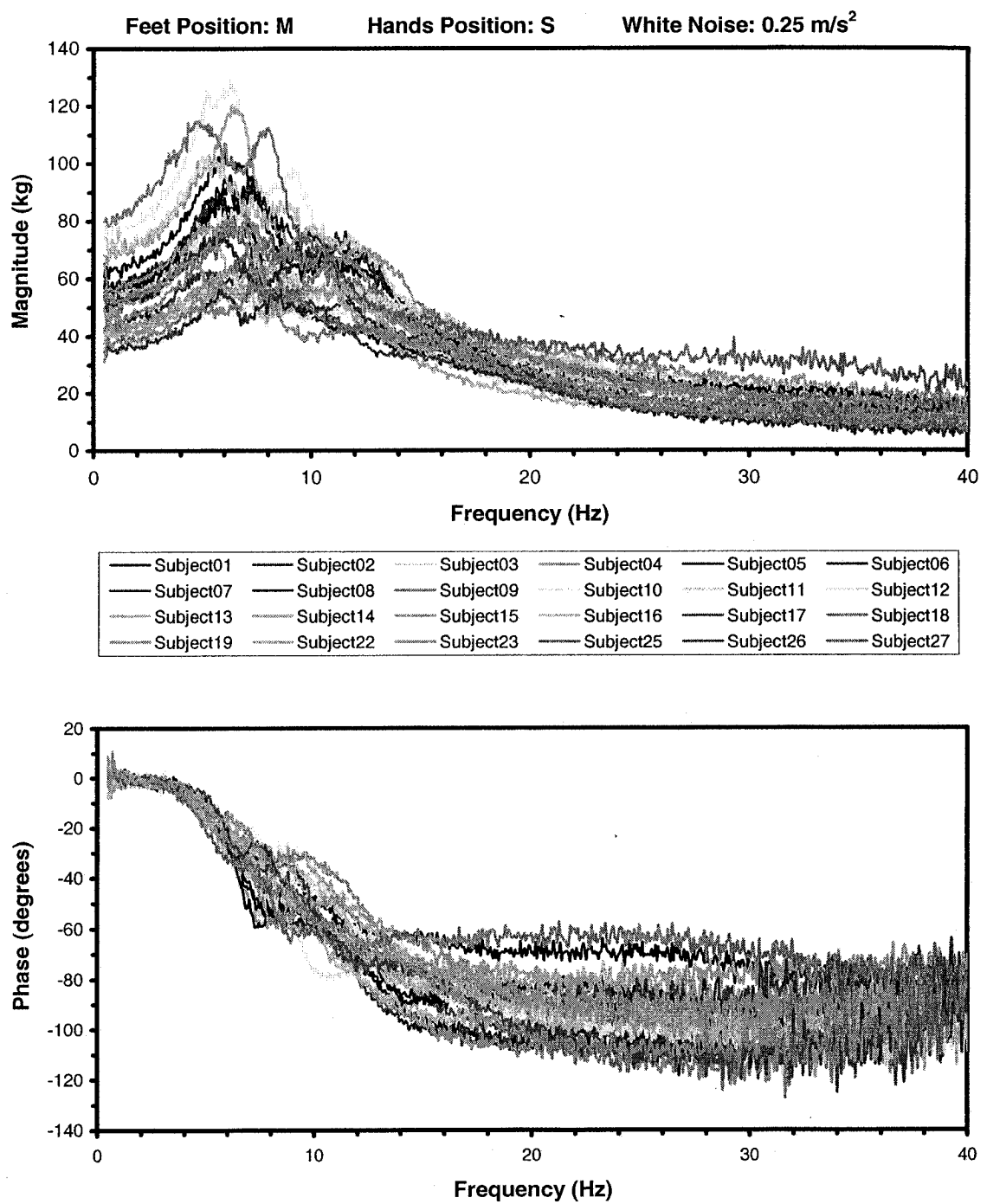


Figure 3.5: Comparison of APMS responses of 24 subjects measured at the seat pan.

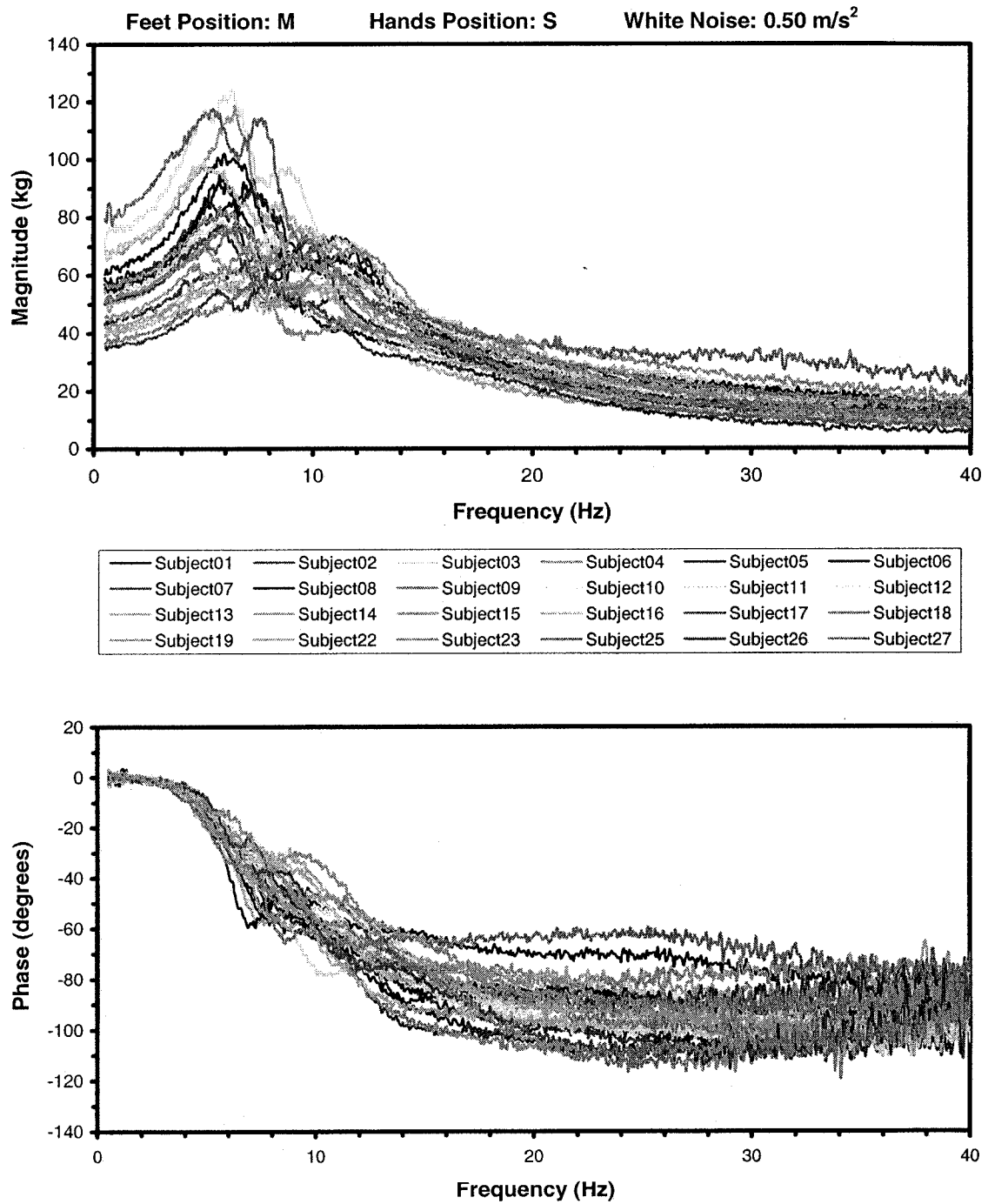


Figure 3.6: Comparison of APMS responses of 24 subjects measured at the seat pan.

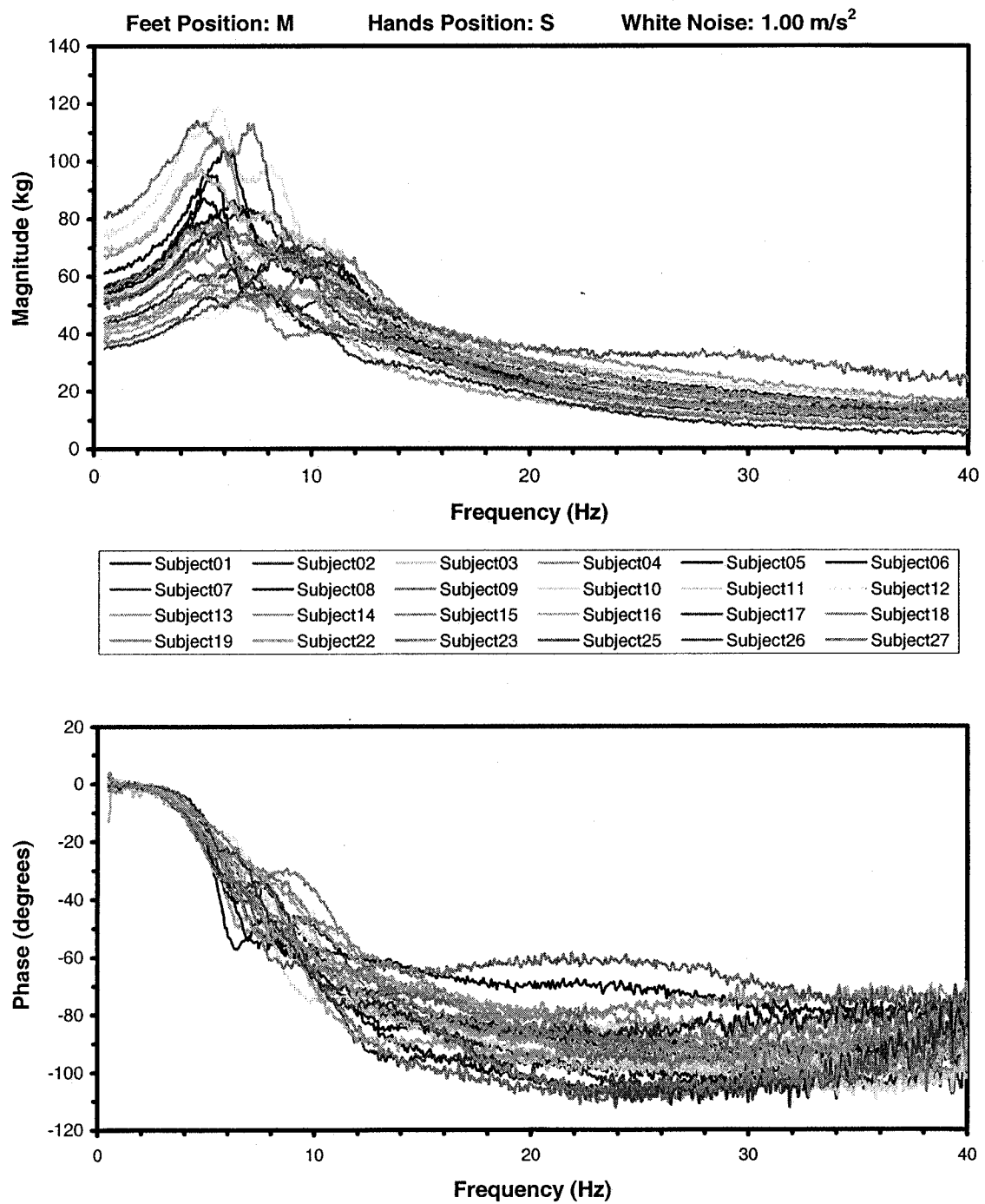


Figure 3.7: Comparison of APMS responses of 24 subjects measured at the seat pan.

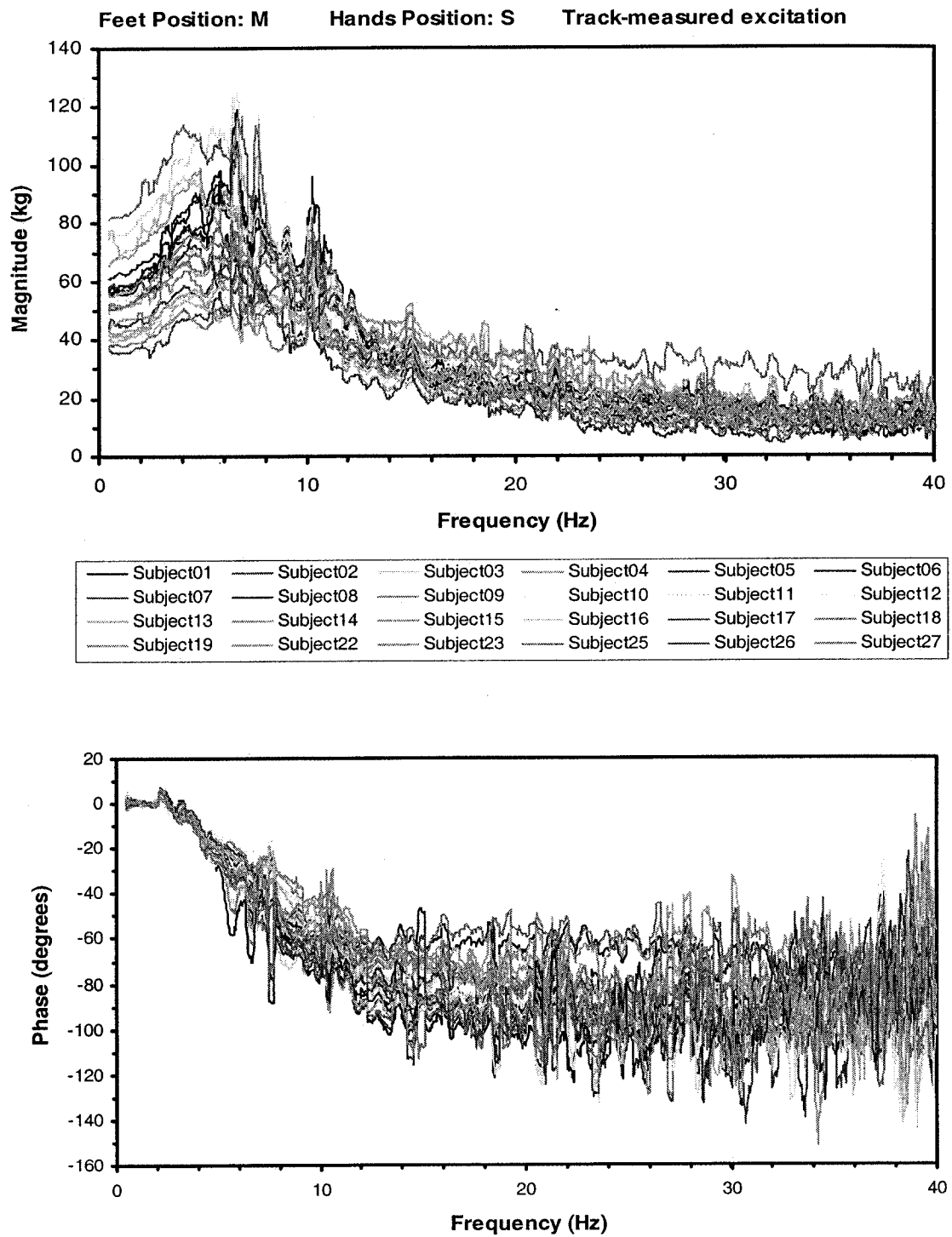


Figure 3.8: Comparison of APMS responses of 24 subjects measured at the seat pan.

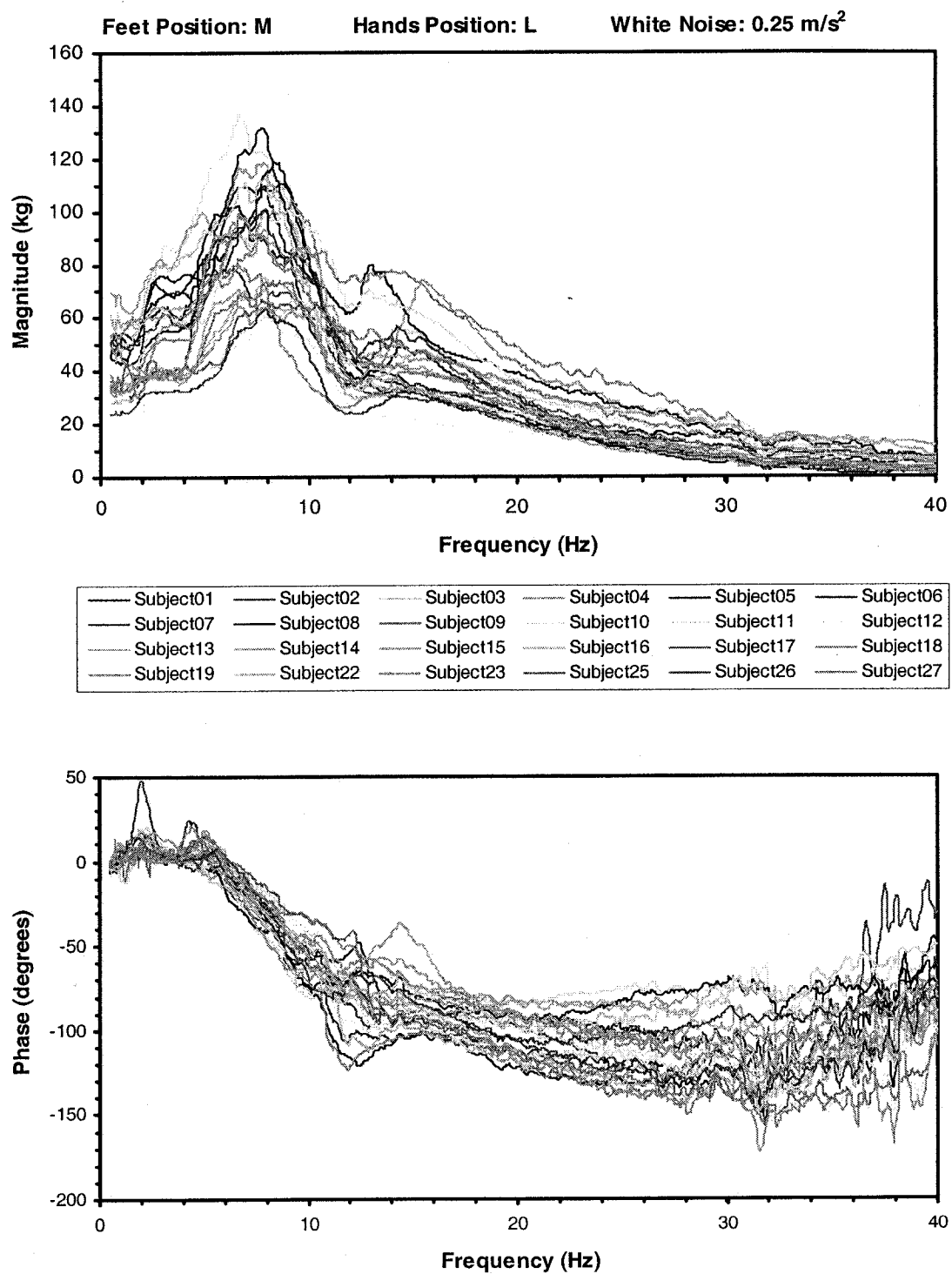


Figure 3.9: Comparison of APMS responses of 24 subjects measured at the backrest.

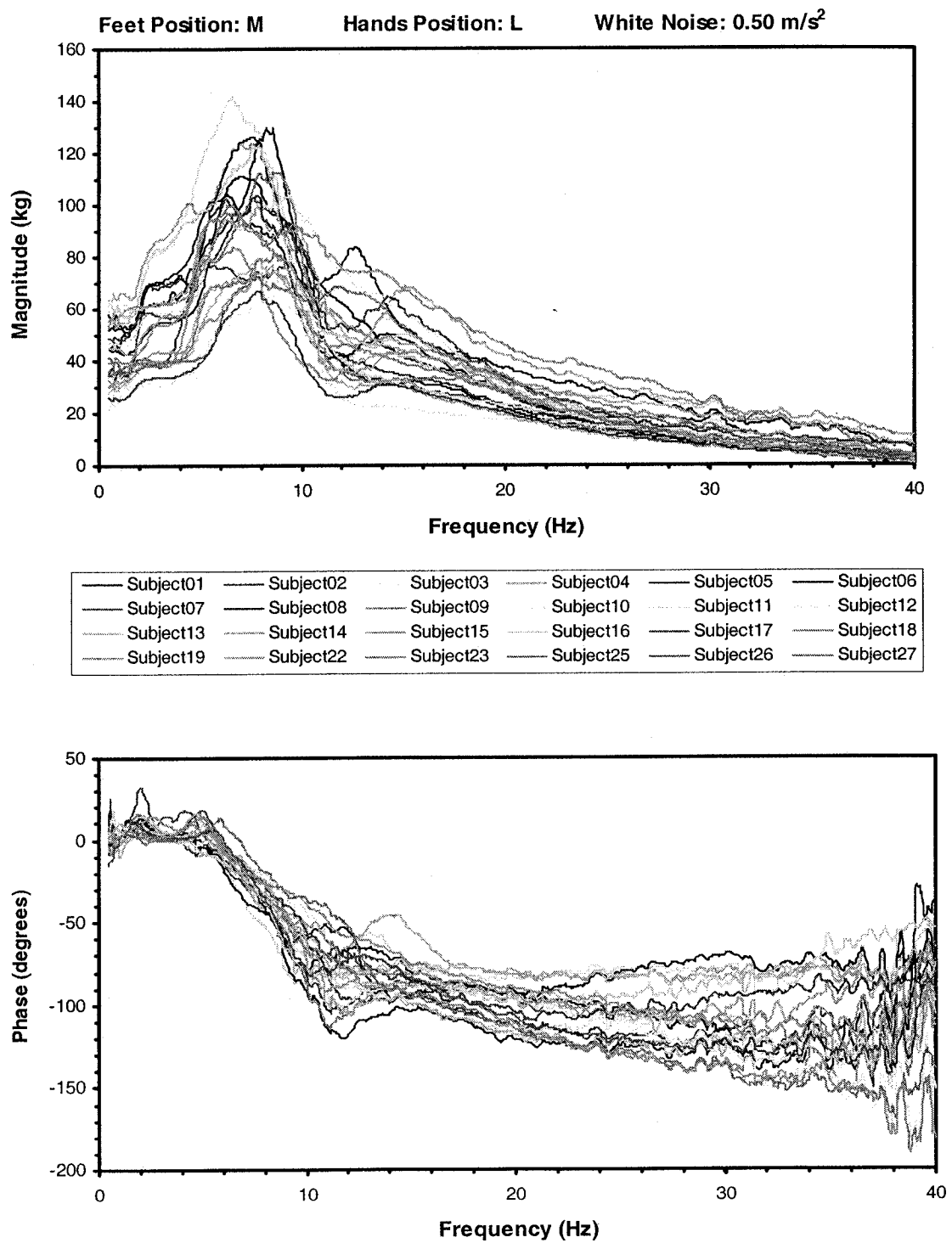


Figure3.10: Comparison of APMS responses of 24 subjects measured at the backrest.

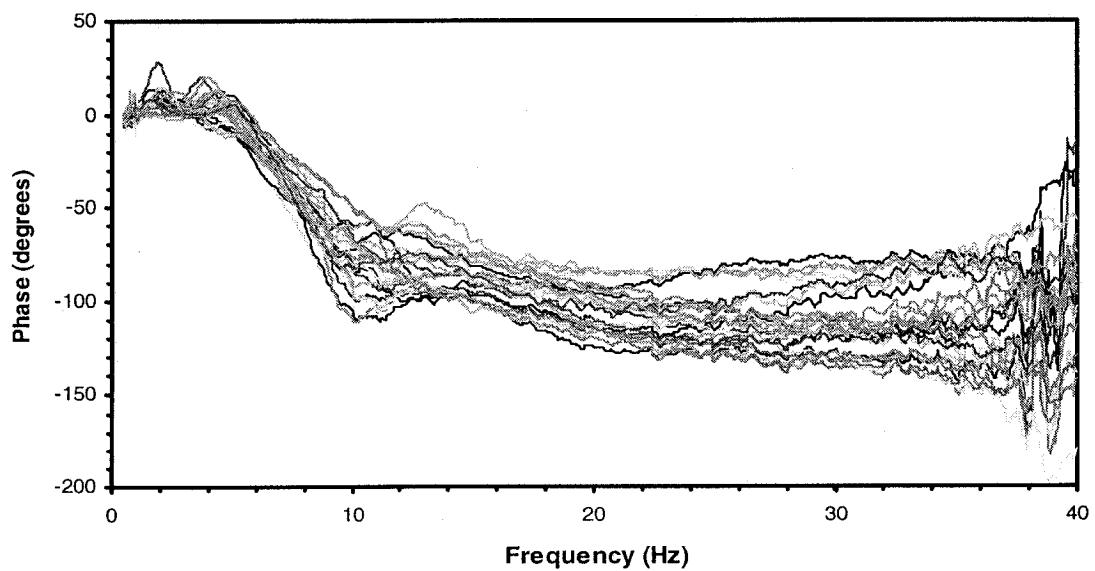
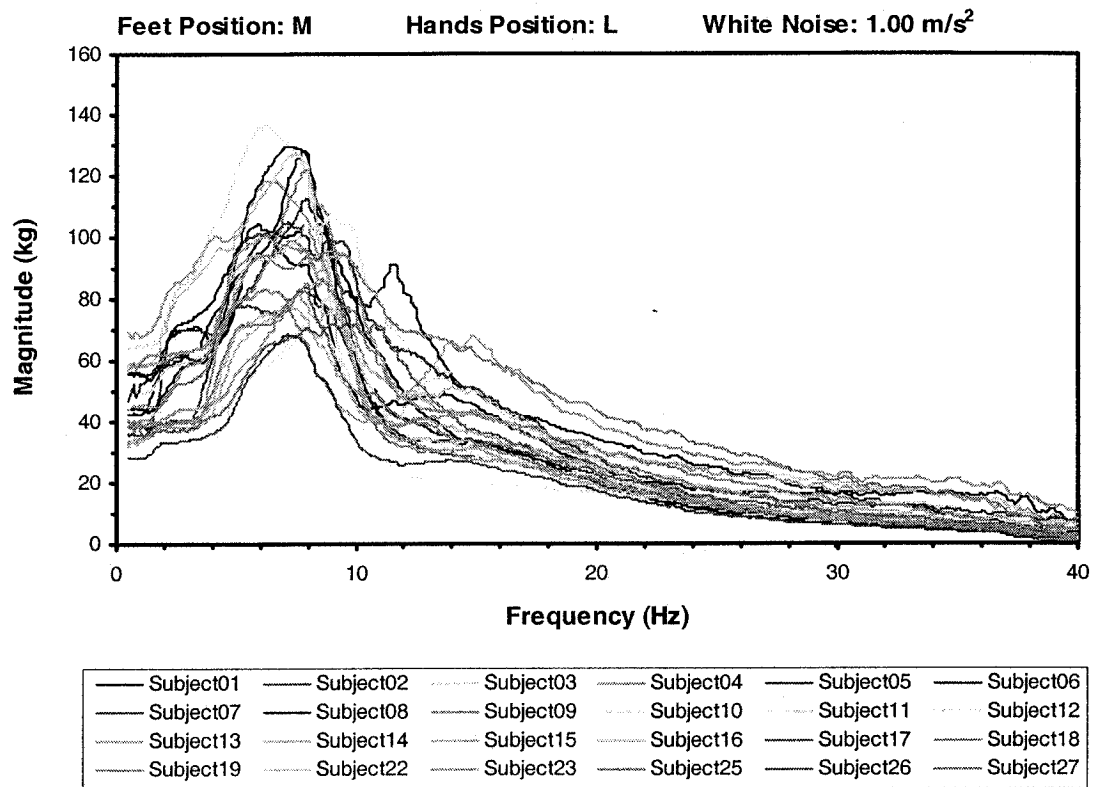


Figure3.11: Comparison of APMS responses of 24 subjects measured at the backrest.

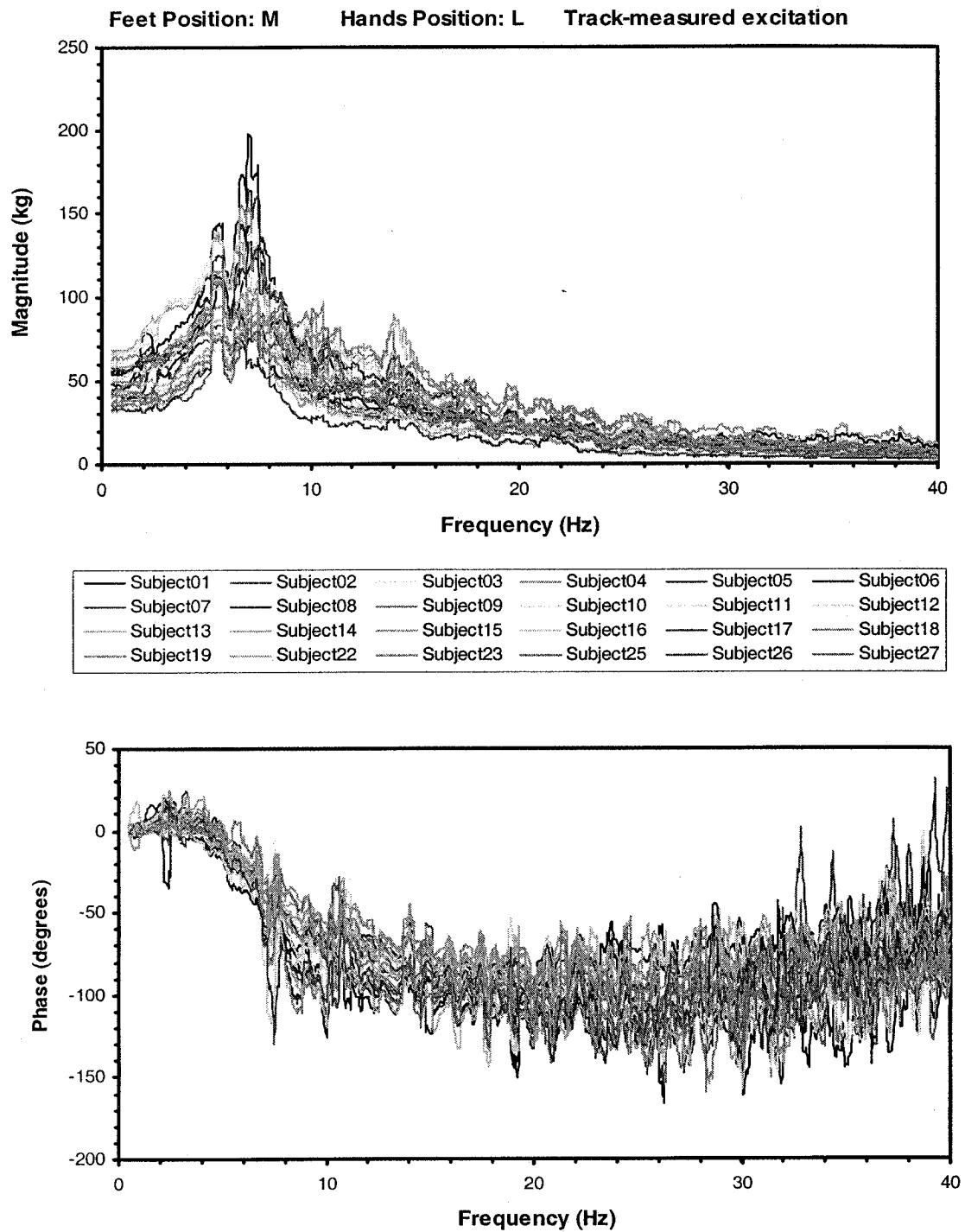


Figure3.12: Comparison of APMS responses of 24 subjects measured at the backrest.

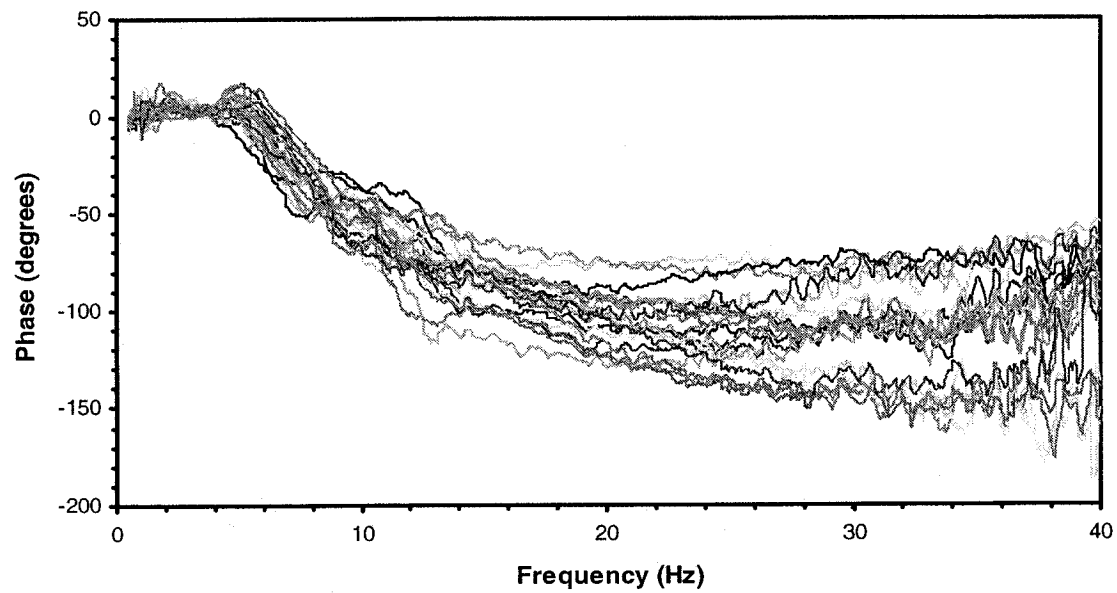
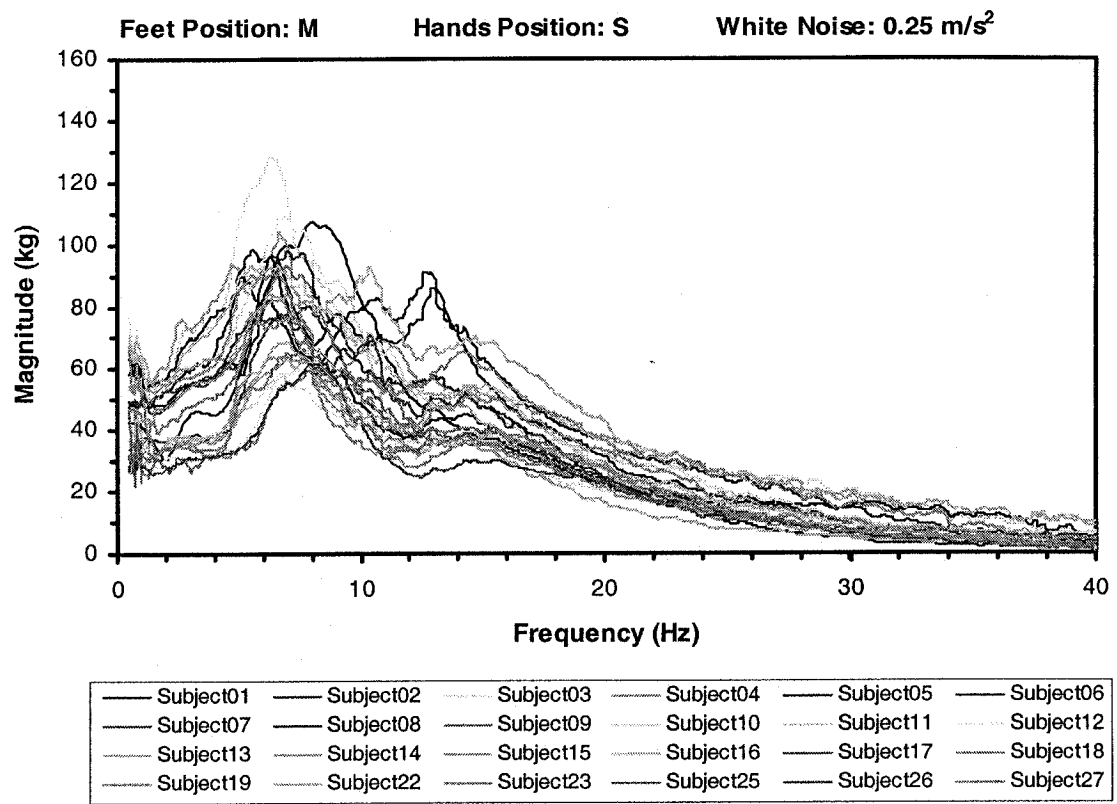


Figure3.13: Comparison of APMS responses of 24 subjects measured at the backrest.

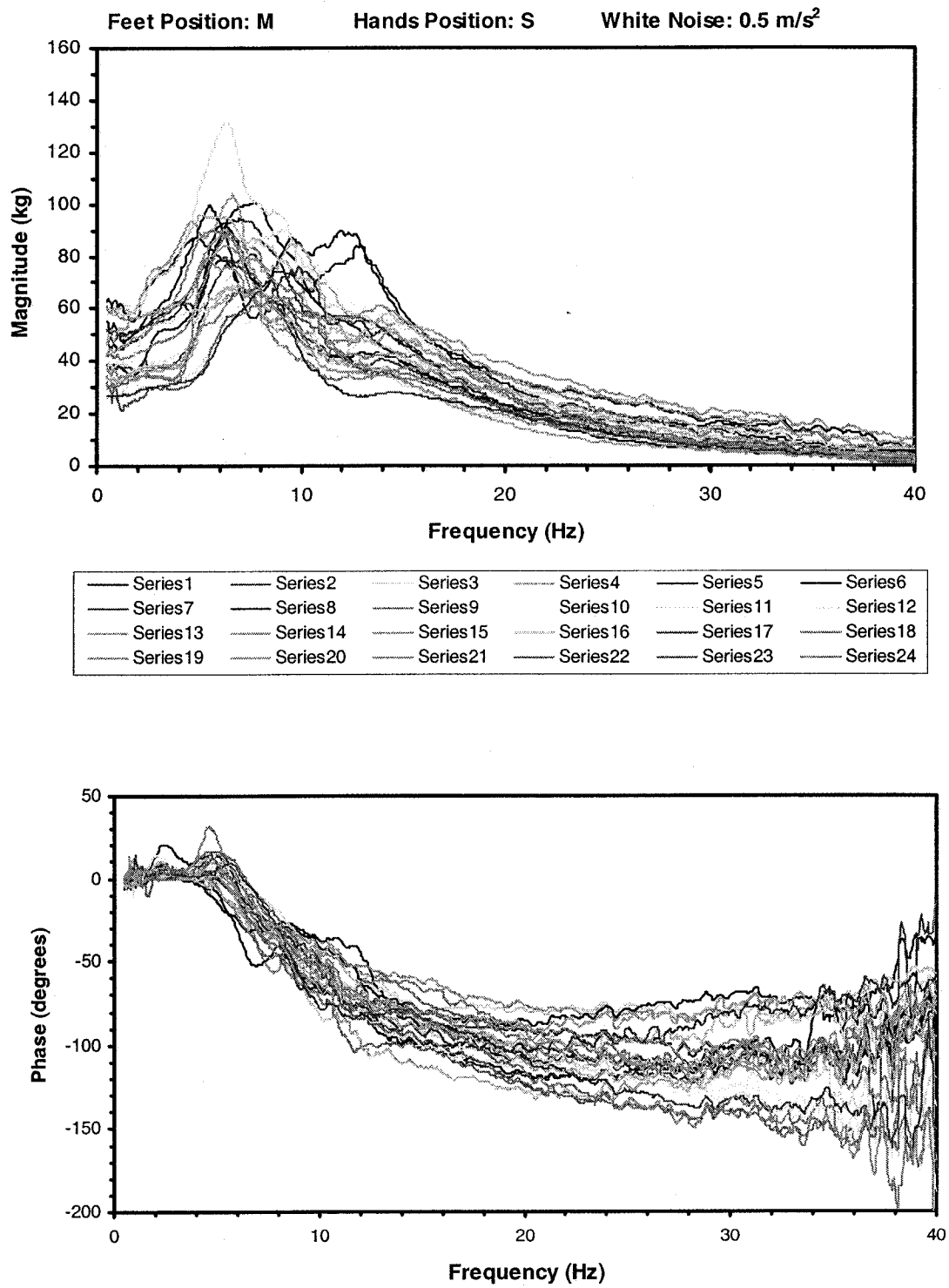


Figure3.14: Comparison of APMS responses of 24 subjects measured at the backrest.

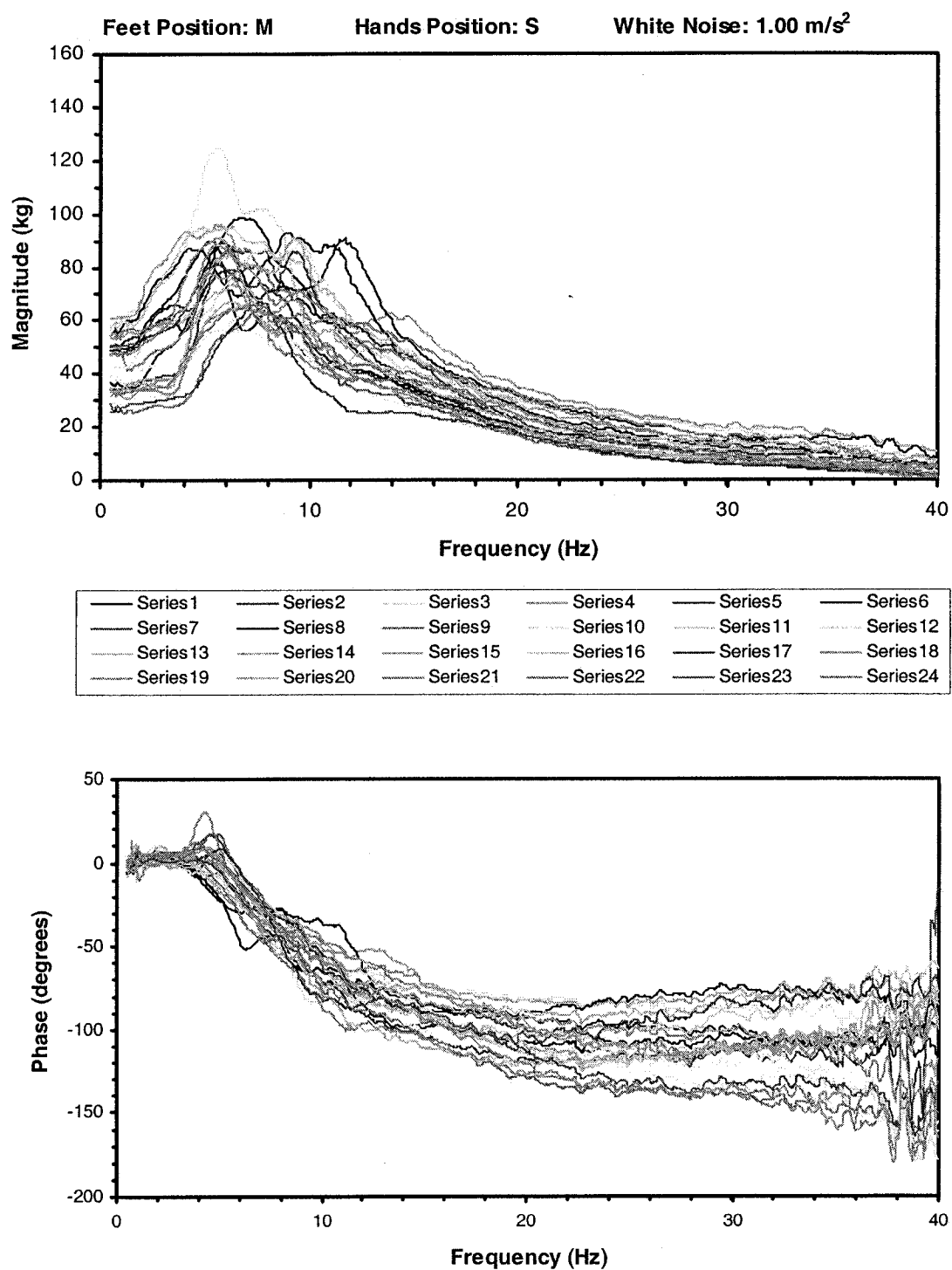


Figure3.15: Comparison of APMS responses of 24 subjects measured at the backrest.

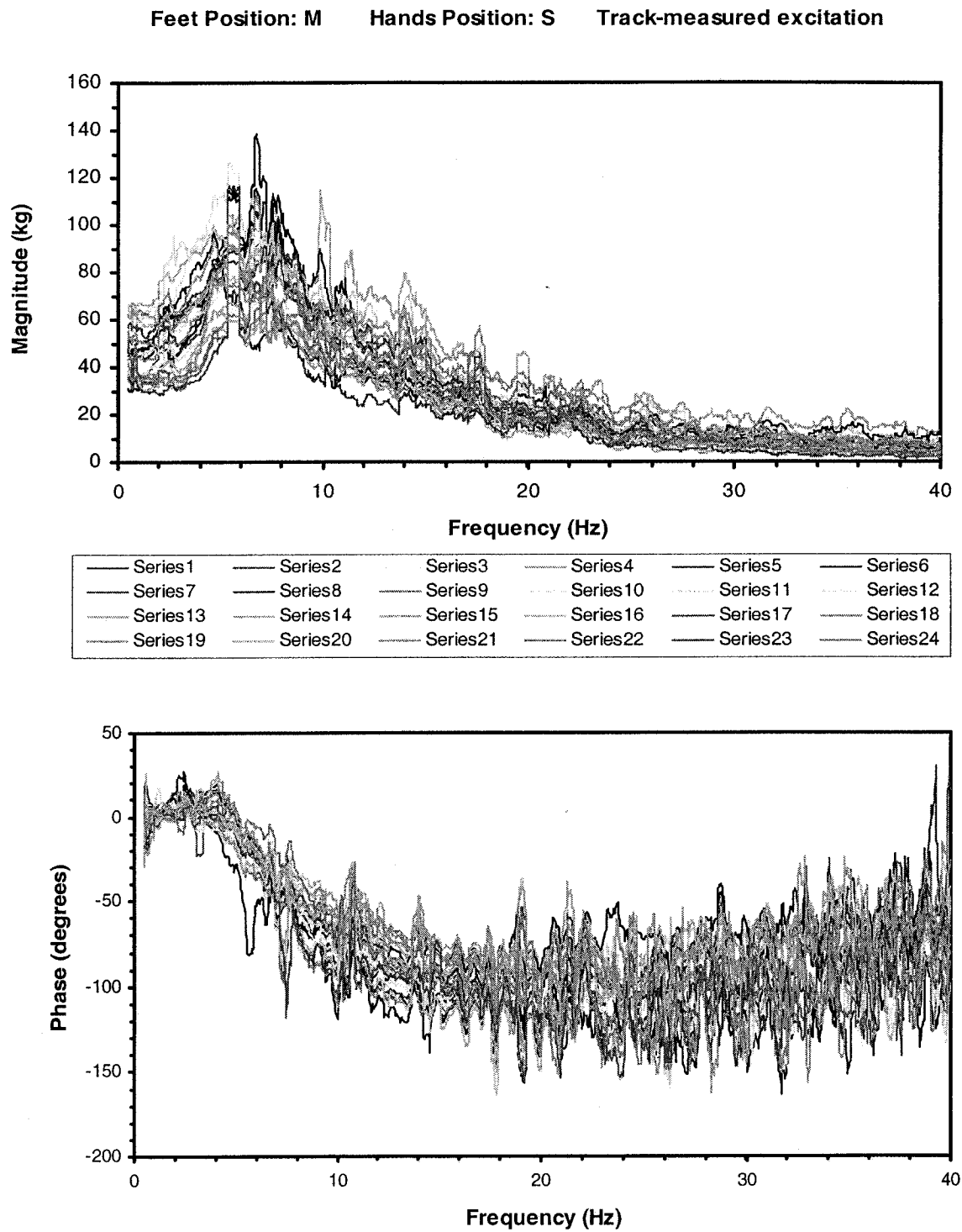


Figure3.16: Comparison of APMS responses of 24 subjects measured at the backrest.

The trends observed in both the pan and the back APMS magnitude data suggest that peak values increase with the increasing body mass, while the corresponding frequency tends to decrease. Figures 3.17 and 3.18 illustrate these trends in the seat pan peak APMS magnitude and the corresponding frequency with the hands in lap and on steering wheel postures, respectively, under $0.5m/s^2$ r.m.s. acceleration excitation (W2). Although considerable dispersion in the data is evident, the trendlines shown in the figure suggest that peak apparent mass magnitude could be positively correlated with the increasing body mass, while the correlation with the corresponding frequency is considerably lower. The correlation coefficients (R^2) in excess of 0.8 are obtained for the seat pan peak APMS magnitude, while those for the corresponding frequency are extremely low.

Figures 3.19 and 3.20 illustrate the relationships between the peak backrest APMS magnitude and the body mass and between the corresponding frequency and the body mass, for the two hands position and W2 excitation. The results show similar degree of positive correlation between the peak magnitude and the body mass ($R^2 > 0.8$) and poor correlation for the corresponding frequency. These results further confirm that the body mass represents an important influence on both the seat pan and the backrest apparent mass response of the seated occupants exposed to vertical vibration.

The influence of the body mass on the APMS response measured at the seat pan and the backrest are further analyzed by grouping the measured datasets in four mass ranges. These included: (i) 8 data sets for subjects' mass below 60 kg with mean mass of 53.4kg; (ii) 5 data sets for subjects' mass between 60.5 and 70 kg with mean mass of 67.6 kg; (iii) 6 data sets for subjects' mass between 70.5 and 80 kg with mean mass of 75.1 kg;

and (iv) 5 data sets for subjects' mass above 80 kg with mean mass of 97.4 kg. The data sets for subjects within each group are averaged to derive the mean APMS magnitude responses at the seat pan and the backrest. The resulting mean data sets are used to demonstrate the strong influence of the body mass on the APMS magnitudes measured at the seat pan and the backrest. Considering the relatively small effects of the magnitude of vibration excitations, the data acquired under three different magnitudes of broadband vibration are combined to derive the mean responses for the four mass groups.

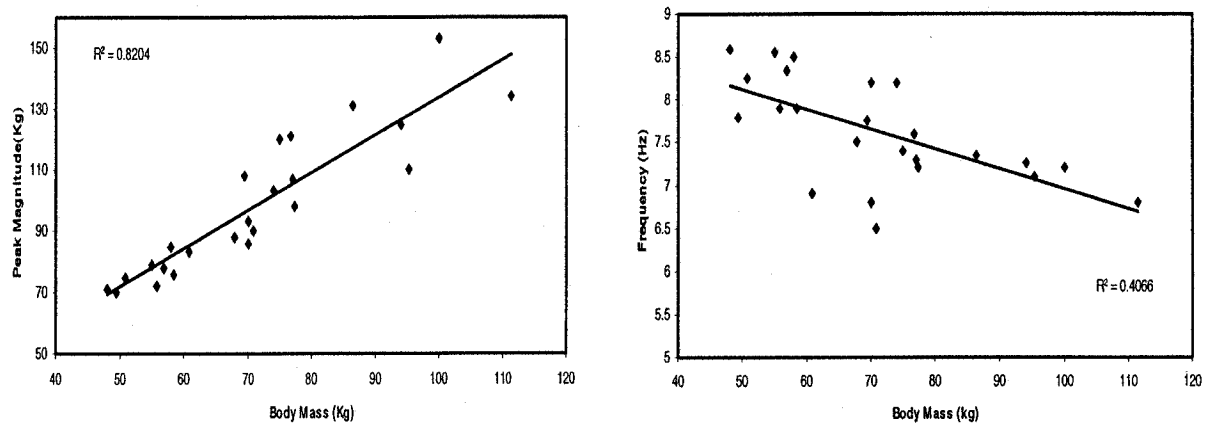


Figure 3.17: Dependence of the peak seat pan APMS magnitude and the corresponding frequency on the body mass (hands-in-lap).

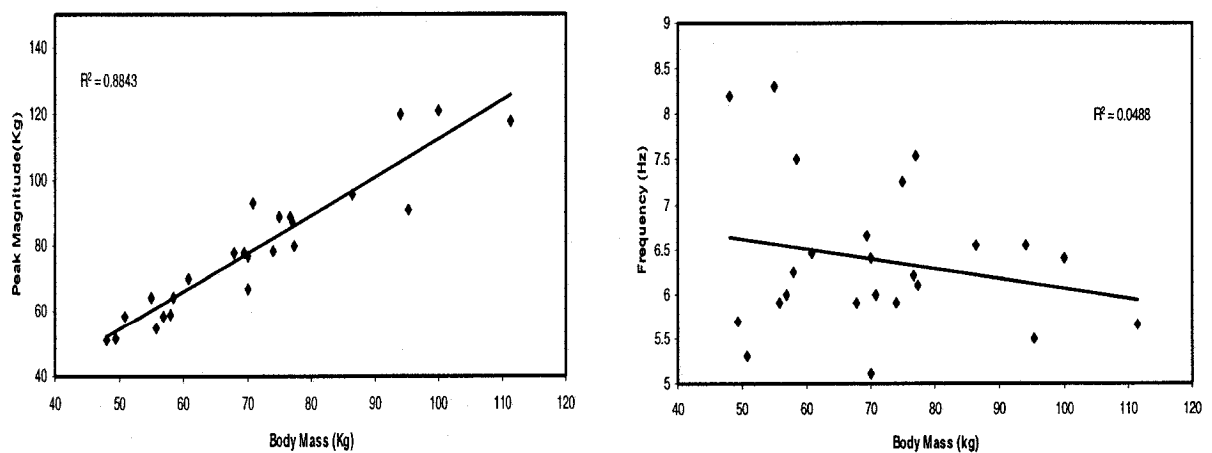


Figure 3.18: Dependence of the peak seat pan APMS magnitude and the corresponding frequency on the body mass (hands-on-steering wheel).

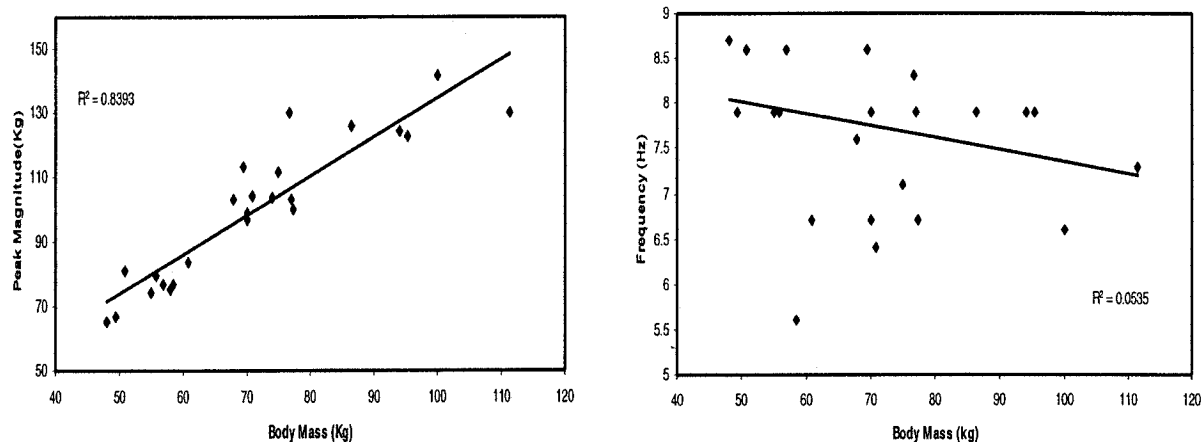


Figure 3.19: Dependence of the peak backrest APMS magnitude and the corresponding frequency on the body mass (hands-in-lap).

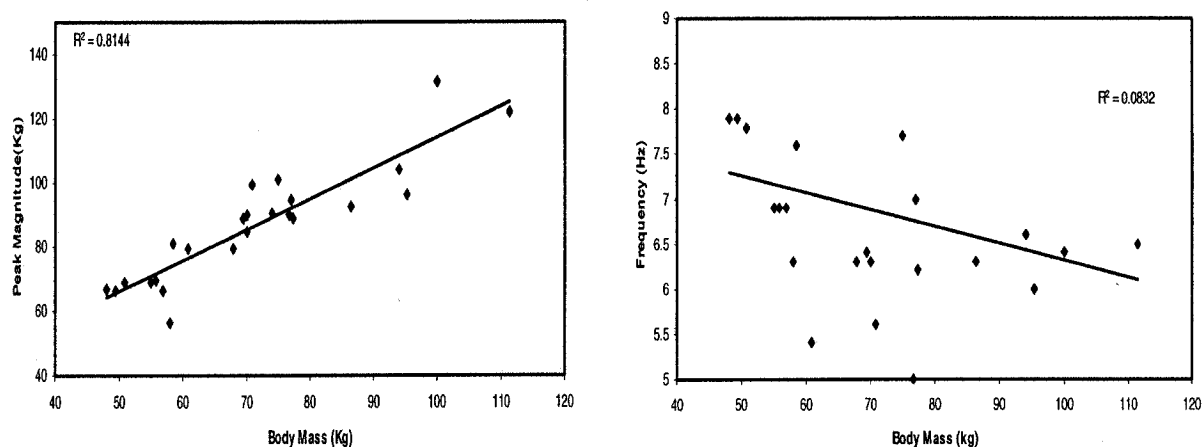


Figure 3.20: Dependence of the peak backrest APMS magnitude and the corresponding frequency on the body mass (hands-on-steering wheel).

Figures 3.21 and 3.22 illustrate both the seat pan and the backrest mean APMS magnitude response characteristics of seated occupants within the four mass ranges for both sitting postures involving hands-in-lap and hands-on-steering wheel. The results show the data obtained for the subject-selected feet position (M). The results also show the overall mean response of all 24 subjects, it is apparent that a heavier occupant yields higher static and peak magnitudes of both the seat pan and the backrest APMS responses. The body weight dependence of the magnitude responses, however, is observed to be

relatively smaller at excitation frequencies above 10Hz. The APMS response of a heavier group thus tends to shift upwards at lower frequencies, irrespective of the hands position and the measurement location. The results also show that the overall mean responses of all 24 subjects (mean mass=71.2 kg) lie between those obtained for the 60.5 – 70 kg and 70.5 – 80 kg mass groups, over majority of the frequency range. The results further show that the primary resonance frequency of light-weight occupants is considerably higher than that of the heavier occupants.

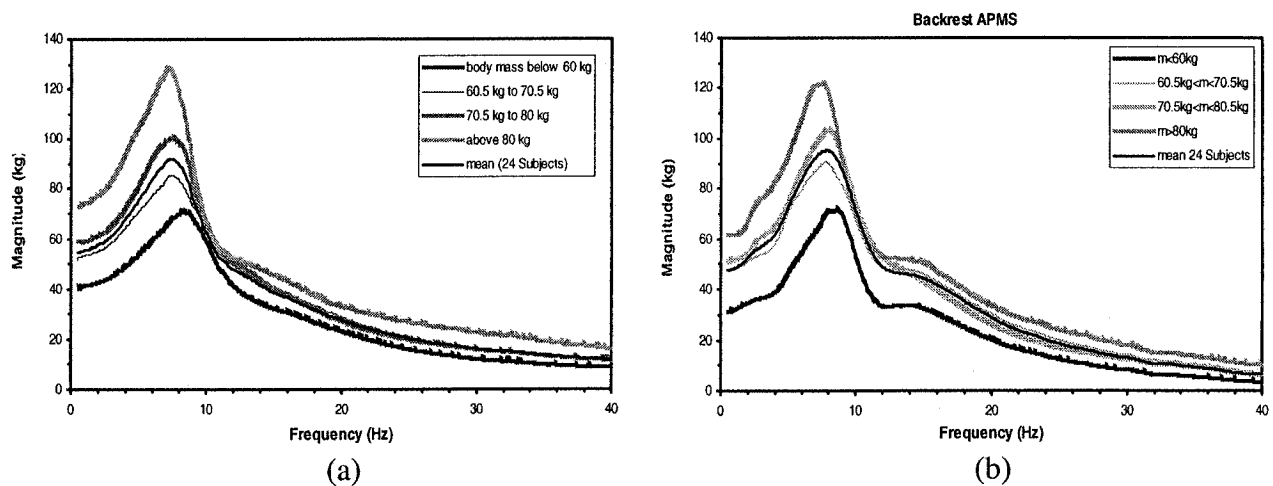


Figure 3.21: Mean APMS magnitude responses measured at: (a) seat pan; and (b) backrest, as a function of body mass (hands-in-lap).

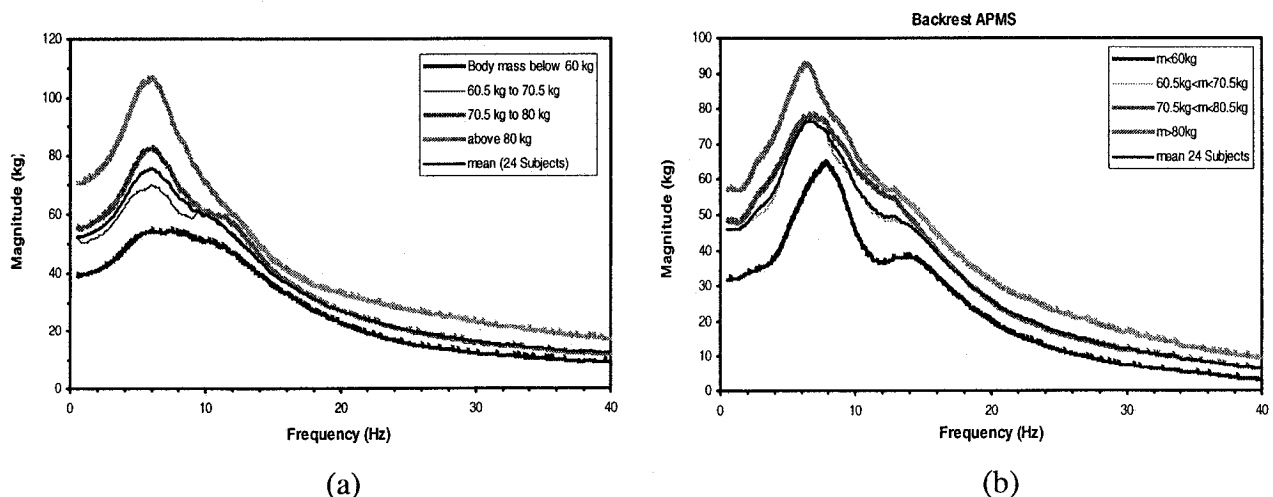


Figure 3.22: Mean APMS magnitude responses measured at: (a) seat pan; and (b) backrest, as a function of body mass (hands-on-steering wheel).

The mean curves, shown in Figures 3.21 and 3.22, are considered to represent the body weight-dependent biodynamic behaviors of seated occupants assuming postures representative of passengers and drivers in automobiles, and exposed to vertical vibration in the $0.25 - 1.0 m/s^2$ r.m.s. acceleration range.

The mean, minimum and maximum values of the apparent mass magnitude and phase responses measured at the seat pan are compared with the range of idealized values proposed in ISO-5982 [59], as shown in Figures 3.23 and 3.24, respectively, for the two hands positions. It should be noted that the limits defined ISO-5982 apply for hands-in-lap posture alone. The fundamental frequency observed from the measured data is considerably larger than that reflected by the idealized values, while the measured seat pan APMS magnitudes are significantly higher than the recommended idealized values. These differences in the magnitude responses and the fundamental frequency are most likely attributed to the automotive posture considered in this study, while the idealized values are reported for the back unsupported posture and relatively higher seats with flat pan. Moreover, the idealized values have been derived from data attained under relatively high magnitudes of vibration ($1-3 m/s^2$ r.m.s. acceleration), which may cause ‘softening’ of the seated body [1]. It should be noted that the seat backrest APMS responses do not yet exist in the published literature to permit a comparison of the measured data. It is found that it is important to include the backrest support as the backrest support increases the natural frequency of the seat-pan APMS significantly [47].

The measured phase data also differs considerably from the reported idealized data at frequencies below 10 Hz. Both the measured and the reported phase responses converge asymptotically towards -90° at frequencies above 10 Hz. Considerable

deviations in the phase response at frequencies below 10 Hz are mostly related to the observed differences in the fundamental frequencies. Although the standardized data are considered valid for the hands-in-lap posture, similar levels of differences are also observed between the measured data at the seat pan and the standardized values. The data acquired for the 24 subjects under same conditions are analyzed to derive the mean responses, which are then examined to response trends in relation to variations in the hands position, and the magnitude of excitation. The data acquired for the individual objects, however, are applied to study the role of a few anthropometric factors.

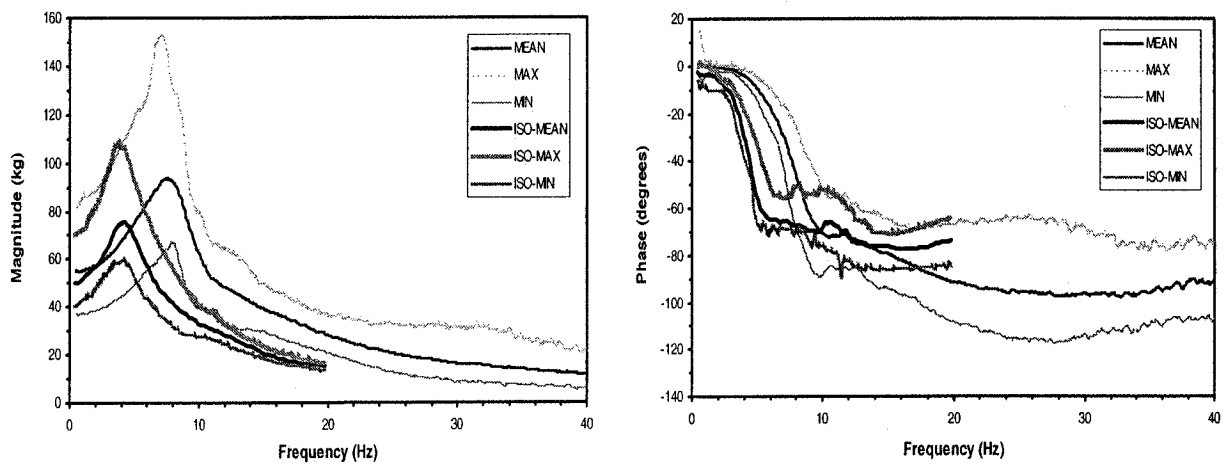


Figure 3.23: Comparisons of mean, maximum and minimum values of the measured seat pan APMS response (hands in lap) with the ranges reported in ISO-5982[59].

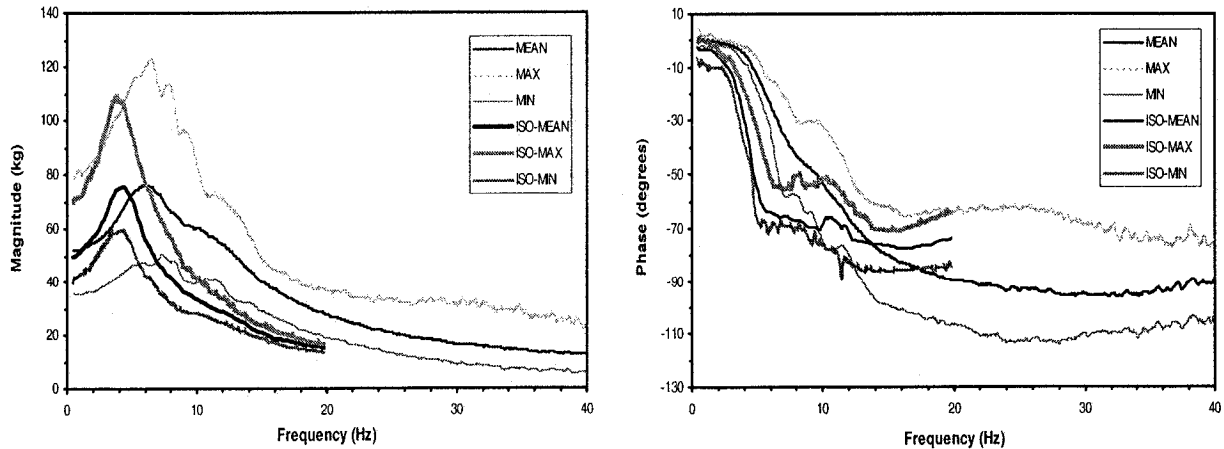


Figure 3.24: Comparisons of mean, maximum and minimum values of the measured seat pan APMS response (hands on steering wheel) with the ranges reported in ISO-5982[59].

3.3.2 Influence of BMI and BF

Apart from the body mass effect, which is quite apparent from the results presented in the previous section, the APMS responses are also influenced by the body build. The effects of body mass build could be investigated using the body mass index (BMI) and the body fat (BF). Figures 3.25 and 3.26 illustrate the relationship between the peak APMS magnitudes derived from the data acquired for individual subjects, with the BMI and BF percentage of the same individual. The results are presented for both hands positions, subject selected feet position (M) and W2 excitation.

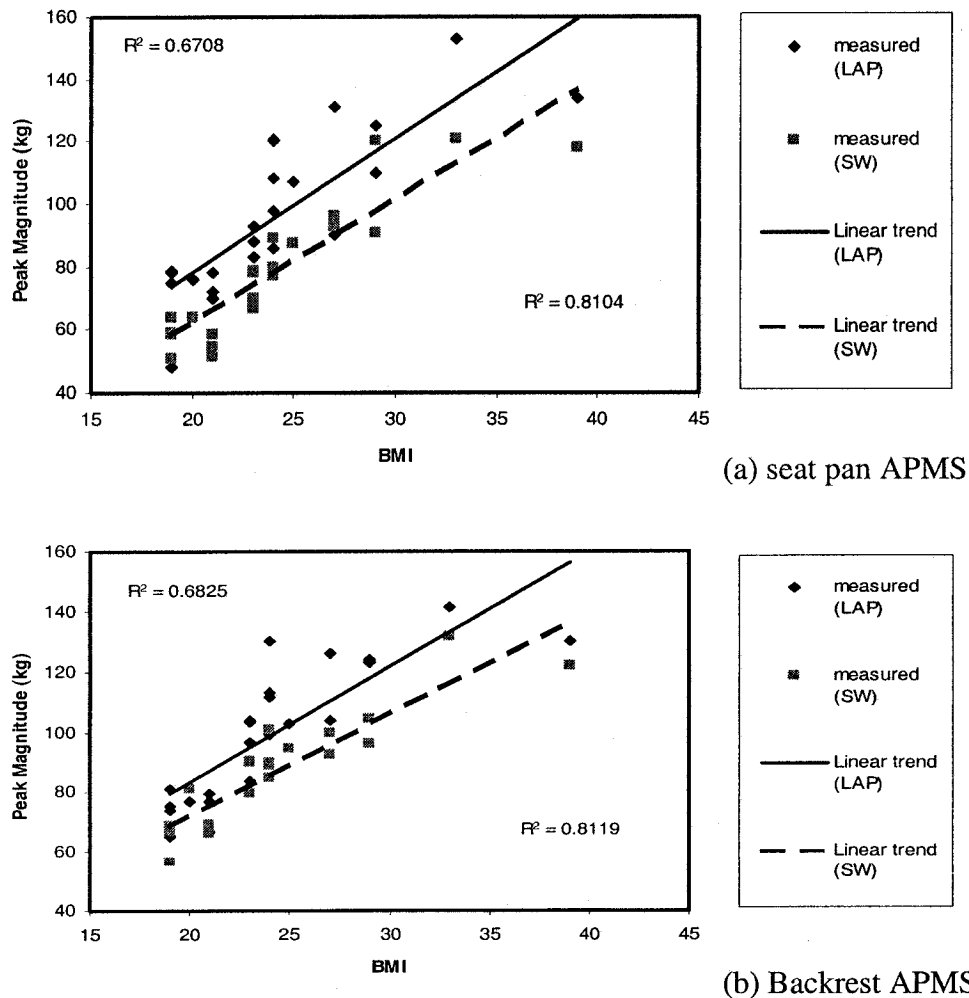


Figure 3.25: Dependence of the peak seat-pan and backrest APMS magnitude on the BMI.

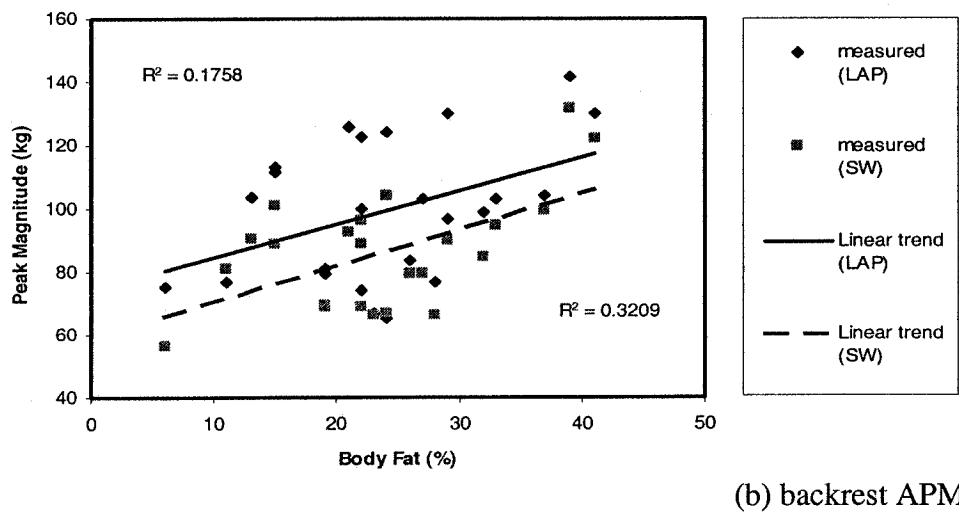
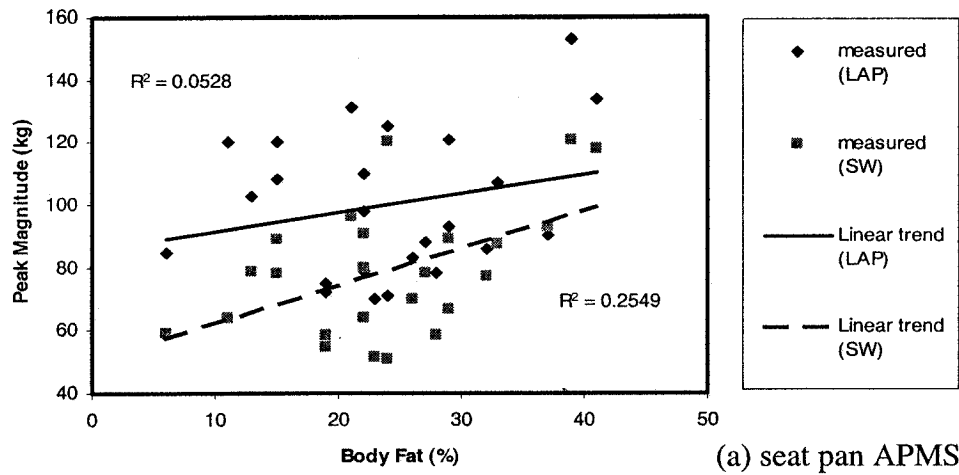


Figure 3.26: Dependence of the peak seat-pan and backrest APMS magnitude on BF.

The results show reasonably good correlations for both the peak seat-pan APMS and the backrest APMS with the BMI, irrespective of the hands position ($R^2 > 0.8$). The results suggest that the peak magnitudes measured at both the seat pan and the backrest increase linearly with the BMI, as observed in the case of the body mass. The results further show that the peak magnitudes of the seat pan and the backrest APMS for hands-in-lap (LAP) posture are higher than those measured for the hands-on-steering wheel (SW) posture. The difference in the peak magnitudes for the LAP and SW postures is

nearly constant for the entire range of BMI considered. Moreover the peak magnitudes of the backrest APMS are comparable with those of the seat-pan, even though the backrest supports a much smaller portion of the body mass. Figure 3.26 also suggests an increasing trend for the seat-pan and backrest peak APMS magnitude with increasing BF. The correlations of the magnitudes with the BF, however, are extremely poor. It may thus be concluded that the peak APMS response does not show a clear trend with respect to body fat.

3.3.3 Correlation between the measured APMS magnitude at seat pan and backrest

A few studies have reported that the magnitude of vibration transmitted to the head of a seated individual increases when the upper body is supported against a backrest, when compared to that encountered while sitting without a backrest [32,47,48]. Sitting with a backrest in an automobile seat helps to reduce the muscle tensions and to maintain a stable and controlled sitting posture in driving [1,8]. The body contact with the backrest also permits for transmission of vibration through the backrest. Recently Nawayseh and Griffin [66,67] measured the forces in the fore-and-aft direction at the backrest for 12 male subjects in four sitting postures, while exposed to four different magnitudes of vibration. The magnitudes of forces measured at backrest were found to be very low due to the vertical backrest used in the study. Thus far, no attempts have been made to study the dynamic interactions of the seated body with an inclined backrest, and the correlation between the APMS magnitudes measured at seat pan and backrest.

The mean APMS data obtained for both the seat-pan and the backrest corresponding to feet position M and W2 excitation are compared to demonstrate the

relative significance of the backrest APMS. Figures 3.27 illustrate comparisons of the mean seat pan and backrest APMS magnitude responses for both hands positions and W2 white noise excitation. The results show that the mean backrest APMS magnitudes are comparable with the seat pan magnitudes in the entire frequency range, even though the backrest supports a significantly smaller proportion of the body mass. The results suggest that the entire upper body experiences horizontal motion under exposure to vertical vibration. The APMS magnitudes at low frequencies, near 0.5 Hz, could be related to the static body mass supported by the seat pan and the backrest. The results show that the magnitude of the backrest APMS is quite comparable to that of the seat pan APMS for both hands position. Relatively larger scatter between the seat pan and the backrest APMS magnitude respond is observed for the hands on steering wheel posture over the entire frequency range, which may be attributed to the additional body support provided by the steering wheel. Another noticeable difference is that the backrest APMS reveals two notable peaks for both hands positions in the vicinity of 8 Hz and 14 Hz.

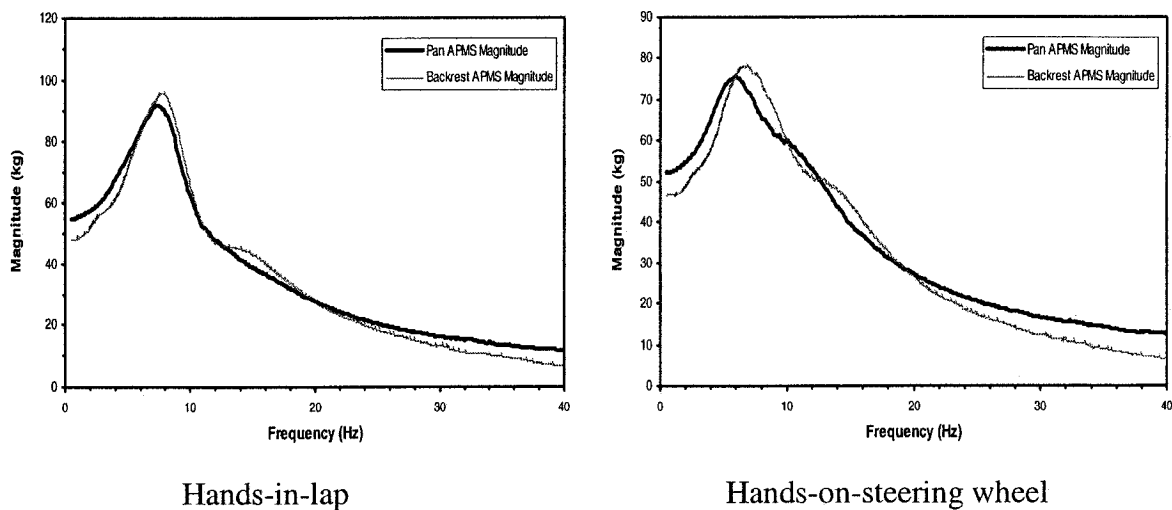


Figure 3.27: Comparisons of the APMS magnitude responses measured on the seat-pan and the backrest.

Figure 3.28 also illustrate the correlation between the measured APMS magnitude at seat pan and the backrest in terms of the ratio of the pan APMS magnitude to the backrest APMS magnitude. The results suggest that the interactions with the backrest constitute an important component of the occupant seating dynamics. The seat backrest APMS thus needs to be considered in the study of biodynamic responses of the seated occupants. At frequencies below 20 Hz, the backrest APMS (M_b) is comparable to that of the pan (M_p). The results further show that at low frequencies around 0.5 Hz, a larger static body weight is supported by the seat pan than that supported by the seat backrest.

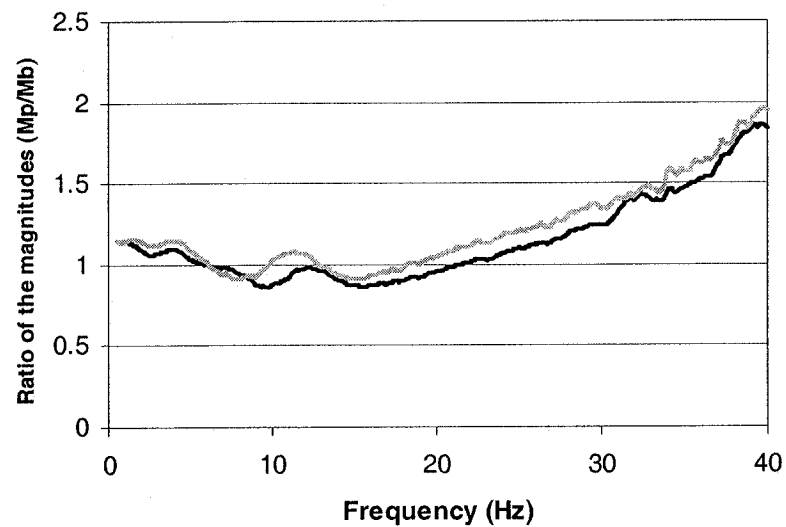


Figure 3.28: Variation in the ratio of the pan APMS magnitude (M_p) to the backrest APMS magnitude (M_b).

3.3.4 The APMS data normalization

Owing to the significant effects of the body mass on the APMS magnitude, the data measured on the seat pan are widely normalized with respect to the static body

weight supported by the pan [1,39,68]. Normalizing the biodynamic response greatly reduces the scatter among the APMS magnitude data acquired for different subjects, and it can eliminate the strong effects of the body mass in order to study the effects of other seat or posture-related factors [68]. Several methods of normalization have been used in the reported studies. Fairley and Griffin [60] derived the “normalized apparent mass” for each subject by dividing the apparent mass of the same subject measured at a low frequency of 0.5 Hz. Holmlund et al. [42], Wu et al. [8], and Rakheja et al. [62] normalized the measured data for each subject corresponding to each posture with respect to the respective static mass supported by the seat. Both the approaches yield comparable results, since the APMS response at 0.5 Hz is close to the static mass on the seat pan. In this study the measured APMS data on the seat pan for each subject is normalized with respect to the static seated weight of the same subject (weight supported by the pan), and the measured APMS data on seat backrest for each subject is normalized by dividing the apparent mass value by the upper body weight, estimated from the anthropometric data [58], for the same subject in order to facilitate the comparison and identification of significant contributing factors. The static body weights supported the seat pan and the backrest have been summarized in Tables 3.2 and 3.3, respectively, for all the subjects.

Figure 3.29 to 3.32 illustrate both pan and back APMS normalized magnitude responses of the 24 subjects, seated with different hands position, under white noise and track measured vertical vibration. A comparison of these results with those presented in Figures 3.1 to 3.16 clearly reveal that normalization reduces the scatter of the magnitude responses at frequencies below 10Hz. The results show good consistency in the normalized magnitude responses of all subjects, irrespective of the excitation level and

hands position. Furthermore the normalized measured data exhibit unity values of the normalized magnitude at very low frequencies suggesting that the APMS magnitude is equal to the static body mass supported by the seat.

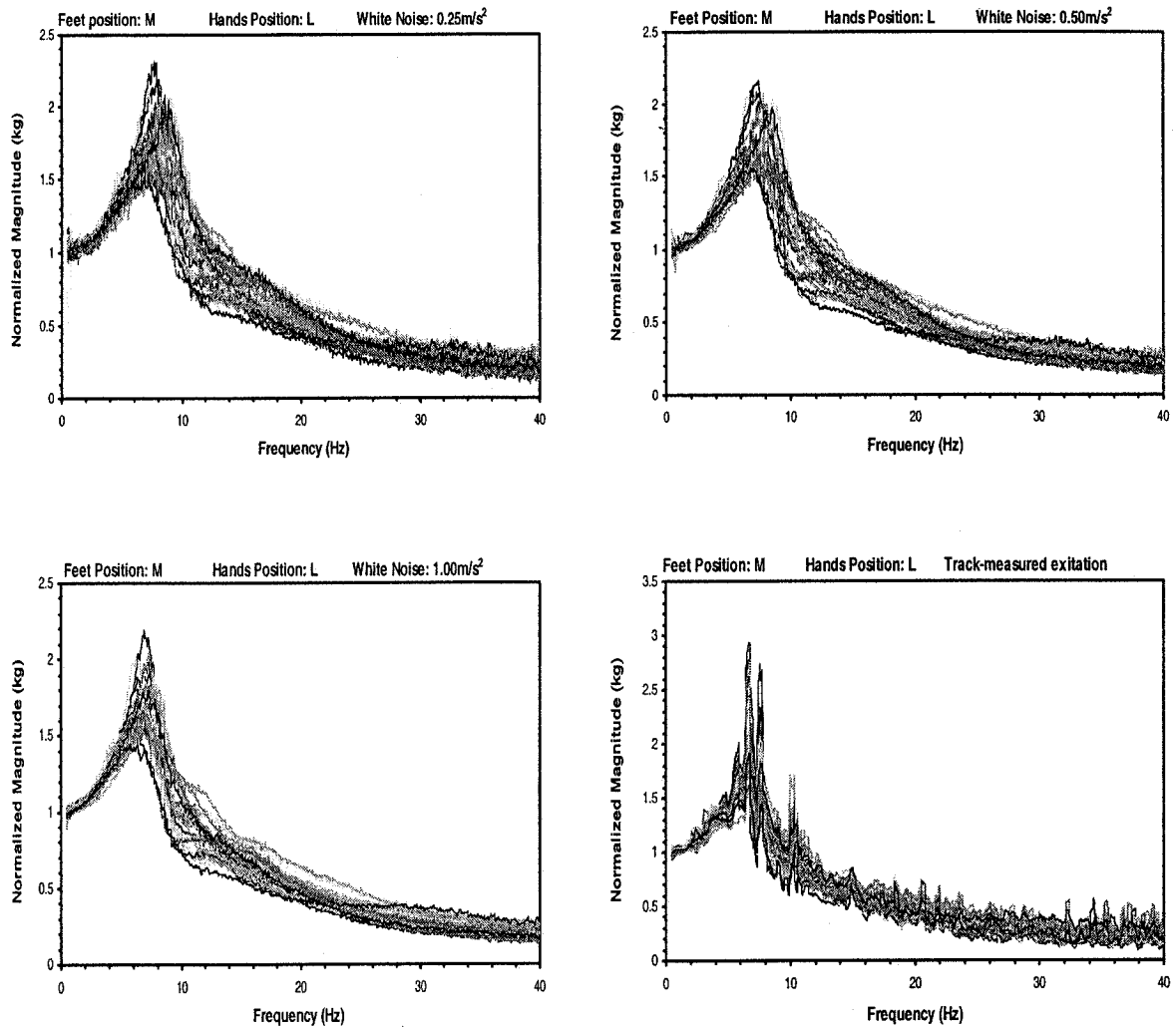


Figure 3.29: The normalized APMS magnitude response of 24 subjects measured at the seat pan under different levels of vertical vibration.

The normalized magnitude response on the seat pan of all the subjects assuming passenger posture exhibits a single peak in the 6.5 to 8.6 Hz frequency range, for all

excitations, as seen in Figure 3.29. The majority of the curves attained for driver posture exhibit two peaks, as shown in Figure 3.30. The primary response peak occurs in the 5.1 to 8.2 Hz range, while the second peak (if present) occurs over a wider frequency range, 10 to 12 Hz, depending upon the excitation level. The normalized magnitude responses of the 24 subjects measured at the seat backrest presented in Figures 3.31 and 3.32 for the two postures show a peak at a lower frequency around 2 Hz, which may be associated with the pitch motion of the upper body [63]. The magnitude responses of the 24 subjects

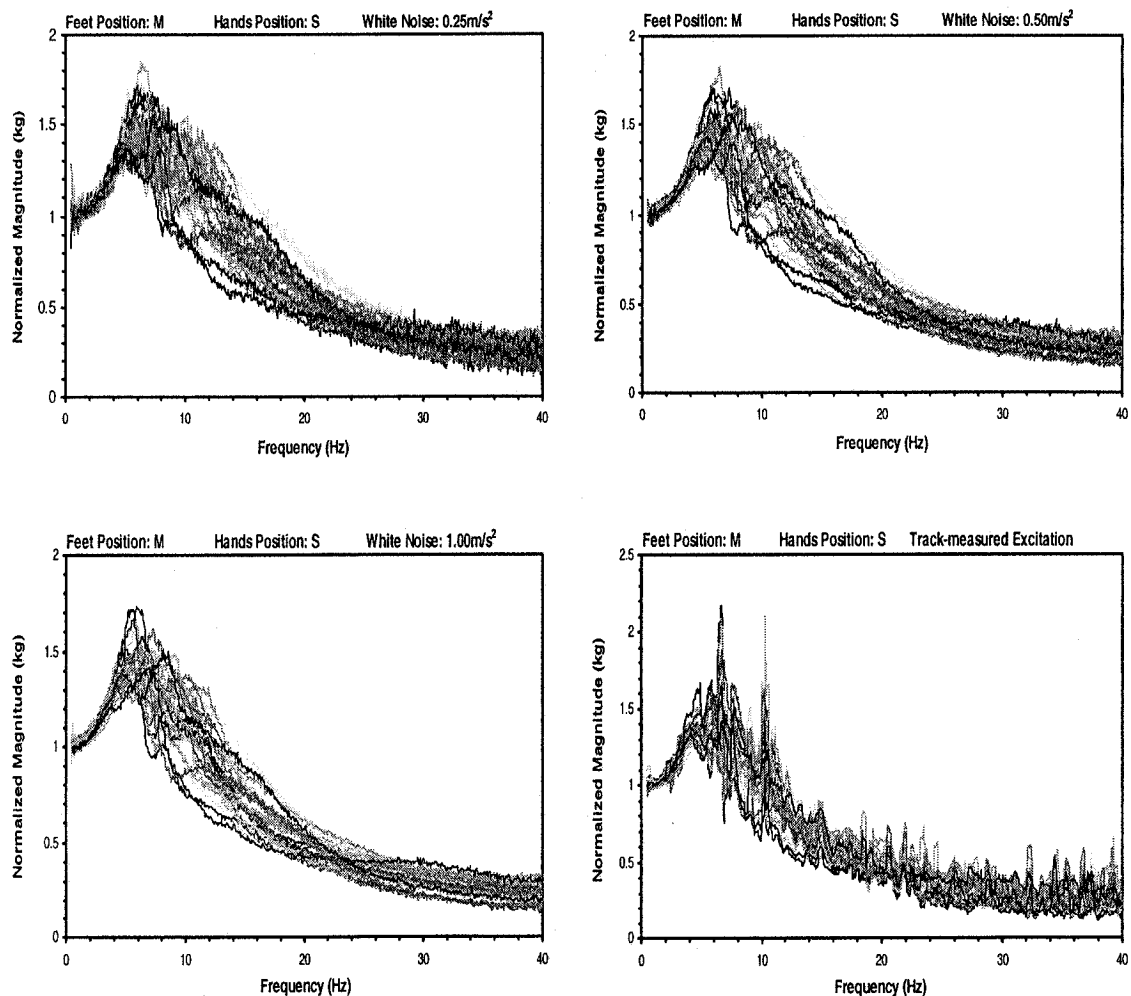


Figure 3.30: The normalized APMS magnitude response of 24 subjects measured at the seat pan under different levels of vibration.

obtained under postures generally show two distinct peaks in the magnitude responses. While the primary peak occurs in the 5.5 to 9.5 Hz range for passenger-like posture and 5 to 9.5 Hz for the driver-like posture, and the secondary peak (if present) occurs in the 10 to 15 Hz range for both postures, depending upon the excitation level. The frequency corresponding to the peak value of the normalized APMS on the seat pan is considered to represent the fundamental resonant frequency of the seated occupant.

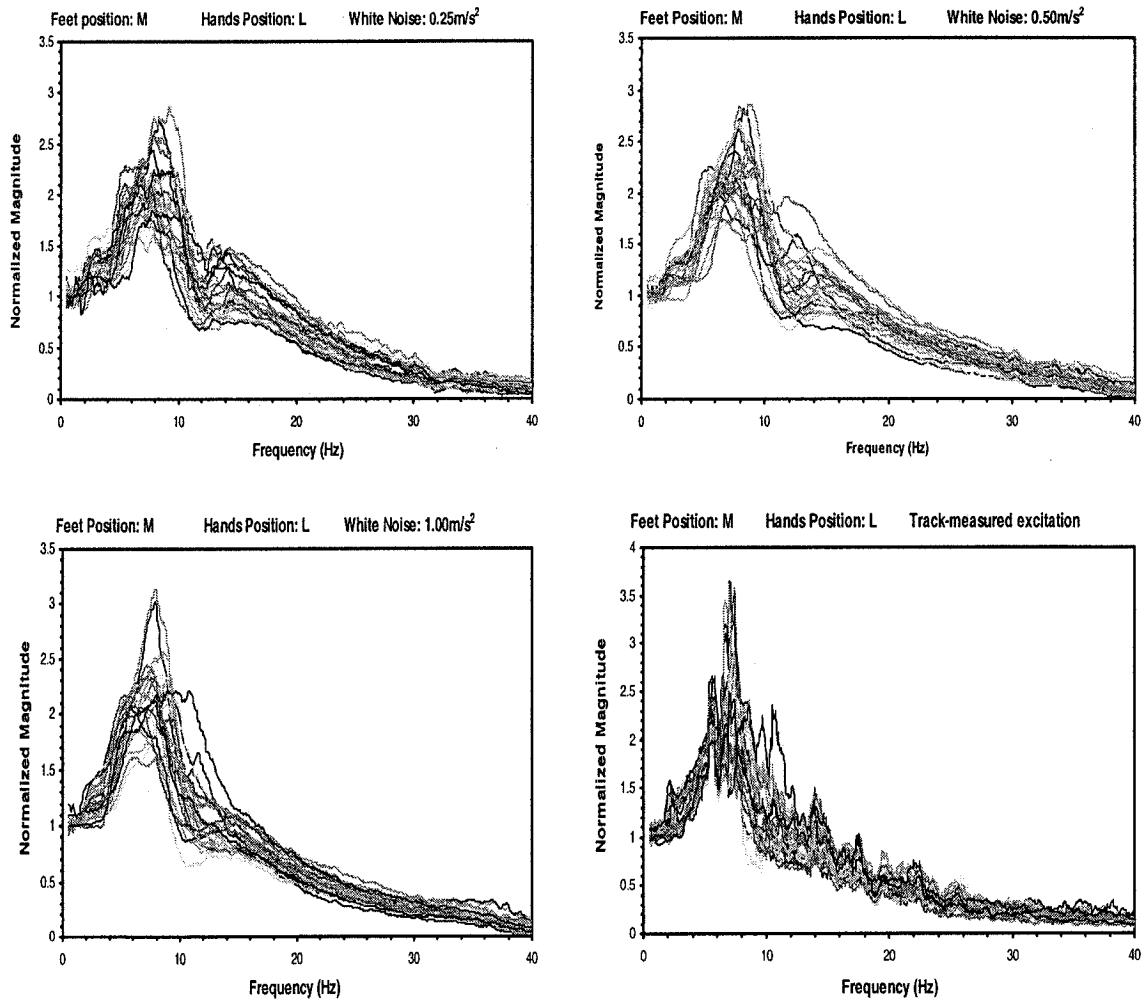


Figure 3.31: The normalized APMS magnitude response of 24 subjects measured at the seat backrest under different levels of vibration.

The frequency corresponding to the peak value of the normalized APMS on the back is used to represent the fundamental resonant frequency of upper body of the seated occupant. The results further show that the peak magnitudes attained with a driving posture are considerably smaller than those obtained with a passenger posture. The data obtained under the track-measured excitations, exhibit larger peak response, which is most likely attributed to the low acceleration signal in the 6 to 8 Hz frequency range.

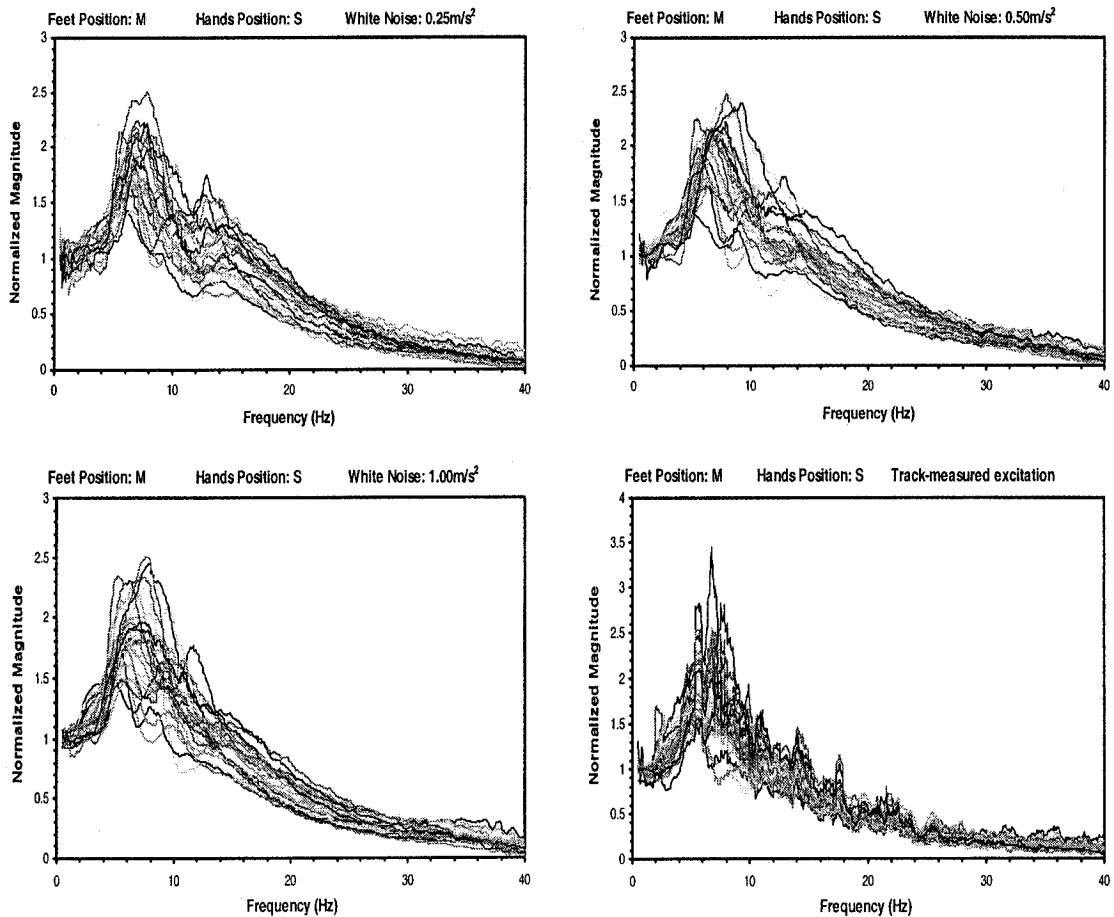


Figure 3.32: The normalized APMS magnitude response of 24 subjects measured at the seat backrest under different levels of vibration.

Figure 3.33 to 3.34 illustrate the mean, maximum, minimum and the standard deviation (SD) of the mean normalized APMS magnitude and phase responses for both

seat pan and the backrest corresponding to the W2 excitation. All the measured data reveal relatively large standard error in the vicinity of the fundamental resonant frequency, where the measured response tends to vary considerably. It should be noted that for the passenger-like posture, all the mean curves exhibit primary peak in the 7 to 8 Hz frequency range, while that for the driving posture it is observed near 6 Hz. The second magnitude peak (if present) occurs near 10.5 Hz for the seat pan data and near 14 Hz for the backrest data. The phase responses for both postures are quite comparable. The mean phase response of the seat pan data converges towards -90° , while that of the seat backrest data converges towards -110° .

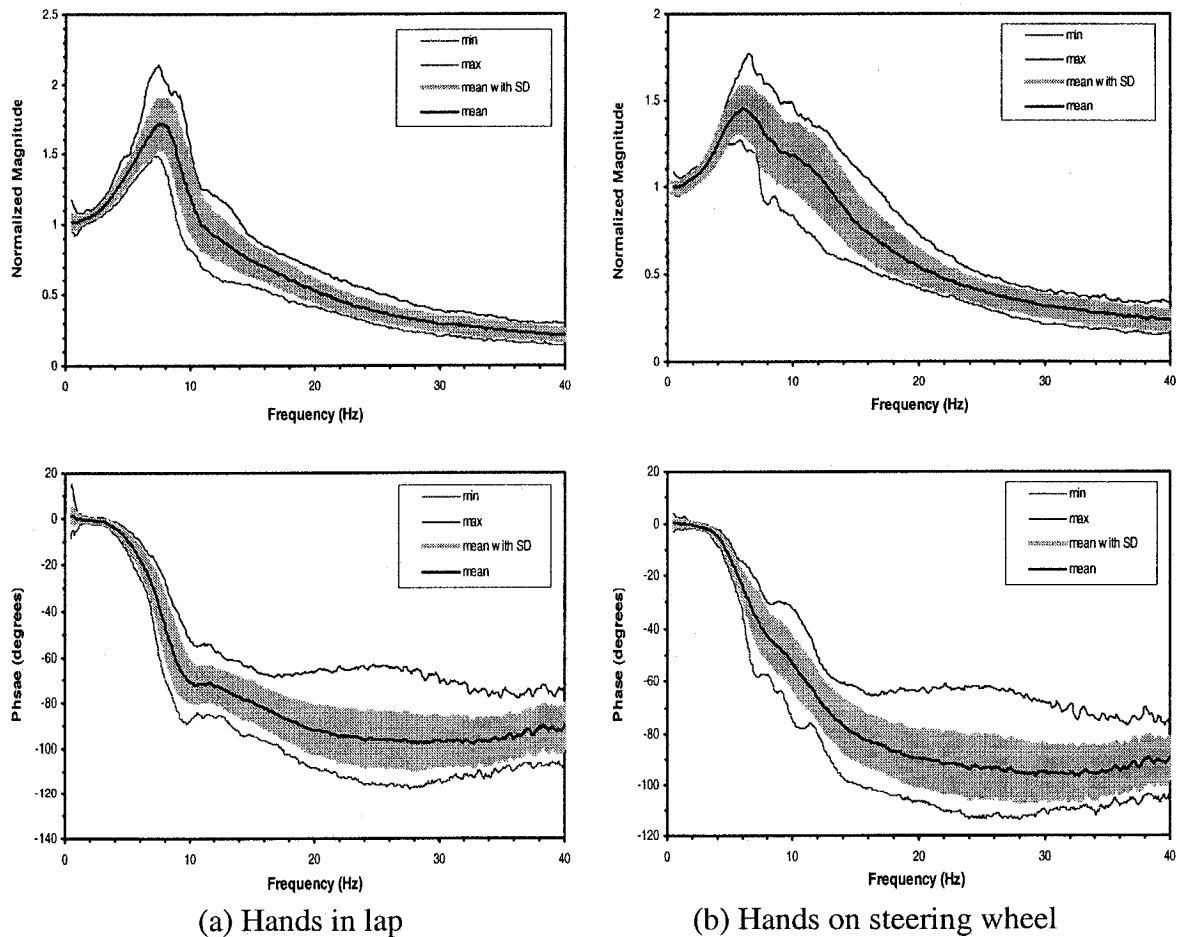
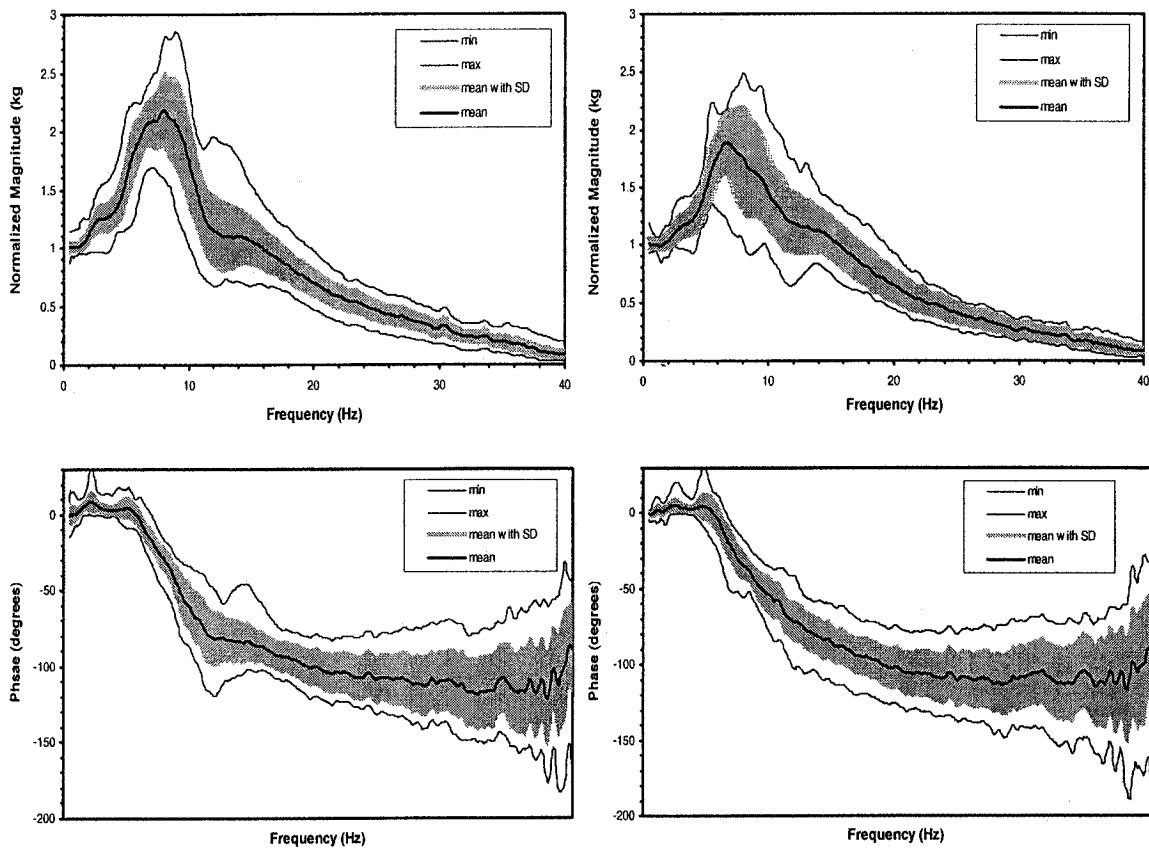


Figure 3.33: The mean, standard deviation, and lower and upper bounds of the normalized APMS magnitude and phase responses measured at the seat pan.



(a) Hands in lap

(b) Hands on steering wheel

Figure 3.34: The mean, standard deviation, and lower and upper bounds of the normalized APMS magnitude and phase responses measured at the seat backrest.

3.3.5 The influence of the magnitude and the type of vibration excitation

The biodynamic response characteristics of the seated human occupants under varying levels of the whole-body vertical vibration have been investigated in many studies, as discussed in chapter 1. The majority of these studies have shown negligible effects of magnitude of broad band random and sinusoidal excitations [42,44]. The measured data attained in this study under different levels of broad-band excitations and track measured excitation are examined to identify the influence of magnitude of

excitation. The mean APMS magnitude and the phase curves obtained under 0.25, 0.5 and 1.0 m/s^2 rms broad-band excitations, and the track-measured excitations are compared in Figures 3.35 and 3.36, for the hands in lap and hands on steering wheel postures, respectively.

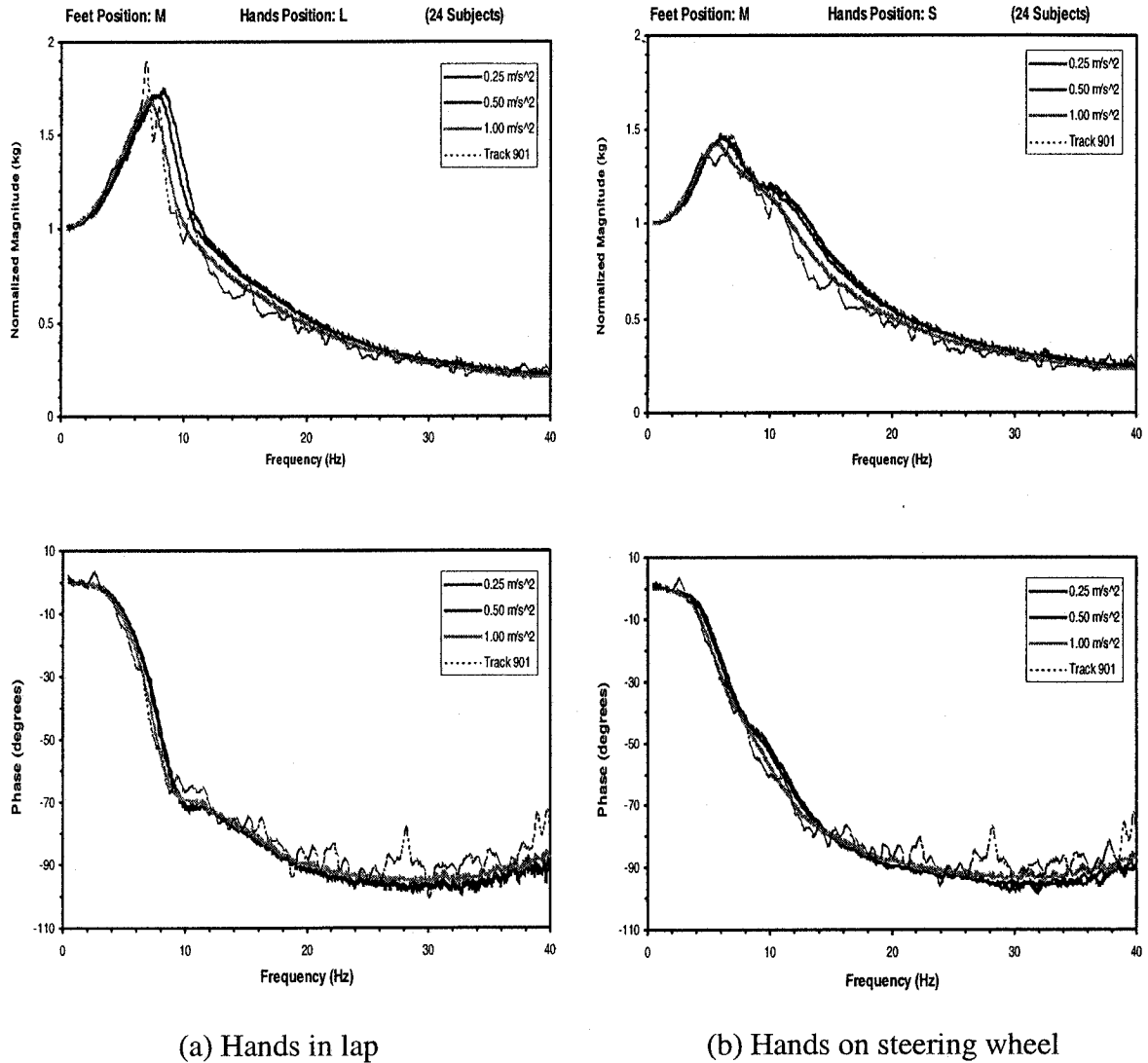


Figure 3.35: The mean APMS response on the seat pan attained for different magnitude and types of vibration excitations.

The mean APMS magnitudes on the seat pan of 24 subjects for both postures are shown in Figure 3.36. The results show that the peak magnitude and the corresponding frequency decrease slightly as the magnitude of broad-band excitation increases. The decrease in the fundamental frequency with increasing level of excitation have been attributed to softening of the seated body under higher excitations [1,8,63]. The mean magnitude response under track-measured excitation is close to that obtained under 1.0 m/s^2 white noise excitation. Since the overall rms acceleration due to the track-measured excitation is 1.07 m/s^2 , the results show insignificant influence of type of vibration excitation. The variations in the peak magnitude and the corresponding frequency of the mean APMS response of the seated occupants with hands on the steering wheel are observed to be considerably smaller. The mean phase response curves show insignificant influence of the magnitude and type of excitation.

The mean APMS magnitude responses measured on the seat backrest also show relatively small effects of magnitude of excitation on magnitude response around the fundamental resonant frequency, while the corresponding frequencies decrease slightly as the magnitude of the excitation increases, for both postures. For hands-on-steering wheel posture, the mean magnitude response curves consistently reveal the presence of a distinct second peak in the 12 to 14 Hz frequency range. The mean phase response tends to increase at frequencies above 20 Hz under the track-measured excitation. This may suggest that the biodynamic response behavior of the seated occupants is somewhat nonlinear. In light of only slight variations in the mean magnitude and phase response due to different excitations, however, the linearity of the response may be justifiable. The mean of the mean data sets is thus considered to represent the mean biodynamic response

of the 24 subjects under different levels and types of vibration excitations. A total of four means of mean data sets are thus defined as the target response functions corresponding to the two different postures (hands in lap and hands on steering wheel) and two different measurement locations (seat pan and backrest).

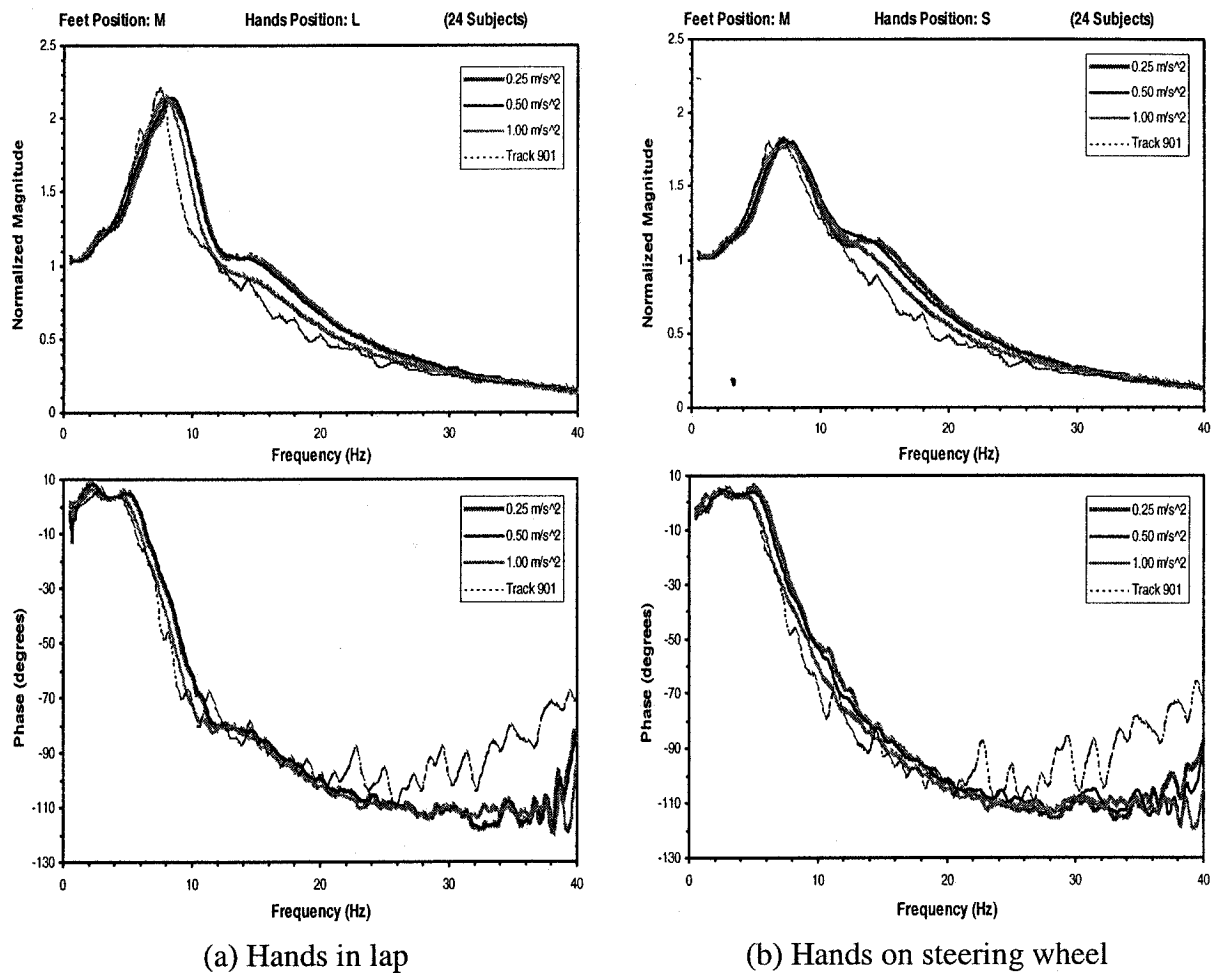


Figure 3.36: The mean APMS response on the seat backrest attained for different magnitude and types of vibration excitations.

3.3.6 Influence of the hands position

The mean data sets obtained upon combining the mean data corresponding to different magnitudes of broad band random excitations and the subject-selected feet

position M are further explored to identify the contributions due to the hands position. Figures 3.37 clearly show important differences in the mean APMS responses due to different hands position. The peak magnitudes of the mean normalized APMS response of occupants sitting with hands-in-lap measured on the seat pan and the backrest is significantly larger than that obtained with hands-on-steering wheel. The primary resonance frequency of the occupants, as observed from the mean magnitude response with hands-in-lap, occurs near 7.8 Hz. The corresponding phase response increases rapidly to approximately -70° at 10 Hz. The hands on steering wheel posture yields two peaks in the mean magnitude response; the primary resonant frequency occurs at a lower frequency around 6.1 Hz. The low magnitude of the primary peak under this posture suggests well-damped behavior of the body, which may be attributed to the additional body support provided by the steering wheel. The secondary resonant frequency appears to be in the vicinity of 10-11 Hz. The corresponding mean phase response increases rapidly to approximately -45° near 8 Hz and remains considerably less than that attained with hands in lap up to approximately 14 Hz. At frequencies above 14 Hz, both postures yield almost identical mean magnitude and phase response.

The influence of the hands position on the APMS response of the seat backrest appears to be similar to that observed for the seat pan APMS response. The only difference is that both hands-in-lap and hands-on-steering wheel postures yield three peaks in the mean APMS magnitude response measured on the backrest, in the vicinity of 2, 6-8, and 14 Hz. The primary resonant frequency of the mean APMS response of occupants sitting with hands in lap and measured on the backrest occurs at 8.1 Hz, with hands on steering wheel it occurs near 6.5 Hz. The secondary resonant frequency with

both postures appears to be in the vicinity of 14 Hz. Moreover, the mean responses show presence of a smaller peak near 2 Hz, which is attributable to the pitch motion of the upper body. The results show that these frequencies corresponding to the peak magnitudes on seat back are slightly higher than those observed from the seat pan response.

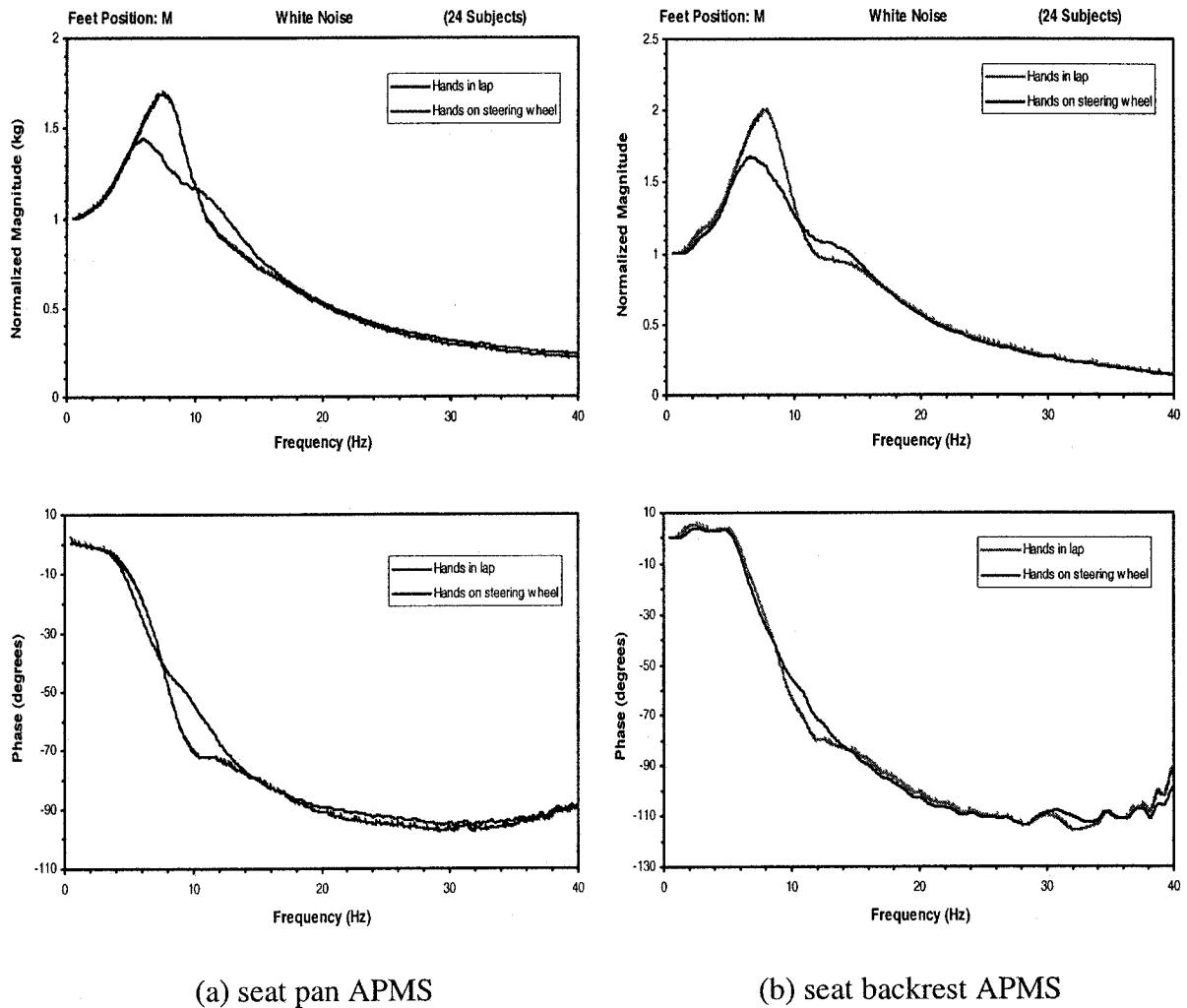


Figure 3.37: The comparison of the mean APMS magnitude responses measured on the seat pan and backrest for different hands positions.

3.3.7 Influence of gender

A few studies have established that the biodynamic response of seated occupants is influenced by the gender, while some of the studies have concluded the gender effect to be mostly insignificant [34,68]. The data measured data in this study were grouped separately for 12 male and 12 female subjects, and hands in the lap and on the steering wheel to study the influence of gender. Figures 3.38 and 3.39 illustrate comparisons of the mean magnitude and phase response characteristics obtained for 12 male and 12 female subjects. The mean curves obtained for white-noise excitations are compared with the overall mean for 24 subjects. All the results show only slight difference in the primary resonant frequency, while the mean magnitude response of male occupants measured on the seat pan is larger than that of the females in the vicinity of the primary resonant frequency. These differences are partly attributed to differences in body mass. The APMS magnitude response of the male subjects, measured on the backrest, is also higher corresponding to the lower resonant frequencies, near 2 Hz, and 8.1 Hz for hands in lap, and 6.5 Hz for hands on steering wheel, as seen in Figure 3.39. The magnitude response of the female subjects, however, trends to be higher near the higher resonant mode around 14 Hz. This trend indicates nonlinear gender effects and biodynamic response characteristics of the seated occupants. A further examination reveals that the mean seat pan phase response of male subjects is slightly larger than that of the female subjects at frequencies above 7 Hz for both postures, which such a trend is not evident in the phase response of APMS measured on the seat back. Owing to the small differences in the magnitude, strong dependence of the body mass and relatively large inter-subject variability of the data, the gender effects on the biodynamic responses may be considered

negligible, specifically for identification of the target data sets for occupant model development.

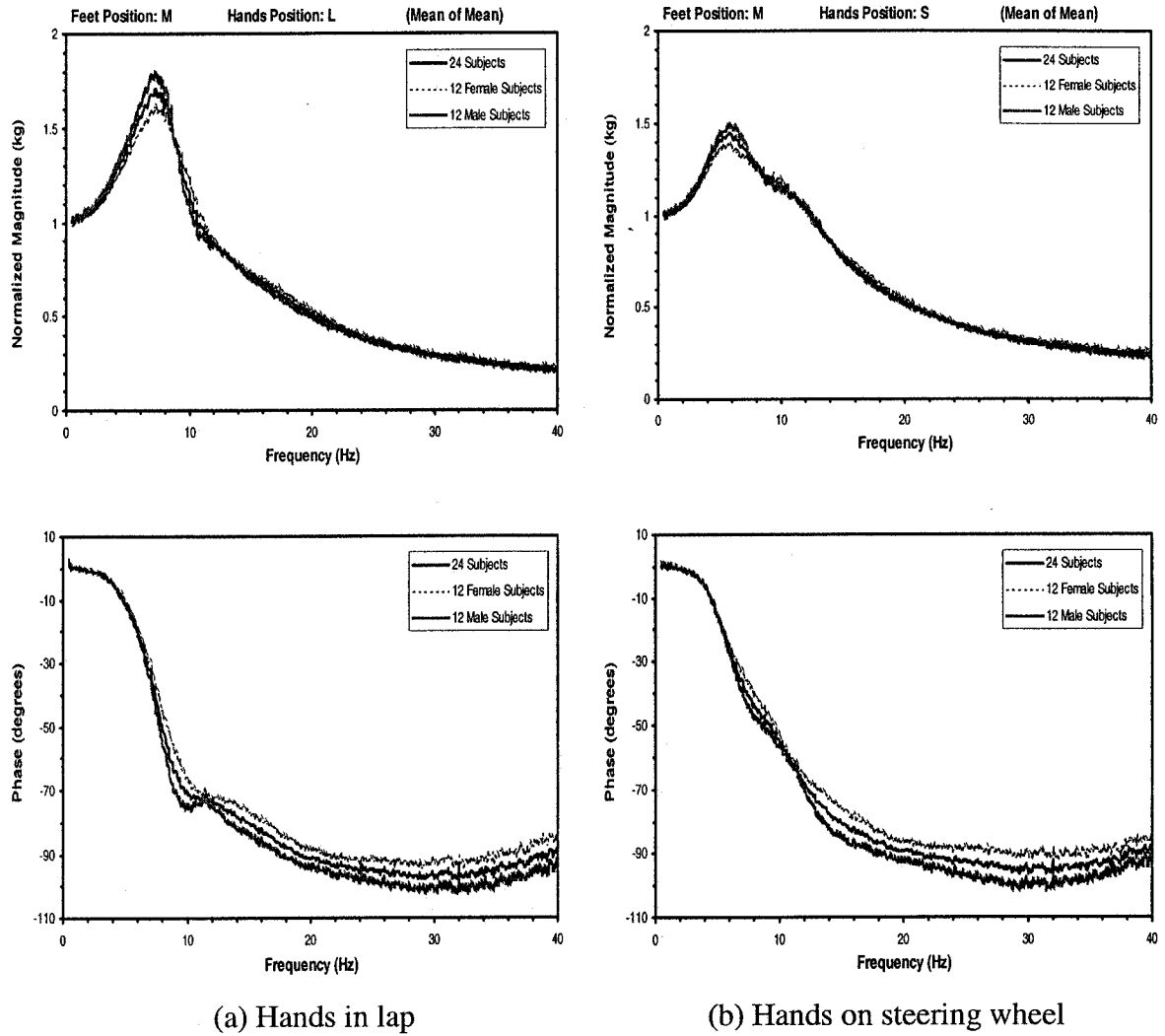


Figure 3.38: Comparisons of mean APMS responses measured on the seat pan with 12 male and 12 female subjects.

3.4 Summary

The biodynamic response characteristics of 24 human subjects (12 male and 12 female) were established under representative automotive postures applicable to drivers and passengers and vertical vibration of different magnitudes in the 0.5-40 Hz frequency

range. The results have shown that the vertical pan APMS responses of the occupants seated under an automotive posture differ considerably from those reported in most other studies, which considered significantly different postures and vibration excitation levels.

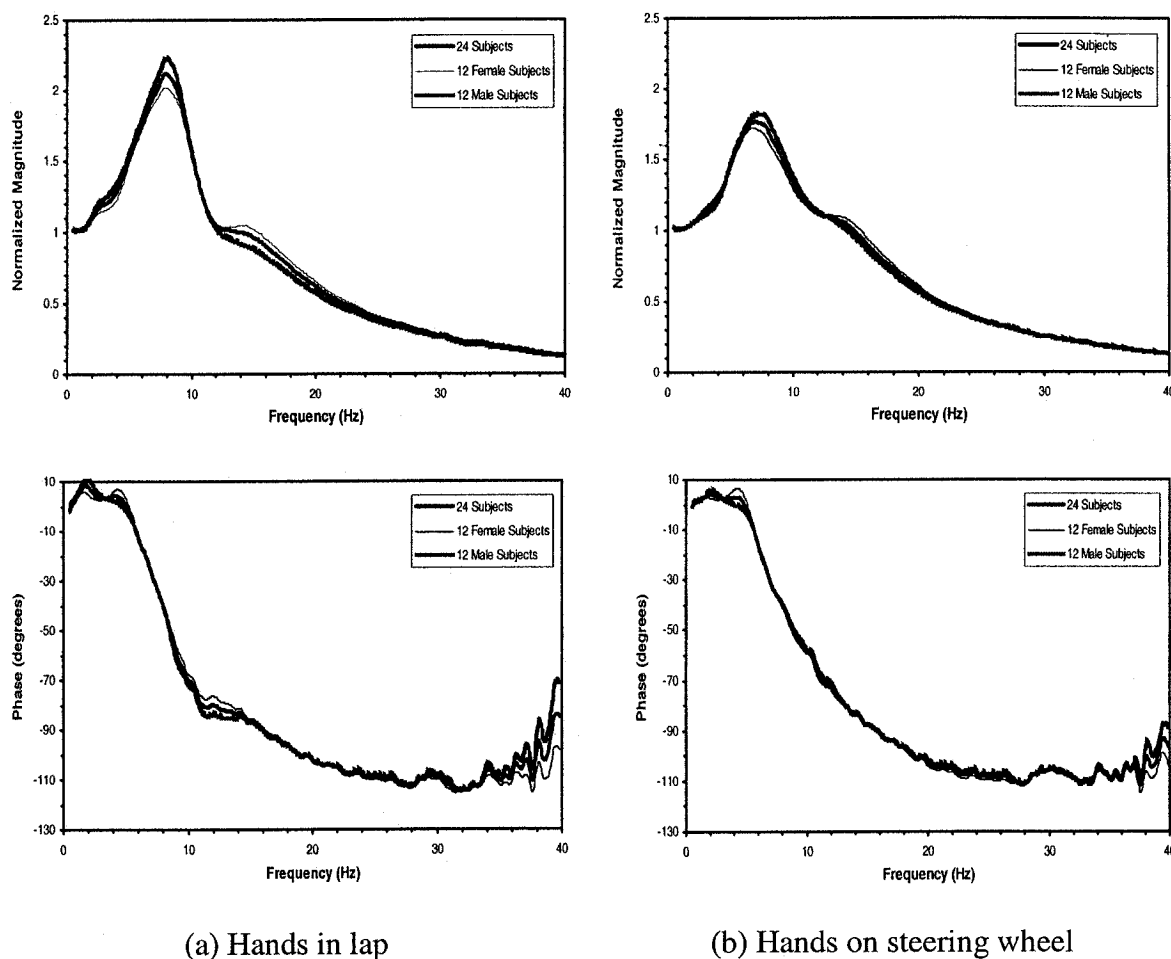


Figure 3.39: The comparisons of mean APMS responses measured on the seat backrest with 12 male and 12 female subjects.

The peak magnitudes of the APMS applicable to automobile passengers with hands in lap posture were observed to occur in 6.5-8.6 Hz frequency range, with mean at 7.8 Hz, which is considerably higher than that usually reported (5Hz) in the literature. The higher resonance frequency is most likely attributed to different sitting posture caused by the inclinations of the pan and the backrest, lower seated height and lower vibration

excitation levels considered for automobile occupants. Moreover, hands position was observed to have the most influential effect on the APMS response, the peak magnitude and corresponding frequency decreasing considerably when hands are moved from lap to the steering wheel (driver posture). A secondary resonance peak in the 10-13 Hz range becomes more apparent with hands-on-steering wheel (driver posture), while the dominant frequency is observed to occur in the 5.1-8.2 Hz range. At frequencies above 14 Hz, the differences in apparent mass response for the two postures become negligible.

Owing to the lack of reported biodynamic response characterizing the interactions of the seated human subjects with the seat backrest, the APMS response data acquired on the seat backrest provide important quantitative information on the interactions. Majority of the magnitude curves exhibit three peaks for both postures, where the first peak occurs near 2 Hz and could be attributed to pitch mode of the upper body. The primary peak magnitude of the APMS applicable to passenger posture were observed to occur in 5.5-9.5 Hz frequency range, with mean at 8.1 Hz. Hands position also was observed to have the most influential effect on the back APMS response; the peak magnitude and the corresponding frequency were considerably lower as the subjects changed their sitting posture from passenger to the driver. The dominant frequency is observed to occur in the 5-9.5 Hz range, with a mean at 6.5 Hz. All the datasets revealed secondary peaks in 10-15 Hz range, with mean around 13.5 Hz.

The body mass forms another most significant factor that affects the apparent mass response of the seated automobile occupants on both the seat pan and the seat backrest. A higher body mass, in general, yields higher peak magnitude response and lower corresponding frequency for both passenger and driver postures. The magnitude is also

observed to be higher over the entire frequency range when the mean body mass is increased. While a positive correlation could be established between peak apparent mass magnitude and the total body mass, the trend in decreasing fundamental frequency with increasing body mass showed a poor correlation. The results also suggest relatively negligible influence of the feet position, types and magnitude of the vibration excitation and gender. From the results, it is concluded that the biodynamic response of occupants seated with automotive postures and subject to vertical vibration need to be characterized, as a minimum, by two distinct functions for two postures: hands-in-lap and hands-on-steering wheel.

Chapter 4 Development of Human Body Model on Seat

4.1 Introduction

The development of an effective occupant-seat model involves four distinct tasks: (i) Characterization of biodynamic response characteristics of seated occupants under conditions representative of automobile environment, specifically the seated posture, and the intensity and frequency contents of vibration; (ii) Development of the occupant model based upon the biodynamic response behavior; (iii) Development of a mechanical model of the seat through characterization of physical and/or chemical properties of the polyurethane foams (PUF) and support mechanism; and (iv) Development and verification of the coupled occupant-seat model through experimentation with wide range of human subjects [55]. While the development of mechanical model of a seat involves characterization of complex properties of the PUF materials and the support mechanism, the occupant modeling task is considered to be far more complex due to extreme variabilities in the anthropometry, and the role of seat design and posture-related factors. Furthermore, considerable efforts are presently being made in developing anthropodynamic manikins for effective experimental assessments of seats, which could be desired on the basis of a reliable biodynamic or mechanical-equivalent model of the occupant [72].

A number of mechanical-equivalent models of the seated human occupant exposed to vertical vibration have been reported in the literature on the basis of the measured biodynamic responses [39,51,53,54,70]. These models have been thoroughly reviewed in Chapter 1. It was concluded that these models are not applicable for automotive seating, since they are developed for sitting without a backrest support, and

relatively high magnitudes of vibration. Moreover, the reported models have been developed on the basis of data acquired on seats with horizontal seat pan and vertical backrest. An automotive sitting posture constitutes considerable inclinations of the seat pan and the backrest, and thus considerably different dynamic interactions with both the seat pan the backrest. Moreover, the dynamic interactions of the occupant are strongly dependent upon the body mass and build, and the hands position. The development of an effective model for automotive seating applications thus necessitates consideration of: (i) dynamic interactions of the occupant with the seat pan and the backrest; (ii) variations in the body mass for representative population; and (iii) sitting posture as determined by the hands position. Furthermore, it is desirable to develop a simple model structure with limited degrees-of-freedom for ease of analyses, anthropodynamic manikin development, and integration to the seat model. Owing to the high degree of uncertainty associated with biomechanical properties of the biological system, it has been suggested that the masses within a multi-DOF model do not need to correspond with any specific body segment mass [8].

In this chapter, a 4-DOF mechanical-equivalent model of the seated occupant is proposed that incorporates adequate portion of the body resting on the seat pan and the backrest support, on the basis of the data acquired. The parameters of the baseline model are identified on the basis of the mean target APMS data, which would represent the mean body mass of 71.2 kg, and exposed to vertical vibration ranging from 0.25 to 1.0 m/s^2 rms acceleration. The proposed model differs from the reported models, since its structure is chosen such as to satisfy simultaneously both APMS responses on the seat pan and the seat back, while minimizing the number of parameters needed to describe the

model. Owing to the strong dependence on the body mass, a non-dimensional model formulation is chosen and parameters for subjects of different mass are identified on the basis of the mean data attained for occupants within four different mass groups. A generalized biodynamic model of the seated occupant is thus derived and its validity is demonstrated by comparing its response with the measured data attained for a few selected subjects.

4.2 Model development

A four-DOF model structure is formulated, as shown in Figure 4.1, to account for dynamic interactions of the body with both the seat pan and the backrest, while exposed to vertical vibration. The model structure also incorporates the geometric effects of typical automotive seat described in section 2.2, and comprises three masses coupled by linear elastic and damping elements constrained to translate along the axes shown in the figure. The rotational stiffness and damping characteristics of the body are neglected, assuming their negligible effect on the pan and the back APMS responses. The friction between the body-backrest interface is also assumed to be negligible. The masses m_1 and m_2 are introduced with an objective to describe the biodynamic behavior related to two resonant peaks observed in the APMS magnitude response in the frequency ranges around 7 Hz and 14 Hz, respectively, as observed from the measured data. The lower mass m_0 is introduced to increase the flexibility for tuning the model parameters without increasing the number of degrees-of-freedom. Although the model is not intended to relate to any anatomical structures of the human body, masses m_1 and m_2 may tentatively be taken to represent the upper body for the purpose of characterizing the back

biodynamic response and computing the static weight on the seat back. The sum of the masses, however, is taken to correspond to the body mass supported by the seat pan and seat back.

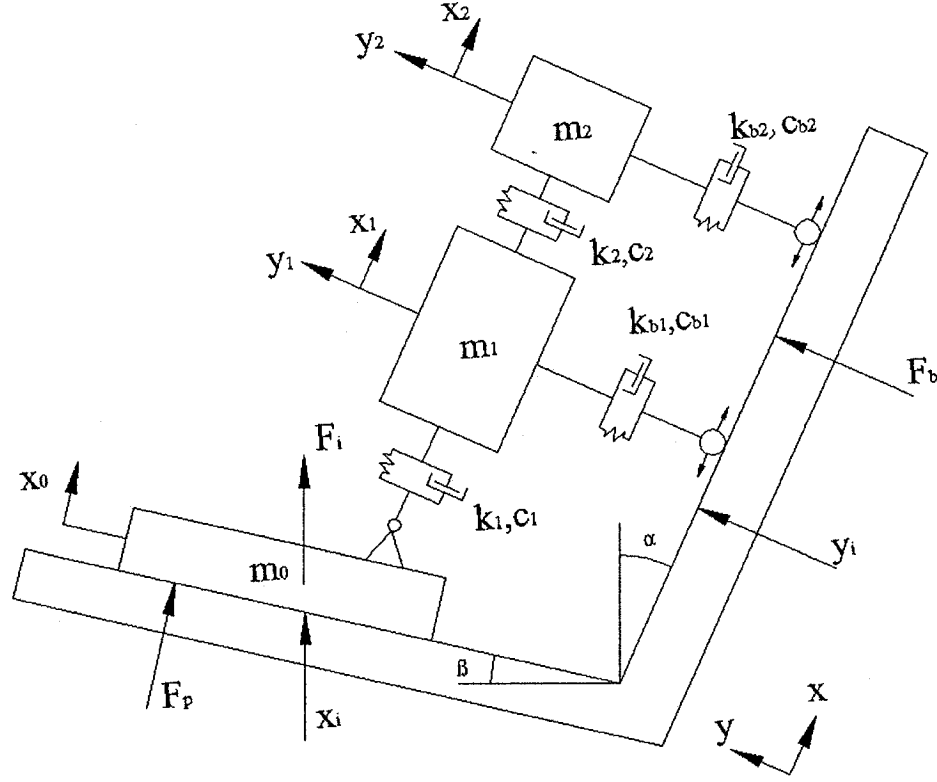


Figure 4.1: The proposed structure of the seated human biodynamic model.

Assuming linear properties of the elastic and damping elements, the motions of the masses along the x -axes can be described by the following differential equations of motion:

$$\begin{aligned} m_2 \ddot{x}_2 + k_2(x_2 - x_1) + c_2(\dot{x}_2 - \dot{x}_1) &= 0 \\ m_1 \ddot{x}_1 + k_2(x_1 - x_2) + c_2(\dot{x}_1 - \dot{x}_2) + k_1[x_1 - x_0 \cos(\alpha - \beta)] + c_1[\dot{x}_1 - \dot{x}_0 \cos(\alpha - \beta)] &= 0 \quad (4.1) \\ m_0 \ddot{x}_0 + k_1[x_0 \cos(\alpha - \beta) - x_1] \cos(\alpha - \beta) + c_1[\dot{x}_0 \cos(\alpha - \beta) - \dot{x}_1] \cos(\alpha - \beta) &= F_p \end{aligned}$$

Where m_0 , m_1 and m_2 are the model masses, as shown in Figure 4.1. The restoring properties of the springs constrained to translate along the x -axis are represented by

constant stiffness coefficients k_1 and k_2 , and c_1 and c_2 are the viscous damping coefficients of the damping elements. The angles α and β define the inclinations of the backrest and the seat pan with respect to vertical and horizontal axis. F_p is the driving point force at the seat pan along an axis normal to the seat pan. The coordinates x_1 and x_2 define the motion of masses m_1 and m_2 , respectively, along the x -axis, and x_0 is the displacement coordinate of base mass m_0 , as shown. The base mass displacement is related to the displacement of the excitation x_i , such that:

$$x_0 = x_i \cos \beta \quad (4.2)$$

The equations of motion for the three displacement coordinates (x_0 , x_1 and x_2) can be combined to yield following expression for the driving-point force, F_p :

$$F_p = m_0 \ddot{x}_0 + (m_1 \ddot{x}_1 + m_2 \ddot{x}_2) \cos(\alpha - \beta) \quad (4.3)$$

The apparent mass due to the model reflected at the seat pan driving point along the true vertical axis can be derived from:

$$APMS_i = \frac{F_i}{\ddot{x}_i} \quad (4.4)$$

The seat-pan APMS, in a similar manner, along the axis of motion of the base mass can be derived from:

$$APMS_p = \frac{F_p}{\ddot{x}_0} = \frac{F_i}{\ddot{x}_i} \quad (4.5)$$

Equation (4.3) yields the following expression for the seat pan driving-point response:

$$APMS_p = m_0 + (m_1 \frac{\ddot{x}_1}{\ddot{x}_0} + m_2 \frac{\ddot{x}_2}{\ddot{x}_0}) \cos(\alpha - \beta) \quad (4.6)$$

The above equation can also be expressed in terms of displacement transmissibility functions, $\frac{X_1}{X_0}(s)$ and $\frac{X_2}{X_0}(s)$, which are derived from Fourier

Transform of the Equation (4.1), such that:

$$APMS_p(s) = m_0 + [m_1 \frac{X_1}{X_0}(s) + m_2 \frac{X_2}{X_0}(s)] \cos(\alpha - \beta) \quad (4.7)$$

The apparent mass magnitude and phase responses at the seat pan driving-point are then evaluated by letting $s \rightarrow j\omega$.

4.2.1 Formulation of a non-dimensional model

Owing to the strong dependence of the APMS responses on the body mass, it is desirable to develop body-mass dependent models of the seated occupant. Alternatively, the model parameters may be normalized with respect to the total body mass, M_T , to derive a non-dimensional model that may be applied to estimate model parameters corresponding to a particular body mass. The non-dimensional model parameters are defined as:

$$\begin{aligned} \mu_0 &= \frac{m_0}{M_T}; \quad \mu_i = \frac{m_i}{M_T} (i=1,2) \\ k_i &= \mu_i \omega_i^2 M_T; \quad c_i = 2\mu_i \xi_i \omega_i M_T (i=1,2) \end{aligned} \quad (4.8)$$

Where M_T is the total body mass; ω_i and ξ_i ($i=1,2$) are the natural frequency and damping ratios of the uncoupled masses, given by:

$$\omega_i^2 = \frac{k_i}{m_i}; \quad \xi_i = \frac{c_i}{2m_i \omega_i} (i=1,2) \quad (4.9)$$

Substituting the non-dimensional quantities in Equation (4.7) yields the following expression for the normalized apparent mass at the seat pan:

$$\frac{APMS_p(s)}{M_T} = \mu_0 + [\mu_1 \frac{X_1}{X_0}(s) + \mu_2 \frac{X_2}{X_0}(s)] \cos(\alpha - \beta) \quad (4.10)$$

The equations of motion of the model masses constrained to translate along x-axis can be rewritten as:

$$\begin{aligned} \ddot{x}_2 + \omega_2^2(x_2 - x_1) + 2\xi_2\omega_2(\dot{x}_2 - \dot{x}_1) &= 0 \\ \ddot{x}_1 + \omega_2^2 \frac{\mu_2}{\mu_1}(x_1 - x_2) + 2\xi_2\omega_2 \frac{\mu_2}{\mu_1}(\dot{x}_1 - \dot{x}_2) + \omega_1^2[x_1 - x_0 \cos(\alpha - \beta)] + 2\xi_1\omega_1[\dot{x}_1 - \dot{x}_0 \cos(\alpha - \beta)] &= 0 \\ \ddot{x}_0 + \frac{\mu_1}{\mu_2}\{\omega_1^2[x_0 \cos(\alpha - \beta) - x_1] + 2\xi_1\omega_1[\dot{x}_0 \cos(\alpha - \beta) - \dot{x}_1]\} \cos(\alpha - \beta) &= \frac{F_p}{\mu_0 M_T} \end{aligned} \quad (4.11)$$

The above equations can be solved to derive the transmissibility functions, such that:

$$\begin{aligned} \frac{X_1}{X_0}(s) &= \frac{\mu_1(2\xi_1\omega_1s + \omega_1^2)(s^2 + 2\xi_2\omega_2s + \omega_2^2)\cos(\alpha - \beta)}{[\mu_1s^2 + (2\xi_1\omega_1\mu_1 + 2\xi_2\omega_2\mu_2)s + (\omega_1^2\mu_1 + \omega_2^2\mu_2)](s^2 + 2\xi_2\omega_2s + \omega_2^2) - (2\xi_2\omega_2\mu_2s + \omega_2^2\mu_2)(2\xi_2\omega_2s + \omega_2^2)} \\ \frac{X_2}{X_1}(s) &= \frac{2\xi_2\omega_2s + \omega_2^2}{s^2 + 2\xi_2\omega_2s + \omega_2^2} \cdot \frac{X_1}{X_0}(s) \end{aligned} \quad (4.12)$$

The above transmissibility functions, when applied to Equation (4.7) yield the normalized APMS response at the seat pan.

4.3.2 Backrest APMS of the model

The APMS response of the model reflected at the back support is derived from the equations of motion for the model masses along the y-axis. Assuming the frictionless and

constant contact of the visco-elastic elements with the backsupport, the equations of motion for the model can be written as:

$$\begin{aligned} m_1 \ddot{y}_1 + k_{b1}(y_1 - x_i \sin \alpha) + c_{b1}(\dot{y}_1 - \dot{x}_i \sin \alpha) &= 0 \\ m_2 \ddot{y}_2 + k_{b2}(y_2 - x_i \sin \alpha) + c_{b2}(\dot{y}_2 - \dot{x}_i \sin \alpha) &= 0 \end{aligned} \quad (4.13)$$

The term $x_i \sin \alpha$ in the above equations represents the excitation along an axis normal to the backrest. The total body force arising from the dynamic interactions between the body and the backrest can be derived as:

$$F_b = m_1 \ddot{y}_1 + m_2 \ddot{y}_2 \quad (4.14)$$

Where c_{bi} and k_{bi} ($i=1,2$) are the damping and stiffness coefficients, respectively, of the contact with the backrest.

The APMS response at the seat backrest could then be derived as follows:

$$APMS_b = \frac{F_b}{\ddot{x}_i \sin \alpha} = \frac{m_1 \ddot{y}_1 + m_2 \ddot{y}_2}{\ddot{x}_i \sin \alpha} \quad (4.15)$$

The APMS response at the backrest can also be expressed as:

$$APMS_b(s) = m_1 \frac{Y_1(s)}{X_i(s) \sin \alpha} + m_2 \frac{Y_2(s)}{X_i(s) \sin \alpha} \quad (4.16)$$

The non-dimensional expression of the APMS response on the seat backrest can then be derived as:

$$\frac{APMS_b(s)}{M_T} = \mu_1 \frac{Y_1(s)}{X_i(s) \sin \alpha} + \mu_2 \frac{Y_2(s)}{X_i(s) \sin \alpha} \quad (4.17)$$

The transfer functions, $\frac{Y_1(s)}{X_i(s)}$ and $\frac{Y_2(s)}{X_i(s)}$, could be computed from the non-dimensional forms of equation (4.13), i.e., $k_{bi} = \mu_i \omega_{bi}^2 M_T$; $c_{bi} = 2\mu_i \xi_{bi} \omega_{bi} M_T$ ($i=1,2$), ω_{bi} and ξ_{bi} are the natural frequencies and the damping ratios, respectively, of the

uncoupled masses m_i , corresponding to motion along the y-axis. The non-dimensional equation of motion are derived as:

$$\begin{aligned}\ddot{y}_1 + \omega_{b1}^2(y_1 - x_i \sin \alpha) + 2\xi_{b1}\omega_{b1}(\dot{y}_1 - \dot{x}_i \sin \alpha) &= 0 \\ \ddot{y}_2 + \omega_{b2}^2(y_2 - x_i \sin \alpha) + 2\xi_{b2}\omega_{b2}(\dot{y}_2 - \dot{x}_i \sin \alpha) &= 0\end{aligned}\quad (4.18)$$

The displacement transfer functions can then be derived as:

$$\begin{aligned}\frac{Y_1(s)}{X_i(s) \sin \alpha} &= \frac{2\xi_{b1}\omega_{b1}s + \omega_{b1}^2}{s^2 + 2\xi_{b1}\omega_{b1}s + \omega_{b1}^2} \\ \frac{Y_2(s)}{X_i(s) \sin \alpha} &= \frac{2\xi_{b2}\omega_{b2}s + \omega_{b2}^2}{s^2 + 2\xi_{b2}\omega_{b2}s + \omega_{b2}^2}\end{aligned}\quad (4.19)$$

4.3 Model parameters estimation

The model parameters are identified using a parametric optimization technique, such that the APMS responses at the seat pan and backrest of the model are comparable to the target responses defined in the previous chapter. An objective function is defined to minimize the error between the model and the measured APMS responses at the seat pan and the backrest over a frequency range of interest. The objective function is defined as the weighted sum of the squared magnitude and phase errors associated with the APMS functions, respectively, and expressed as:

$$U(\chi) = \min[U_p(\chi) + U_b(\chi)] \quad (4.20)$$

Where $U(\chi)$ is the weighted minimization function, and $U_p(\chi)$ and $U_b(\chi)$ are sum of the squared errors resulting from APMS response at the seat pan and the seat back, respectively, given by:

$$\begin{aligned}U_p(\chi) &= \psi \sum_{i=1}^n \{[|M_p(\omega_i)| - |M_{pt}(\omega_i)|]^2\} + \sum_{i=1}^n \{[|\phi_p(\omega_i)| - |\phi_{pt}(\omega_i)|]^2\} \\ U_b(\chi) &= \rho \sum_{i=1}^n \{[|M_b(\omega_i)| - |M_{bt}(\omega_i)|]^2\} + \sum_{i=1}^n \{[|\phi_b(\omega_i)| - |\phi_{bt}(\omega_i)|]^2\}\end{aligned}\quad (4.21)$$

Where $M_p(\omega_i)$ and $\phi_p(\omega_i)$ are the magnitude and the phase of the pan APMS response of the model corresponding to the excitation frequency ω_i . $M_{pt}(\omega_i)$ and $\phi_{pt}(\omega_i)$ represent the corresponding measured values. $M_b(\omega_i)$ and $\phi_b(\omega_i)$ are the magnitude and phase of the back APMS response of the model, and $M_{bt}(\omega_i)$ and $\phi_{bt}(\omega_i)$ are the corresponding measured values. n is the number of discrete frequencies selected in the 0.5 to 40 Hz frequency range. χ is a vector of model parameters to be identified, expressed as:

$$\chi = \{\mu_0, \mu_1, \mu_2, \omega_1, \omega_2, \xi_1, \xi_2, \omega_{b1}, \omega_{b2}, \xi_{b1}, \xi_{b2}\}^T \quad (4.22)$$

where ‘T’ designates the transpose. ψ and ρ are the weighting factors used in the pan and back APMS error functions, respectively, to ensure somewhat comparable contributions of the magnitude and phase errors in the objective function. The magnitude of the normalized APMS varies in the 1.5 to 2.5 range, which is considerably smaller than its phase range of 0° to -120° over the frequency range of interest. The weighting factors ψ and ρ , however, are taken as of 10^4 to emphasize the contribution due to the APMS magnitude.

The minimization problem expressed in Equation (4.20) is solved subject to a number of constraints imposed on the model parameters. Limit constraints are applied to the model masses considering that the mean measured data are related to the mean body mass of 76.6% of the total body mass supported by the seat pan corresponding to a passenger posture, and 73.5% of the total body mass corresponding to a driver posture, the body mass supported by the backrest is also considered to be 30.4% of the total body

mass for the passenger posture and 28.1% for the driver posture. The limit constraints are defined to allow the total mass to vary within a narrow band ($\pm 4\%$), such that:

$$\begin{aligned}
0.735 &\leq \sum_{i=0}^2 \mu_i \leq 0.797 && \text{Hands in lap sitting posture} \\
0.292 &\leq (\mu_1 + \mu_2) \sin 24^\circ \leq 0.316; \\
0.706 &\leq \sum_{i=0}^2 \mu_i \leq 0.764 && \text{Hands on steering wheel posture} \\
0.270 &\leq (\mu_1 + \mu_2) \sin 24^\circ \leq 0.292;
\end{aligned}$$

The measured seat pan APMS magnitudes mostly predominate around a single frequency in the 6-8 Hz range, the backrest APMS magnitude reveals two notable peaks in the vicinity of 6-8 Hz, and 12-16 Hz. The uncoupled natural frequencies of the model are constrained to lie between 25 rad/s and 125 rad/s, while the uncoupled damping ratios are also limited to 0.6, such that:

$$\begin{aligned}
25 &\leq \omega_i \leq 125; & 0 < \xi_i < 0.6; \\
25 &\leq \omega_{bi} \leq 125; & 0 < \xi_{bi} < 0.6;
\end{aligned} \quad (i=1,2)$$

The minimization problem is solved using the proposed occupant model structure and the mean values of the measured responses for both sitting postures. The solutions were obtained for different starting values of the parameter vector χ and the resulting model parameters were examined to obtain minimal value of the error functions. The resulting model parameters were identified as:

$$\text{Hands-in-lap: } \chi = \{0.05, 0.43, 0.3, 100, 55.7, 0.27, 0.40, 52.5, 86.5, 0.22, 0.34\}^T$$

$$\text{Hands-on-steering wheel: } \chi = \{0.05, 0.42, 0.28, 100, 46.0, 0.295, 0.57, 50.8, 84.9, 0.28, 0.297\}^T$$

The model parameters derived from the above optimal non-dimensional values are summarized in Table 4.1. These model parameters, derived on the basis of the mean

target data for the entire test population, would correspond to mean body mass of 71.2 kg. The model masses obtained for the hands on steering wheel posture are in general lower than those achieved for the hands in lap sitting posture. The total model mass for hands on steering wheel sitting posture is also lower which conforms with the trends in the measured data. A comparison of the stiffness and damping parameters of the two models reveals that the stiffness parameters of the hands on the steering wheel model are lower than those of the hands in lap model. This is attributed to lower primary frequency observed with the hands on steering wheel posture. The damping parameters of the hands on steering wheel model, however, are generally higher than those of the hands in lap model, with the exception of the c_{b2} . Higher damping parameters of the hands on steering wheel model also confirm with relatively lower peak magnitude observed for this posture.

Table 4.1: Model Parameters based upon the mean mass of 71.2 kg.

Parameter	Parameter values	
	Hands-in-lap	Hands-on-steering wheel
$\mu_0 (m_0)$	0.05(3.56 kg)	0.05(3.36 kg)
$\mu_1 (m_1)$	0.43(30.62 kg)	0.42(29.9 kg)
$\mu_2 (m_2)$	0.3(21.36 kg)	0.28(19.94 kg)
$\Sigma \mu_i (m_i)$	0.78(55.54 kg)	0.75(53.4 kg)
k_1	306.2 kN/m	299 kN/m
k_2	66.4 kN/m	42.7 kN/m
k_{b1}	84.4 kN/m	77.1 kN/m
k_{b2}	159.8 kN/m	143.5 kN/m
c_1	1673 Ns/m	1764 Ns/m
c_2	946 Ns/m	1047 Ns/m
c_{b1}	698 Ns/m	859 Ns/m
c_{b2}	1244 Ns/m	1006 Ns/m

The eigenvalue solution of the dynamic matrix yield two pairs of complex conjugates eigenvalues for each model, which are $-50.31 \pm 98.39i$ and $-14.60 \pm 48.29i$ for

the hands-in-lap model, and $-51.95 \pm 86.17i$ and $-21.32 \pm 40.78i$ for the hands-on-steering wheel model. These results suggest two natural frequencies of the hands in lap model with frequencies of damped oscillations being 7.68 and 15.66 Hz, and the corresponding damping ratios of 0.46 and 0.29. For the hands on steering wheel model, the frequencies were obtained as 6.49 Hz and 13.7 Hz, with corresponding damping ratios of 0.52 and 0.46, respectively. The damped natural frequencies related to the seat backrest APMS responses are 8.35 Hz and 13.77 Hz and the corresponding damping ratios are 0.22 and 0.34 for the hands in lap posture. For the hands-on-steering wheel model the damped natural frequencies are 7.08 Hz and 13.5 Hz, and the corresponding damping ratios are 0.28 and 0.3.

The validity of the proposed models and their parameters, corresponding to the mean body mass of 71.2 kg is further examined by comparing the model responses with the mean measured responses under both sitting postures. Figures 4.2 and 4.3, respectively, illustrate comparisons of seat pan and backrest magnitude and phase responses of the models and the mean measured data for both postures. The results in terms of magnitude and phase show reasonably good agreements between the mean measured and model response characteristics for both postures. Both the seat-pan and the backrest magnitude responses of the model correlate very well with the mean measured data corresponding to both postures in majority of the frequency range, although some deviations are observed at frequencies above 25 Hz in the pan response. While the models phase responses generally agree with the measured data, larger deviations are observed for the back APMS phase responses, irrespective of the posture. The peak phase error in the order of 20% occurs near 10 Hz, which is most likely attributed, in part, to the

nonlinear occupant behavior of the upper body. The high magnitude of error in the phase response may also be partly attributed to relatively high inter-subject variations in the back APMS response observed in the measured data near 10 Hz. The magnitude of the error in the phase response, however, is well below 10% at frequencies above 15 Hz. The proposed models can thus be considered to characterize the mean biodynamic response of human occupants at the seat pan and the backrest, when seated with hands in lap or on the steering wheel, and exposed to vertical vibration of magnitude ranging from 0.25 m/s^2 to 1.0 m/s^2 rms acceleration. The validity of the model, however, may be limited to total body mass in the vicinity of 71.2 kg.

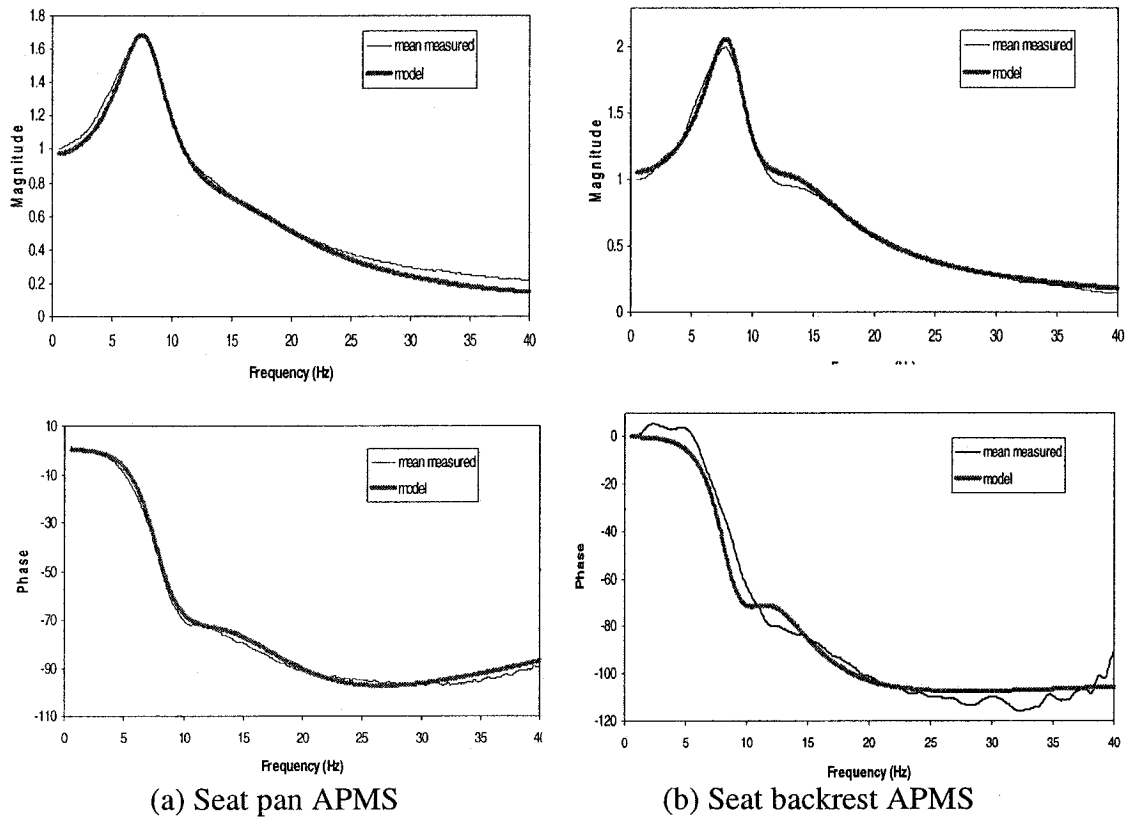


Figure 4.2: Comparisons of apparent mass responses of the seated occupant model with the mean measured response (hands-in-lap posture).

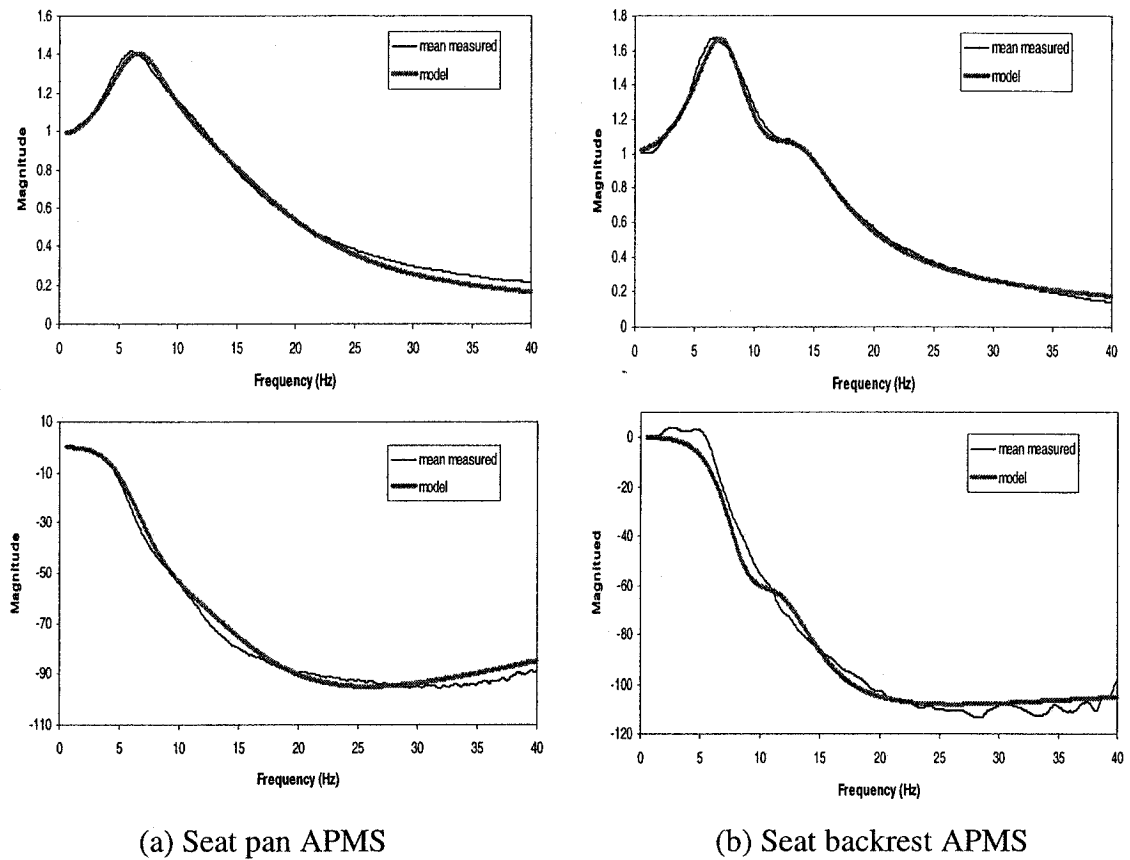


Figure 4.3: Comparisons of apparent mass responses of the seated occupant model with the mean measured response (hands-on-steering wheel posture).

4.4 Body weight-dependent seated occupant model

The measured data acquired at the seat pan and the backrest clearly revealed the strong influence of the body mass on the APMS responses. The occupant models derived in the preceding section can be considered to characterize the biodynamic response of a wide range of seated occupants with mean body mass of 71.2 kg exposed to vertical vibration. The strong dependency of the biodynamic response on the body mass thus can not be characterized using the models based on mean population mass. It is thus vital to derive body weight dependent occupant models, such that vibration transmission analysis

of the coupled occupant-seat system may be performed as a function of the occupant's weight.

In this study, the model parameters are identified on the basis of the mean target curves attained for different ranges of body mass. The measured apparent mass response characteristics of the 24 subjects were grouped into four different sets corresponding to occupants' mass lying in four different ranges: less than 60 kg; between 60.5 and 70.5 kg; between 70.5 and 80 kg; and above 80 kg. The subject population considered in this study resulted in a total of 8 data sets in the category of occupants with mass below 60 kg; 5 data sets in the 60.5 to 70.5 kg range; 6 data sets in the 70.5 to 80kg range; and 5 data sets for above 80 kg mass range. The mean occupant masses corresponding to the four groups were attained as 53.4 kg, 67.6 kg, 75.1 kg and 97.4 kg, respectively. The mean response curves attained for the four body mass groups, presented in Figures 3.21 and 3.22, are applied in the minimization problem of Equations (4.20) and (4.21), in order to identify parameters of the body-weight dependent biodynamic models.

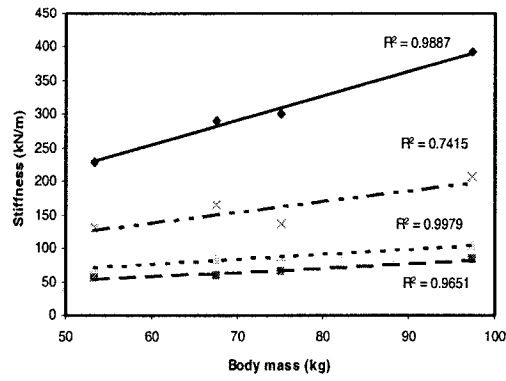
The minimization problem is solved for each mass group, where the limit constraint on the total body mass is defined by the lower and upper limit of the group range. The model parameters identified for the different mass groups are in Table 4.2. The identified parameters indicate that the model masses increase with the mean group mass. The stiffness and damping parameters also increase with the body mass, in general, with a few exceptions in the 60.5 to 70.5 kg and 70.5 to 80kg group. This is likely attributed to the relatively close mean mass values of the groups. The increasing trend is more obvious, when parameters attained for the highest and the lowest mass groups are

compared. The dispersion in the model parameters is believed to be caused by variations in the body masses, while little is known on the nature of the dependence.

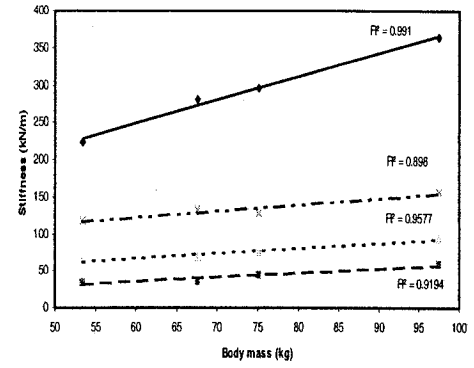
Table 4.2: Parameters of the automotive body weight-dependent occupant models.

Parameters	Mass range				
	< 60kg	60.5-70kg	70.5-80kg	> 80kg	Mean
	53.4kg	67.6kg	75.1kg	97.4kg	71.2kg
Hands-in-lap					
m0 (kg)	2.67	3.38	3.755	4.87	3.56
m1 (kg)	22.962	29.068	32.293	41.882	30.62
m2 (kg)	16.02	20.28	22.53	29.22	21.36
k1 (kN/m)	229.6	290.7	300.7	392.2	306.2
k2 (kN/m)	54.9	59.2	66	83.2	66.4
c1 (Ns/m)	1198	1360	1700	2551	1673
c2 (Ns/m)	871	1011	969	1014	946
kb1 (kN/m)	71.6	83.5	88.2	104.3	84.4
kb2 (kN/m)	130	165	160.8	207.3	159.8
cb1 (Ns/m)	427	722	719	944	698
cb2 (Ns/m)	759	1236	1240	2468	1244
Hands-on-steering wheel					
m0 (kg)	2.67	3.38	3.755	4.87	3.56
m1 (kg)	22.428	28.392	31.542	40.908	29.9
m2 (kg)	14.7918	18.92	21.028	27.292	19.936
k1 (kN/m)	224.3	281.2	295.8	364.3	299
k2 (kN/m)	34.4	35.4	43	58.1	42.7
c1 (Ns/m)	1173	1762	1763	2683	1764
c2 (Ns/m)	856	982	1017	1155	1047
kb1 (kN/m)	65.3	69.5	79.5	93.6	77.1
kb2 (kN/m)	117.1	133.5	127.6	157.3	143.5
cb1 (Ns/m)	493	822	1022	1535	859
cb2 (Ns/m)	580	1005	1017	2018	1006

Figures 4.4 and 4.5 illustrate the variations in the stiffness and damping parameters, respectively, of the hands in lap and hands on steering wheel models with the total body mass. The results show high linear correlation ($R^2 > 0.88$) between the model stiffness and damping parameters and the body mass, except for c_2 and k_{b2} for the hands-in-lap posture model ($R^2 = 0.58$ and 0.74 respectively). The results further show that the variations in the damping coefficient are quite small. The linear regression functions of all the model parameters are further established and summarized in Table 4.3.

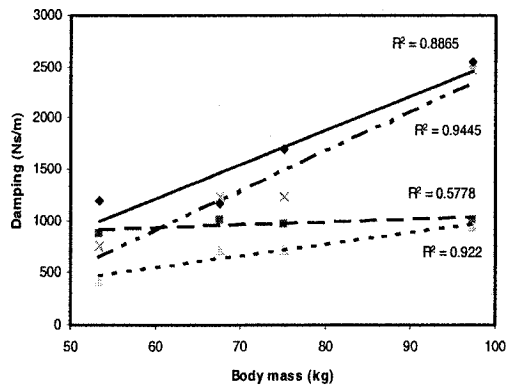


(a) Hands-in-lap

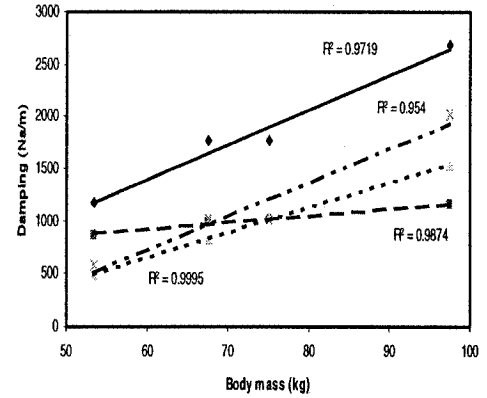


(b) Hands-on-steering wheel

Figure 4.4: Correlations of the model stiffness parameters with the body mass.



(a) Hands-in-lap



(b) Hands-on-steering wheel

Figure 4.5: Correlations of the model damping parameters with the body mass.

Table 4.3: Regression functions of the model parameters.

Parameter	Hands-in-lap	Hands-on-steering wheel
k_1 (kN/m)	$k_1 = 3.631M_t + 36.892$	$k_1 = 3.119M_t + 62.531$
k_2	$k_2 = 0.666M_t + 16.966$	$k_2 = 0.571M_t + 0.806$
k_{b1}	$k_{b1} = 0.736M_t + 32.874$	$k_{b1} = 0.665M_t + 27.162$
k_{b2}	$k_{b2} = 1.646M_t + 38.991$	$k_{b2} = 0.878M_t + 69.437$
c_1 (Ns/m)	$c_1 = 33.159M_t + 780.01$	$c_1 = 33.475M_t - 610.95$
c_2	$c_2 = 2.762M_t + 763.62$	$c_2 = 6.65M_t + 514.54$
c_{b1}	$c_{b1} = 11.082M_t - 110.15$	$c_{b1} = 23.749M_t - 774.59$
c_{b2}	$c_{b2} = 38.65M_t - 1410.2$	$c_{b2} = 32.441M_t - 1225.4$

The validity of the identified body mass-dependent models is examined using two approaches. In the first approach, the effectiveness of the models is evaluated by comparing the model responses with the mean responses measured for the corresponding body mass group. In the second approach, the regression functions are applied to derive the model parameters and responses for three particular subject masses. The model responses are then compared with the measured data attained for the subjects of identical masses. Figures 4.6 and 4.7 illustrate the modulus and phase response characteristics of the models derived for four different mass groups with the corresponding mean measured data obtained for the respective mass groups. The figures show the magnitude and phase responses at the seat pan and the backrest, and for hands in lap and hands on steering wheel posture, respectively.

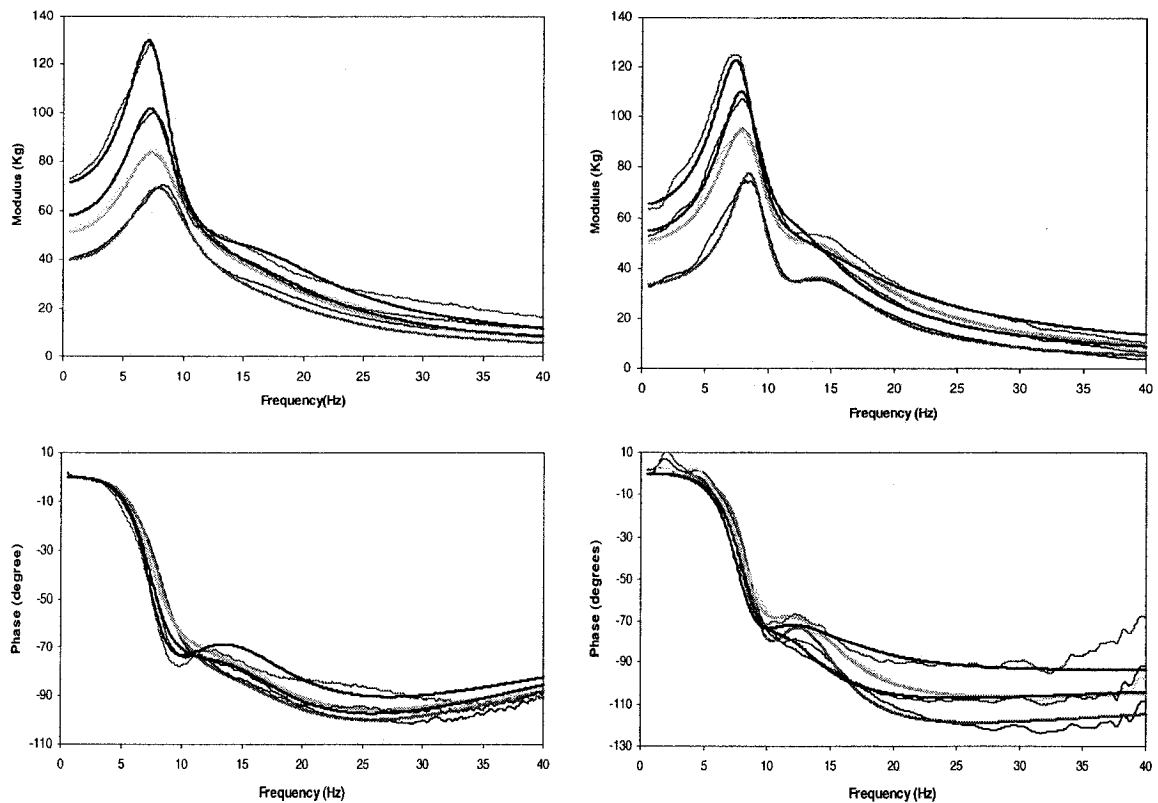


Figure 4.6: Comparisons of the mass-dependent model results with the mean measured response of seated occupants within different mass ranges (hands-in-lap).

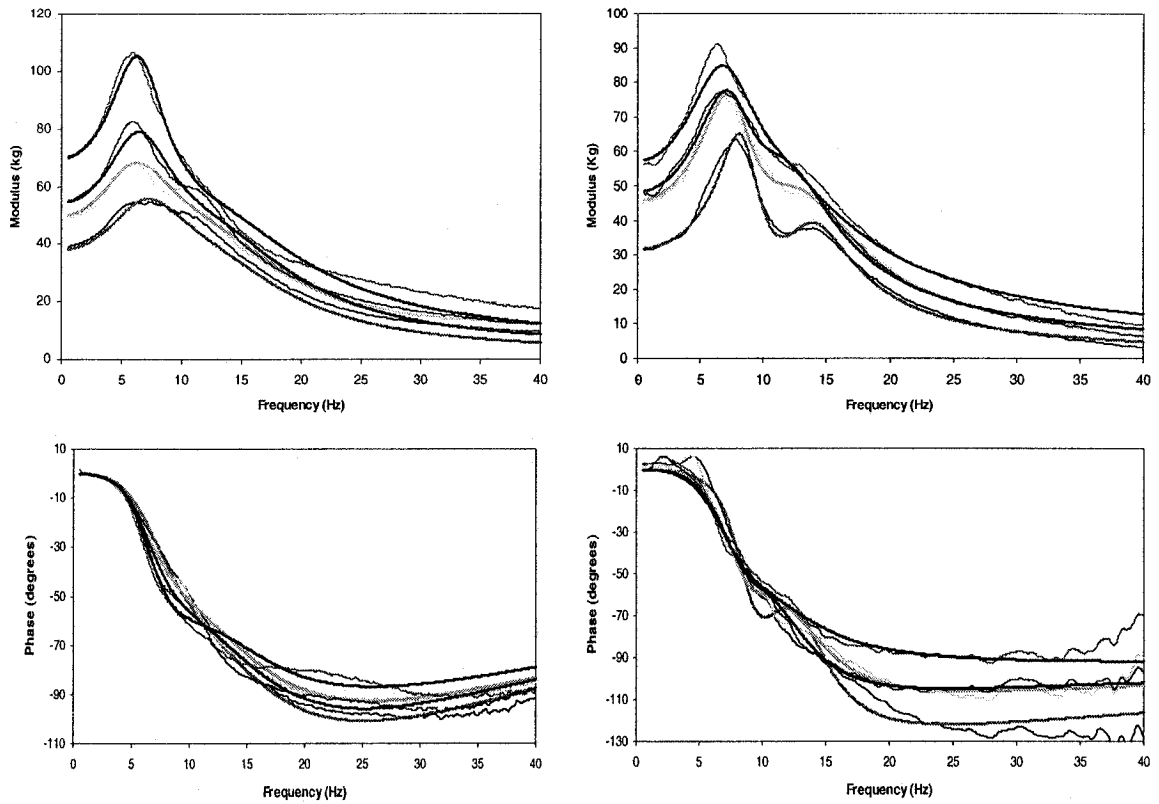


Figure 4.7: Comparisons of the mass-dependent model results with the mean measured response of seated occupants within different mass ranges (hands on steering wheel).

The results show reasonably good agreements between the models results and mean measured response characteristics. Both the proposed mass-dependent model and the mean measured data exhibit a decrease in primary resonant frequency and an increase in the modulus response with the increase in the occupant mass. The modulus response of the hands-on-steering wheel sitting posture model, however, reveals more deviations from the mean measured modulus than that of the hands-in-lap sitting posture model. These discrepancies between the model and measured response are most likely attributed to non-linear biodynamic behavior of the seated occupants. The apparent mass phase response characteristics of the passenger and driver mass-dependent models also exhibit

reasonably good agreement with the mean measured data in most of the frequency range for all the mass groups, as shown in Figures 4.6 and 4.7.

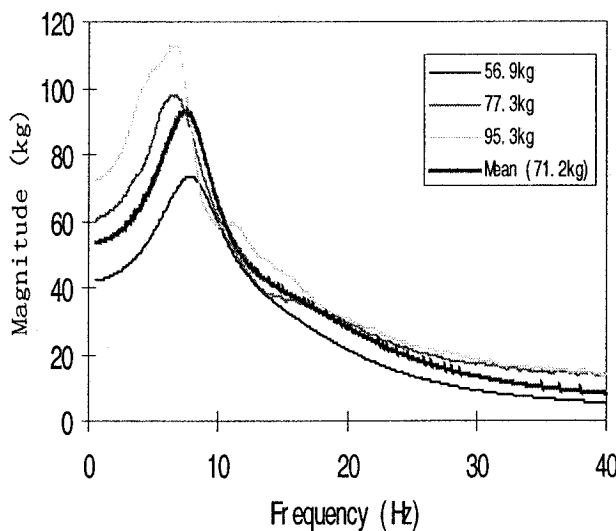
The validity of the body mass-dependent models are further examined by evaluating the seat-pan and backrest APMS responses of three particular subjects of body masses of 56.9 kg, 77.3 kg and 95.3 kg. The regression functions, presented in Table 4.3, are applied to estimate the model parameters for the three body masses, which are summarized in Table 4.4, and the corresponding the estimated seat pan APMS responses for two sitting postures are presented in Figure 4.8. The seat pan and backrest APMS magnitude and phase responses of the models with estimated parameters are evaluated and compared with those derived from the data acquired with individuals of identical masses. The analyses and comparisons are performed for both postures involving hands in lap and hands on the steering wheel.

Table 4.4: The estimated model parameters of three selected subjects.

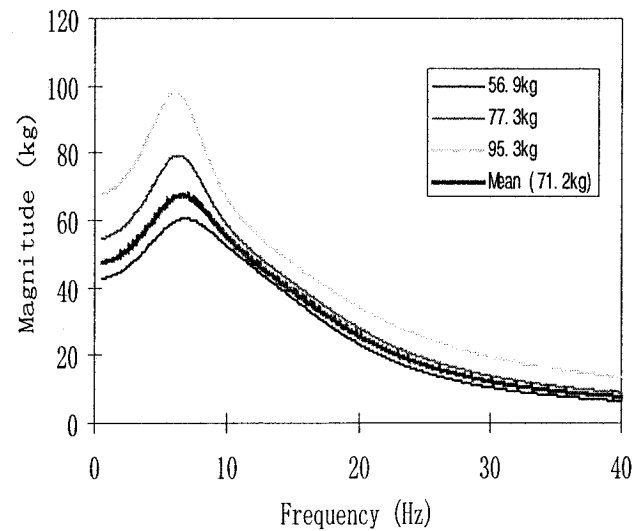
Parameter	$M_T=56.9$ kg		$M_T=77.3$ kg		$M_T=95.3$ kg	
	LAP	SW	LAP	SW	LAP	SW
m_0 (kg)	2.85	2.85	3.87	3.87	4.765	4.765
m_1	24.5	23.94	33.24	32.5	41	40
m_2	17.1	15.96	23.2	21.64	28.6	26.7
k_1 (kN/m)	243.8	240.3	317.6	303.7	382.9	359.8
k_2	54.9	33.4	68.44	44.97	80.4	55.25
k_{b1}	74.8	65	89.79	78.54	103	90.5
k_{b2}	132.8	119.5	166.2	137.3	195.9	153
c_1 (Ns/m)	1110	1297	1783	1977	2380	2579
c_2	921	894	977	1029	1027	1148
c_{b1}	521.5	579	746.5	1061	946	1488.7
c_{b2}	793	623	1578	1282	2273	1866

The comparisons of the model predictions of the APMS magnitude and phase responses with the measured responses of the selected subjects are presented in Figures 4.9 to 4.11 for both hands-in-lap and hands-on-steering wheel postures. The estimated

apparent mass responses generally show close agreements with the measured values in both the magnitude and the phase, as shown in Figures 4.9 to 4.11. Some deviations between the resonant frequency of the model and that observed from the measured data are evident for the hands on steering posture of the subjects with body masses of 56.9 kg and 95.3 kg (Figures 4.9(b) and 4.11(b)). Greater phase lags can also be observed in Figure 4.9 (a) for the subject with body mass of 56.9 kg. The results, in general, showed a reasonably good agreements between the measured and the estimated APMS response characteristics, which validate the modeling procedure and provide a reliable seated human body model, irrespective of the body mass.

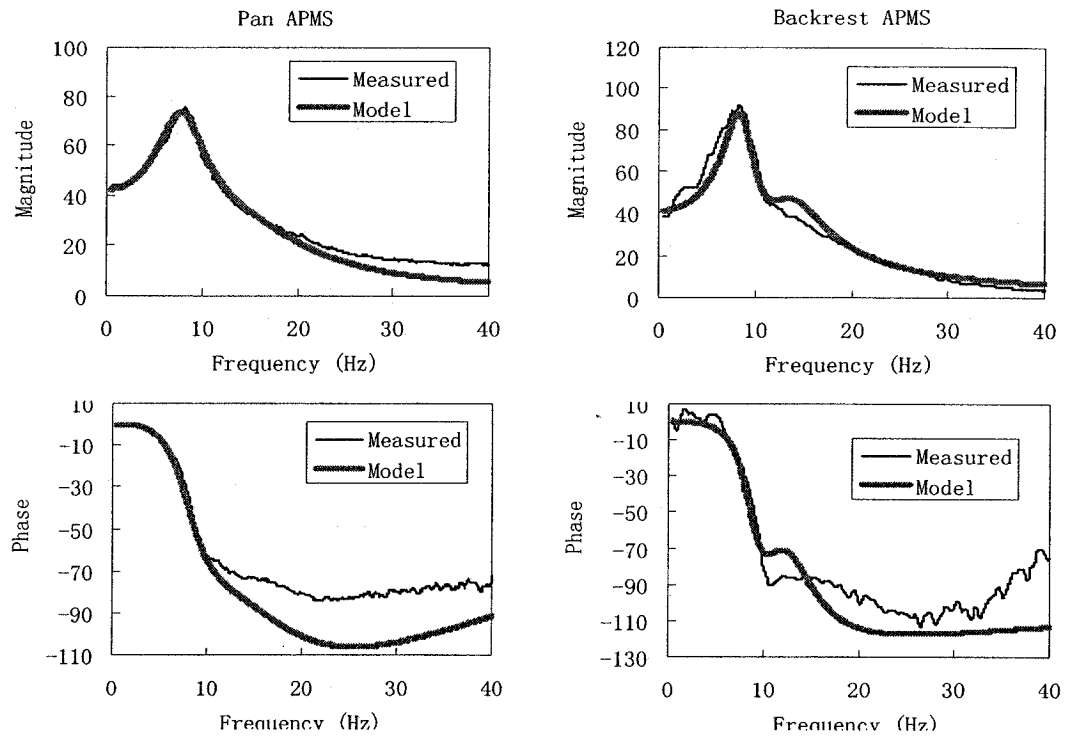


(a) Hands in lap

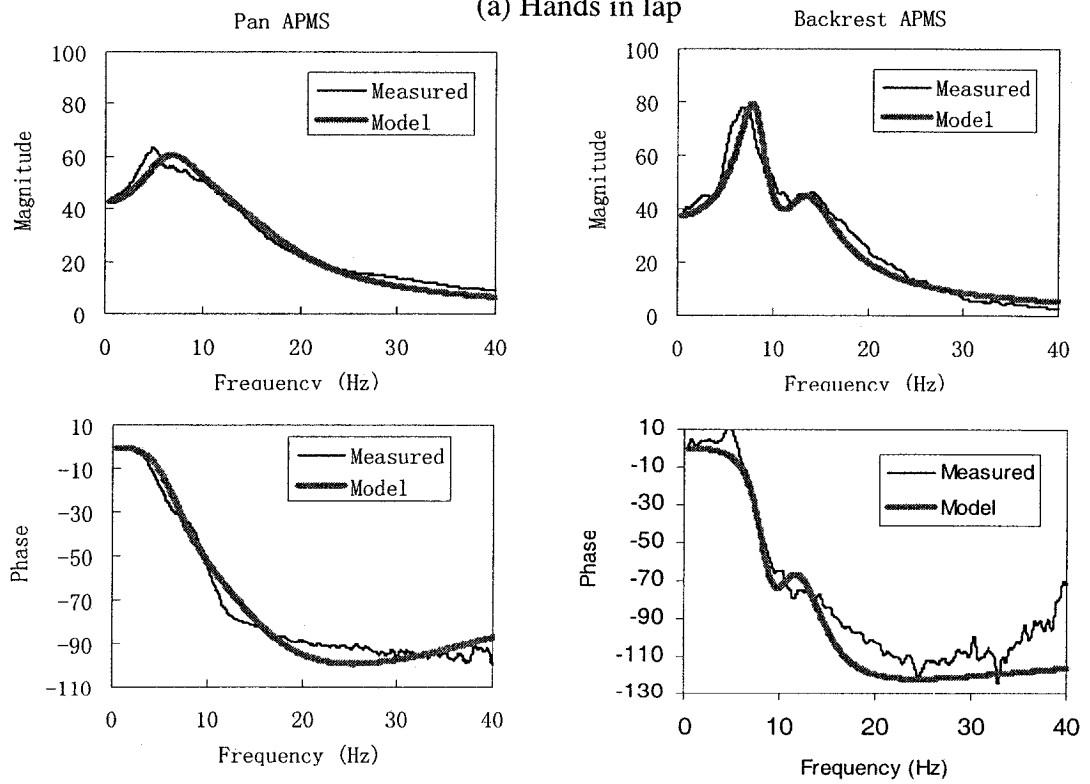


(b) Hands on steering wheel

Figure 4.8: The comparison of the estimated seat pan APMS response with the body weight dependent model response.



(a) Hands in lap



(b) Hands on steering wheel

Figure 4.9: Comparisons of the estimated APMS magnitude and phase responses with the measured responses of the subject with total body mass of 56.9 kg.

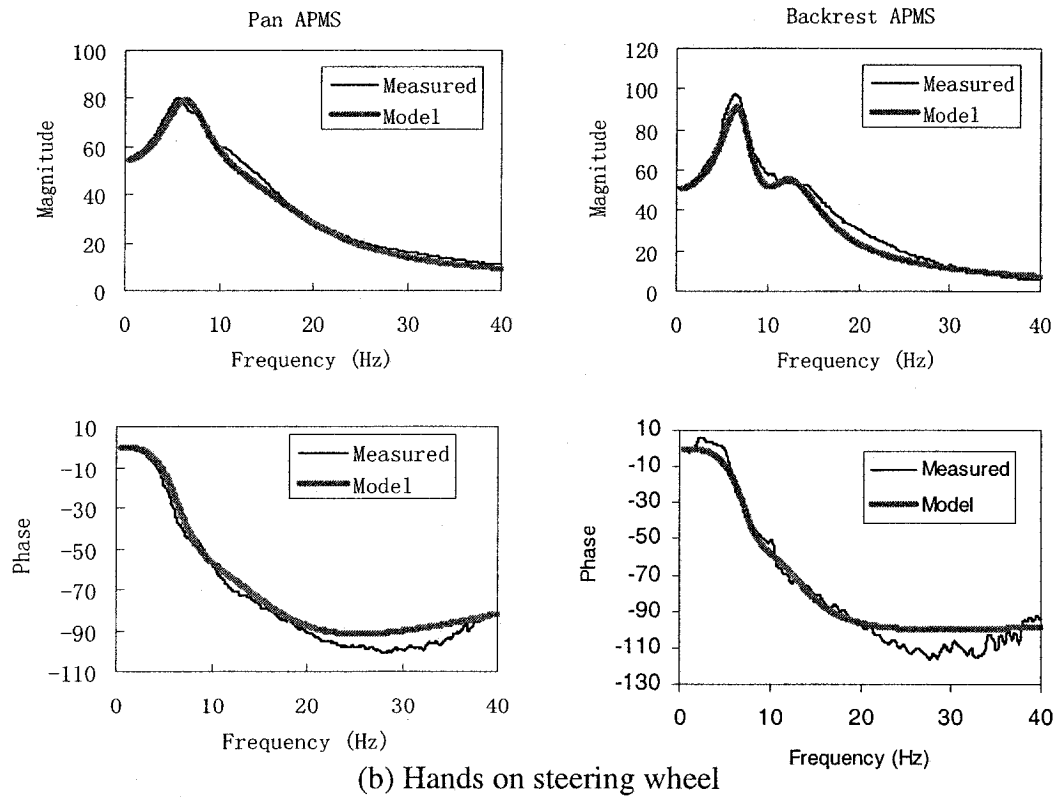
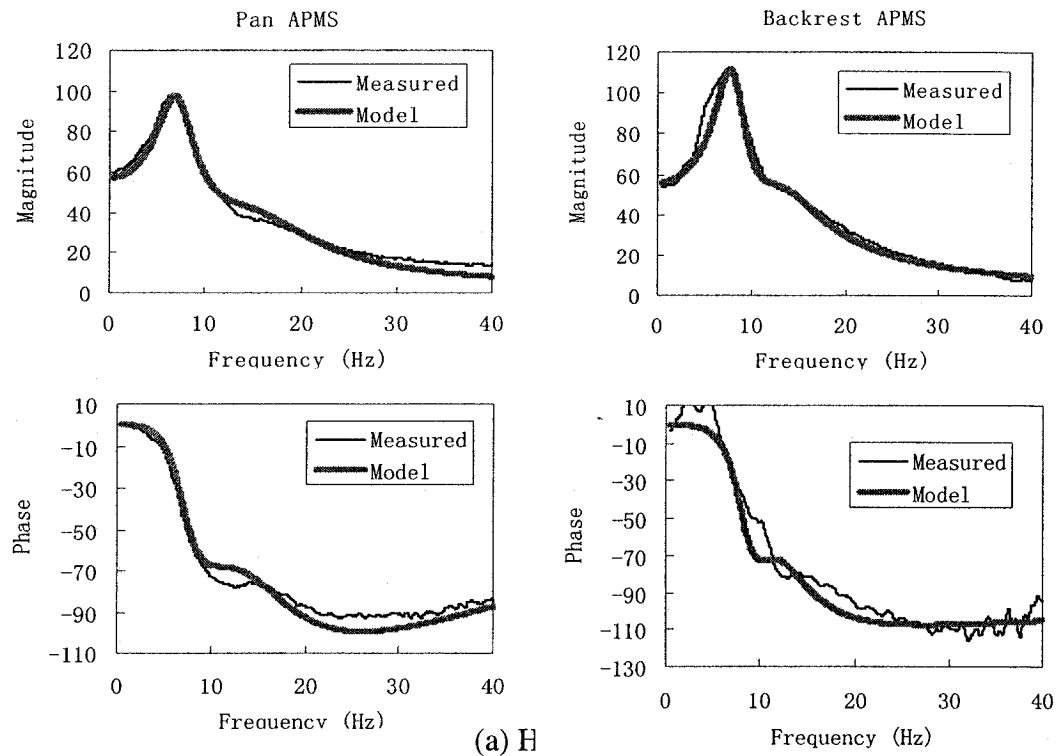
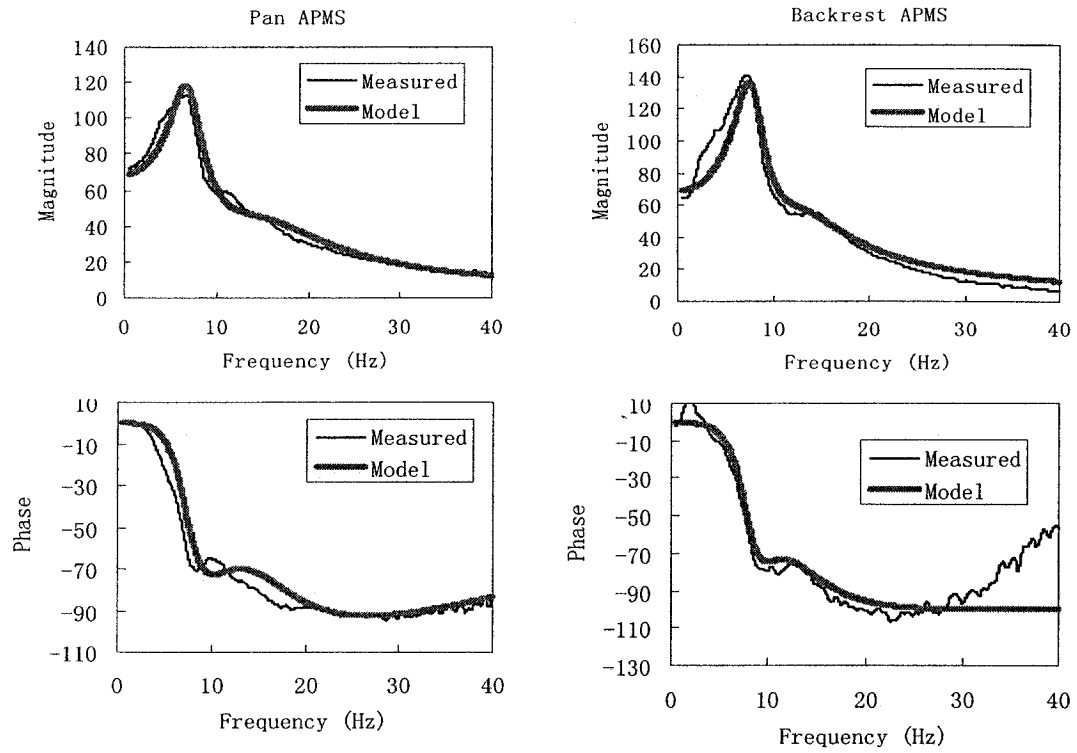
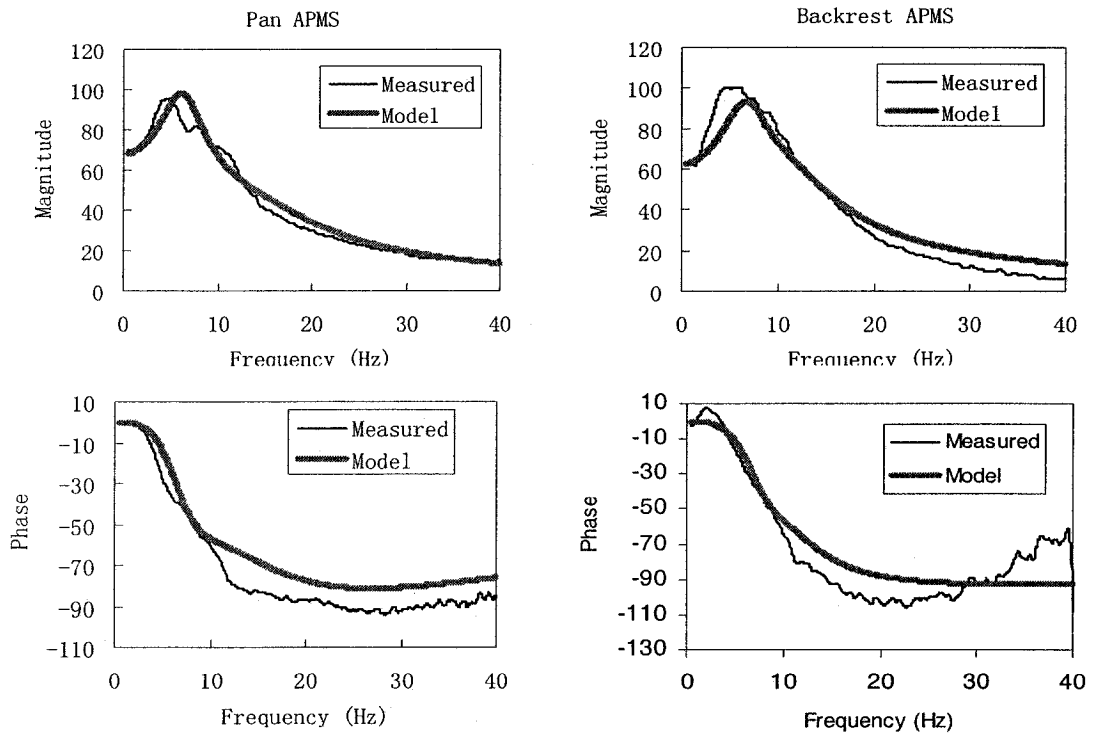


Figure 4.10: Comparisons of the estimated APMS magnitude and phase responses with the measured responses of the subject with total body mass of 77.3 kg.



(a) Hands in lap



(b) Hands on steering wheel

Figure 4.11: Comparisons of the estimated APMS magnitude and phase responses with the measured responses of the subject with total body mass of 95.3 kg.

4.5 Summary

The proposed mechanical-equivalent model can be effectively used to characterize the biodynamic response of seated occupants reflected on both the pan and the backrest under vertical vibration with mean body mass of 71.2 kg. The contributions due to variations in the body weight, however, cannot be derived using this model. In order to account for the significant influence of body weight, the proposed models are refined to provide a reasonable characterization of the biodynamic response of subjects of different body weight. The measured data for 24 subjects is grouped into four classes on the basis of the total body weight. These include 8 data sets for subjects' mass below 60 kg, 5 data sets for subjects' mass between 60.5 and 70 kg, 6 data sets for mass ranging from 70.5 to 80 kg, and 5 data sets for mass above 80 kg. The measured response characteristics of the subjects within each group are analyzed to derive the mean values corresponding to two different postures and three different levels of vibration excitations. Owing to the relatively small contributions due to level of vibration excitations, the mean data sets obtained for 0.25 m/s^2 , 0.5 m/s^2 and 1.0 m/s^2 rms acceleration excitations, are further analyzed to derive mean of mean biodynamic response of occupants in the different mass ranges. A total of 16 mean data sets are thus derived to describe the both pan and back biodynamic response of subjects in the four different weight groups and two different postures.

The occupant models developed for the mean biodynamic response are refined to account for the dependence on the body weight. The optimization problem is solved subject to identify the model parameters for each body mass range. This method thus allows the masses to vary in order to derive reasonable agreement with the mean

biodynamic response characteristics corresponding to different weight groups. In view of lack of knowledge of the trends related to variations in the visco-elastic properties of the human body in different weight ranges, the optimization problem is subject to equality constraints on various stiffness and damping elements of the models. The results derived from the models showed reasonably good agreements with the mean measured data sets. The proposed models are thus considered to characterize the biodynamic response behavior of seated occupants of different weight groups and different sitting postures under vertical automotive vibration.

Chapter 5 Conclusions and recommendations for further work

5.1 Major highlights and contributions

This study on biodynamic responses and body interactions with the seat pan and the backrest under vertical vibration involved: (i) Measurement of the apparent mass response characteristics under automotive vibration environment with appropriate considerations of the interactions with backrest and the pan; (ii) Identification of the important contributing factors and target response curves for model development; (iii) Development and validation of a linear biodynamic model of the seated occupant. The major contributions and highlights of this investigation are summaries below:

Measurement of the apparent mass response

No attempts have been made thus far to characterize the force-motion relationship at the seated upper body and the seat backrest interface, when the backrest is inclined as in the case of automobile seats. In this study, the apparent mass response characteristics are derived through measurements of force and motions on both the seat pan and the backrest using 24 individuals under postural and vibration conditions representative of those applicable to automobile drivers and passengers. The APMS response data acquired on the seat backrest provide important quantitative information on the interactions. The study revealed that the backrest APMS magnitudes are quite comparable with the seat pan magnitudes in the entire frequency range for both hands position, even though the backrest supports a significantly smaller proportion of the body mass. The results suggest that the entire upper body experiences horizontal motion under exposure to vertical vibration.

Factors Influencing the APMS response characteristics of seated occupant

The influence of various factors on the measured APMS response is investigated in this study. The results show that the body mass forms the most significant factor that affects the apparent mass response of the seated automobile occupants on both the seat pan and the seat backrest. A higher body mass, in general, yields higher peak magnitude response and lower corresponding frequency for both passenger and driver postures. While a positive correlation could be established between the peak apparent mass magnitude and the total body mass, the trend in decreasing fundamental frequency with increasing body mass showed a poor correlation. The results also suggest relatively negligible influence of the feet position, magnitude of the vibration excitation and the gender. From the results, it is concluded that the biodynamic response of occupants seated with automotive postures and subject to vertical vibration need to be characterized, as a minimum, by two distinct functions for two postures: hands-in-lap and hands-on-steering wheel.

Human body model development

Current experimental data are insufficient to define the relevant movements of the human body during vibration and, therefore, they are also insufficient to determine the relevant masses, stiffness and damping of structure that moves like the body during vibration. The experimental data suggest that just two or three degrees-of-freedom models could accurately represent a subject's apparent mass over the 0.5-40 Frequency range. It is therefore reasonable to seek a model which does not related with the biological system but has the same apparent mass. In this study a linear 4-DOF

mechanical-equivalent model of the seated occupant is developed that incorporates adequate portion of the body resting on the seat pan and the backrest support, on the basis of the data acquired. The validity of the proposed models and their parameters, corresponding to the mean body mass of 71.2 kg is examined by comparing the model responses with the mean measured responses under both sitting postures. The results in terms of magnitude and phase show reasonably good agreements between the mean measured and model response characteristics for both postures.

Development of body weight-dependent seated occupant models

The occupant models derived in the preceding section can be considered to characterize the biodynamic response of a wide range of seated occupants with mean body mass of 71.2 kg. The strong dependency of the biodynamic response on the body mass thus can not be characterized using the models based on mean population mass. Thus a body weight-dependent seated occupant model is derived in this study. The validity of the identified body mass-dependent model is examined by comparing the model responses with the mean responses measured for the corresponding body mass groups. Further validation is demonstrated by applying the regression functions to derive the model parameters and responses for three particular subject masses, then comparing with the measured APMS responses of the same subjects. The results showed a reasonably good agreement between the measured and the estimated APMS response characteristics, which validate the modeling procedure and provide a reliable seated human body model.

5.2 Conclusions

On the basis of the studies conducted in this dissertation, the following major conclusions are drawn:

- The biodynamic response behavior of seated subjects is invariably described in terms of driving-point mechanical impedance (DPMI) or apparent mass (APMS) and seat-to-head transmissibility (STHT). From the study of reported biodynamic characteristics, it is apparent that the DPMI/APMS and STHT are influenced by many factors related to subject characteristics and test conditions.
- The APMS response data acquired on the seat backrest provide important quantitative information on the interactions. The study revealed that the backrest APMS magnitudes are quite comparable with the seat pan magnitudes in the entire frequency range for both hands position (in the lap and on the steering wheel).
- The results have shown that the seat pan APMS responses of occupants seated with an automotive posture differ considerably from those reported in most other studies, which consider significantly different postures and vibration excitation levels. The peak magnitudes of APMS applicable to automobile passengers with hands in lap posture were observed to occur in 6.5-8.6 Hz frequency range, with mean frequency in the area of 7.8 Hz, which is considerably higher than that usually reported (5Hz) in the literature.
- The higher resonance frequency is most likely attributed to different sitting postures caused by inclinations of the seat pan and the backrest, the lower seated height and the lower vibration excitation levels considered for automobile occupants.
- Hands position is observed to have the most influential effect on APMS response. The peak magnitude and corresponding frequency decrease considerably when the hands are moved from lap to the steering wheel.
- The body mass forms another most significant factor that affects the vertical apparent mass response of seated automobile occupants on both the seat pan and the seat backrest. A higher body mass in general yields higher peak magnitude response and lower corresponding frequency for both passenger and driver postures. The magnitude is also observed to be higher over the entire frequency range when the mean body mass is increased. While a positive correlation could be established between peak apparent mass magnitude and the total body mass, the trend in decreasing fundamental frequency with increasing body mass showed a poor correlation.
- The results suggest relatively negligible influence of the feet position, body fat percentage, magnitude of vibration excitation and the gender.

- The biodynamic response of occupants seated with automotive postures and subject to vertical vibration need to be characterized, as a minimum, by two distinct functions for two postures: hands-in-lap and hands-on-steering wheel.
- Majority of the reported biodynamic models, are not applicable for automotive applications. Moreover all the reported biodynamic models are based upon the force-motion relationship at the seat-pan alone, while the sitting posture is limited to unsupported back only, and the interactions with the backrest are ignored.
- The proposed linear 4-DOF model can be effectively used to characterize the biodynamic responses of the seated occupants on both the seat pan and the backrest under vertical vibration. The model, however, could be considered applicable for seated subjects of mean mass of 71.2 kg.
- The non-dimensional modeling approach could be effectively applied to account for the significant effects of the body mass on the APMS response of both the seat pan and the backrest.
- The proposed body weight-dependent seated occupant model can provide a reasonable characterization of the biodynamic response of subjects of different body weight.

5.3 Recommendations for further work

- The human body model developed in this study is actually a mathematical curve-fitting model. In order to develop anatomical subsystem model describing accurately the body dynamics, more measurements at multiple vibration entry points are needed. The measurements should include the tri-axial forces at the seat pan and backrest and the vibration transmission along the pitch direction. The model may have degrees-of-freedom in the pitch mode.
- The human body model developed in this study is primarily applicable to the study of off-road vehicle driver and passenger seating, where the seated posture is usually making a full use of backrest. Errors may be expected, when the model is applied to study the seating dynamics in vehicles where the seat backrest angle is adjust less or more than 24° with respect to the vertical. The human body model parameters should thus be identified to characterize the biodynamic response for the different seat backrest angle.
- The biodynamic responses characterized in this study as well as all other reported studies can be considered valid when the body is uncoupled from the seat. Owing to considerable compliant properties of the seat, the biodynamic behavior of the occupant seated on a flexible surface may change. The development of an

effective model for seating application thus requires additional attempts to characterized the responses while seated on curved elastic surfaces.

REFERENCES

1. M.J. Griffin (1990) Handbook of Human Vibration, Academic Press, London.
2. D.G. Wilder (1993) American Journal of Industrial Medical 23, 577-588. The biomechanics of Vibration and low back pain.
3. D.G. Wilder and M.H. Pope (1996) Clinical Biomechanics 11, 67-73. Epidemiological and aetiological aspects of low back pain in vibration environments – an update.
4. B.O.Wikstrom, A-Kjellberg and U. Landstrom (1994) International Journal of Industrial Ergonomics 14, 273-292. Health effects of long-term occupational exposure to whole-body vibration: a review.
5. C.T.J.Hulshof and O.B.A.Veldhuijzen Van Zanten (1987) International Archives of Occupational and Environmental Health 59, 205-220. Whole-body vibration and low back pain – a review of epidemiologic studies.
6. M.Bovenzi and C.Hulsshof (1998) An updated review of epidemiologic studies on the relationship between exposure to whole-body vibration and low back pain. Journal of Sound and Vibration; 215(4): 595-611
7. Comite European de Normalisation (1996) Mechanical vibration – Guide to health effects of vibration on human body, CEN Report 12349. Bressels, CEN.
8. Xuting Wu (1998) Study of driver-seat interactions and enhancement of vehicular ride vibration environment. A PHD thesis Concordia University.
9. G.S.Paddan and M.J.Griffin (1998) A review of the transmission of translational seat vibration to the head. Journal of Sound an Vibration 215(4), 863-882.

10. International Organization for Standardization 2000 ISO-5982. Mechanical vibration and shock-range of idealized values to characterize seated-body biodynamic response under vertical vibration.
11. F.Pradko and R.A.Lee (1966) SAE Paper No. 660139 Vibration comfort criteria.
12. R.Lundstrom and P.Holmlund Absorption of energy during whole-body vibration exposure. Journal of Sound and Vibration (1998) 215(4) 789-799.
13. J.C.Guignard (1959) Air Ministry Flying Personnel Research Committee Report 1062. The physical response of seated men to low-frequency vertical vibration. Some preliminary studies.
14. J.C.Guignard and A.Iriving (1960) Engineering 190(4952), 364-367. Effects of low-frequency vibration on man.
15. Coermann R.R.(1962) "The mechanical impedance of the human body in sitting and standing position at low frequencies", Human Factors,227-253.
16. M.A.Schmitz and A.K.Simons (1960) The American Society of Mechanical Engineers ASME Paper. 59-A-200,1-11. Man's response to low-frequency vibration.
17. Edwards, R.G. and Lange, K.O.(1964) "A mechanical impedance investigation of human response to vibration", AMRL-TR-64-91 Aerospace Medical Research Laboratories, Wright-Patterson Air Force Base, Ohio.
18. J.P.Dennis (1965) Journal of Applied Psychology 49,245-252. Some effects of vibration upon visual performance.
19. Vogt, H.L., Coermann, R.R. and Fust, H.D.(1968) "Mechanical impedance of the sitting human under sustained acceleration", Aerospace Medicine,39,675-679.
20. Suggs, C.W., Abrams, C.F. and Stikeleather, L.F. (1969) "Application of a damped spring-mass human vibration simulator in vibration testing of vehicle seats", Ergonomics, 12, 79-90.

21. Miwa T. (1975) "Mechanical Impedance of Human body in Various Postures", *Industrial Health*, 13, 1-22.
22. G.R.Barnes and B.H.Rance (1975) *Aviation, Space, and environmental Medicine* 46, 987-993. Head movement induced by angular oscillation of the body in the pitch and roll axes.
23. G.F.Rowlands (1977) Royal Aircraft Establishment, Farnborough Technical Report 77068. The transmission of vertical vibration to the heads and shoulders of the seated man.
24. H.H.Cohen, D.E.Wasserman and R.W.Hornung 1977 *Ergonomics* 20, 207-216. Human performance and transmissibility under sinusoidal and mixed vertical vibration.
25. M.D.Bennett, B.Farmilo, S.H.Cole, S.J.Page, W.R. Witney and R.D.G.Webb (1978) Mechanical Engineering Department, The Royal Military College of Science, Report No.78003. An investigation into some of the human responses to sinusoidal and random vibration in the upright and semi-reclined seated posture.
26. M.J.Griffin and E.M. Whitham (1978) *Journal of Sound and vibration* 58, 239-250. Individual variability and its effect on subjective and biodynamic response to whole-body vibration.
27. M.J.Griffin, C.H.Lewis, K.C.Parsons and E.M. Whitham (1979) AGARD Conference Proceedings CP-253. Paper A28 in Models and analogues for the evaluation of human biodynamic response, performance and protection. The biodynamic response of the human body and its application to standards.
28. Mertens H. (1978) " Nonlinear behavior of sitting humans under increasing gravity", *Aviation, Space, and Environmental Medicine*, 287-298.
29. M.J.Moseley, C.H. Lewis and M.J.Griffin (1981) United Kingdom Informal Group Meeting on Human Response to Vibration, Heriot-Watt University, Edinburgh. The influence of seating conditions on head vibration and visual performance.

30. T.A.Furness (1981) [Ph.D. Thesis] Institute of Sound and Vibration Research, University of Southampton, Hampshire. The effects of Whole-body vibration on the perception of the helmet-mounted display.
31. B.K.N.Rao (1982) Shock and Vibration Bulletin 52, 89-99. Biodynamic response of human head during whole-body vibration conditions.
32. Sandover, J. (1982) "Measurements of the frequency response characteristics of man exposed to vibration", Ph.D Thesis, Loughborough University of Technology.
33. Donati, P.M. and Bonthous, C. (1983) "Biodynamic response of the human body in the sitting position when subjected to vertical vibration", Journal of Sound and Vibration, 90, 423-442.
34. Fairley, T.E. and Griffin, M.J. (1983) "Application of mechanical impedance methods to seat transmissibility", International Conference on Noise Control Engineering, Edinburgh, 533-536.
35. Fairley, T.E. and Griffin, M.J. (1986) "A test method for predicting of seat transmissibility", Society of Automotive Engineer International Congress and Exposition, Detroit, 24-28 February, SAE 860046.
36. F.W.Hagena, J.Piehler, C.J.Wirth, G.O.Hofmann and TH.Zwingers (1986) Neuro-Orthopedics 2, 29-33. The dynamic response of the human spine to sinusoidal Gz-vibration. In-vivo-experiments.
37. Hinz, B. and Seidel, H. (1987) "The nonlinearity of the human body's dynamic response during sinusoidal whole body vibration", Industrial Health, 25, 169-181.
38. Paddan, G.S. and Griffin, M.J. (1988) "The transmission of translational seat vibration to the head-I. Vertical seat vibration", Journal of Biomechanics, 21, 191-197.
39. Fairley T.E. and Griffin M.J. (1989) "The apparent mass of the seated human body: vertical vibration", Journal of Biomechanics, 22, 81-94.

40. G.S.Paddan (1991) [Ph.D Thesis] Institute of Sound and Vibration Research, University of Southampton, Hampshire. Transmission of vibration through the human body to the head.
41. Smith, S.D. (1993) "Comparison of the driving-point impedance and transmissibility techniques in describing human response to whole-body vibration", Proceedings U.K. Informal Group Meeting on Human Response to Vibration, APRE, Farnborough, The United Kingdom.
42. Holmlund P., Lundstrom R. and Lindberg L. (1995) "Whole-body vibration mechanical impedance of human body in the vertical direction", Proceedings of the UK Informal Group Meeting on Human Response to Bibration, Silsoe, United Kingdom.
43. Seidel, H. (1996) "A contribution to the revision of ISO 5982: Mechanical driving-point impedance and transmissibility of the human body", Personal Communications to A.J.Brammer.
44. Boileau, P.E. and Rakheja S. (1998) "Whole-body vertical biodynamic response characteristics of the seated vehicle driver: Measurement and model development", International Journal of Industrial Ergonomics, 22, 449-472.
45. R.Lundstrom and P.Holmlund (1998) "Absorption of energy during whole-body vibration exposure", Journal of Sound and Vibration (1998) 215(4), 789-799.
46. Kobo, Terauchi, Aoki and Matsuoka (1999) "An investigation into a synthetic vibration model for humans: An investigation into a mechanical vibration human model constructed according to the relations between the physical, psychological and physiological reactions of humans exposed to vibration", International Journal of Industrial Ergonomics 27 (2001) 219-232.
47. Younggun Cho and Yong-san Yoon (2001) "Biomechanical model of human on seat with backrest for evaluating ride quality", International Journal of Industrial Ergonomics 27(2001) 331-345.
48. N.J.Mansfield and M.J.Griffin (2001) "Effects of posture and vibration magnitude on apparent mass and pelvis rotation during exposure to whole-body vertical vibration", Journal of Sound and Vibration (2002) 253(1), 93-107.

49. W.N.Patten (1998) "A vibration model of open celled polyurethane foam automotive seat cushions", *Journal of Sound and Vibration* 217,145-161.
50. Hinz, Seidei, Menzel and Bluthner (2001) "Transfer functions as a basis for the verification of models – variability and restraints", *Clinical Biomechanics* 16 supplement No.1 (2001) S93-S100.
51. Boileu,P.E. (1995) "A study of second suspension and human driver response to whole-body vehicular vibration and shock", PhD. Thesis, Concordia University.
52. G.Allen (1978) "A critical look at biodynamic modeling in relation to specifications for human tolerance of vibration and shock", Paper A25-5, AGARD Conference Proceedings No.253.
53. Demic,M. (1987) "Investigation of human body oscillatory parameters under the action of shock excitations", ISO document TC108/SC/WG ZN158.
54. Payne,P.R. and Band,E.G.U.(1971) "A 4-DOF lumped parameter model of the seated human body", Aerospace Medical Research Laboratories Report AMRL-TR-70-35, Wright-Patterson Air Force Base, Ohio.
55. M.J.Griffin (2001) "The validation of biodynamic models", *Clinical Biomechanics* 16 Supplement No.1 (2001) S81-S92.
56. Yasunao and Griffin (2001) "Modeling the dynamic mechanisms associated with the principal resonance of the seated human body", *Clinical Biomechanics* 16. No.1 (2001) S31-44.
57. Rakheja,S., Tchernychouk,V. and Stiharu, I., "Measurement of vibration transmissibility and ride performance of seat-human system", Concave Report 15-96, 1996.
58. Winter DA *Biomechanics of human movement* p.151 (1979); Now published as *Biomechanics and Motor Control of Human Movement*.
59. International Organization for Standardization (1998), ISO-5982. Mechanical vibration and shock-range of idealized values to characterize seated-body biodynamic response under vertical vibration.

60. L. Wei and M.J. Griffin "Mathematical models for the apparent mass of the seated human body exposed to vertical vibration", *Journal of Sound and Vibration* (1998) 212 (5), 855-874.
61. Allen, G., "A Critical Look at Biodynamic Modeling in Relation to Specifications for Human Tolerance of Vibration and Shock", AGARD Conference Proceedings No.253, Paper A25-5, Paris, France, November 6-10, 1978
62. Boileau, P.E., X. Wu and S. Rakheja Definition of a range of idealized values to characterize seated body biodynamic response under vertical vibration. 1998 *Journal of Sound and Vibration* 215, 841-862.
63. G. S. Paddan and M. J. Griffin, The transmission of translational seat vibration to the head. Horizontal seat vibration, *Journal of Biomechanics* 21, 1998 1269-1278.
64. Alexander Cullmann and H.P. Wolfel Design of an active vibration dummy of sitting man. 2001 *Clinical Biomechanics* 16 Supplement No.1 (2001) S64-S72.
65. International Organization for Standardization (1993) ISO-5982. Mechanical vibration and shock-range of idealized values to characterize seated-body biodynamic response under vertical vibration.
66. N. Nawayseh and M. J. Griffin Tri-axial forces at the seat and backrest during whole-body fore-and-aft vibration. *Journal of Sound and Vibration*, in press, 2005.
67. N. Nawayseh and M. J. Griffin Tri-axial forces at the seat and backrest during whole-body vertical vibration. *Journal of Sound and Vibration* 227 (2004) 309-326.
68. W. Wang, S. Rakheja and P. E. Boileau Effects of sitting postures on biodynamic response of seated occupants under vertical vibration. *International Journal of Industrial Ergonomics*, Volume 34, Issue 4, October 2004.
69. S. Rakheja, I. Stiharu and P. E. Boileau Seated occupant apparent mass characteristics under automotive postures and vertical vibration. *Journal of Sound and Vibration* (2002) 253 (1), 57-75.

70. P. E. Boileau, S. Rakheja and X. Wu A body mass dependent mechanical impedance model for applications in vibration seat testing. *Journal of Sound and Vibration* (2002) 253 (1), 243-264.
71. Body fat percentage and body mass index calculator: <http://top.monad.net/~vsi/java/wbf/bf/calc.html>
72. Alexander Cullmann and H.P. Wolfel Design of an active vibration dummy of sitting man. *Clinical Biomechanics* 16 Supplement No.1 (2001) S64-S72.